UNIVERSITÉ DU QUÉBEC À MONTRÉAL

VERS UNE COMPRÉHENSION MÉCANISTIQUE DES INTERACTIONS INDIRECTES ENTRE LES PROIES DE LA TOUNDRA ARCTIQUE

THÈSE

PRÉSENTÉE

COMME EXIGENCE PARTIELLE

DU DOCTORAT EN BIOLOGIE

PAR

ANDRÉANNE BEARDSELL

MAI 2023

Remerciements

Mes premiers mots sont offerts à mon directeur, Joël Bêty. Jojo, Captain, Joey le touriste, Joji, ta passion pour l'écologie et la recherche est contagieuse (et infinie) et tu m'as offert un environnement idéal pour réaliser ma thèse. Un environnement de soutien, de confiance, d'opportunités et d'échanges, sur la science, la politique, la chasse et sur la vie. Je n'imagine pas de meilleur encadrement et j'en suis extrêmement reconnaissante. Je garderai un excellent souvenir de mes études doctorales.

Je tiens également à remercier mon codirecteur, Dominique Gravel, pour nos échanges scientifiques, pour les dessins sur un coin de table à Bylot, pour tes danses en "Waders", pour les balades toundriques et pour ton accueil lors de mes visites (un peu trop rares à mon goût) à Sherbrooke. Merci aussi à Dominique Berteaux pour ton support dans cette aventure et pour le maintien du suivi de la population de renards. J'aimerais aussi remercier Gilles Gauthier pour ta lecture approfondie de chacun de mes articles et pour tes judicieux conseils.

Ce projet, synthétisant des données accumulées depuis plus de 25 ans à l'île Bylot dans le Haut-Arctique, a été possible grâce à la contribution de nombreuses personnes envers qui j'ai beaucoup de reconnaissance. Sincères remerciements à toute la communauté Bylotienne avec qui j'ai eu la chance de partager des moments de vie et des aventures inoubliables entre 2012 et 2019. Ces étés de terrain ne seraient pas les mêmes sans le travail incroyable de Marie-Christine Cadieux et de Marie-Jeanne Rioux. J'aimerais aussi souligner la contribution de Jeanne Clermont, Éliane Duchesne, Jean-François Lamarre, Dominique Fauteux, Madeleine-Zoé Corbeil-Robitaille, Frédéric Dulude-De-Broin, Frédéric Letourneau, Louis Moisan et Alexis Grenier-Potvin. Merci à vous pour nos échanges scientifiques (ou pas), les crêpes nordiques,

nos moments magiques sur le terrain et pour votre support. Éliane, Lilou la loutre, merci pour les baignades (au moins 8) et ton soutien (te souviens-tu des brownies que tu as amené pendant mon examen doctoral?). Je termine avec un merci à toi Jeanne, pour nos milliers milliers d'échanges et je suis chanceuse d'avoir pu marcher à tes côtés pendant toutes ces années.

La faune du sous-sol de l'aile B de l'UQAR! Grande soeur cosmique, dès mon arrivée à l'UQAR, ton bureau a été un lieu d'échanges sur la vie, de conseils, de douceur, de câlins et le corridor un lieu de roulades. Lulu, Ludo, merci d'avoir accepté comme source de perturbations (très) fréquentes. Ces moments de folies ont embelli mes journées (j'espère aussi un peu les tiennes!).

Merci à Marie-Pier Landry, Samuel Dufour et leur fils Henri Dufour, spécialement pour m'avoir chanté cette chanson à ma fête (paroles modifiées de *Ricky Baker Happy Birthday Song*), le jour où mon article venait d'être refusé dans un journal:
DD Beardsell
Happy birthday
Once rejected, now accepted
By us, and Henri

Merci aux organismes subventionnaires qui m'ont permis d'embarquer pleinement dans l'aventure doctorale sans soucis financier. Merci à la fondation Garfield-Weston, au Conseil de Recherches en Sciences Naturelles et en Génie du Canada, au Fonds de Recherche du Québec - Nature et Technologies, à la fondation de l'UQAR, au Centre d'Études Nordiques et au programme de formation en sciences et services de la biodiversité computationnelle (BIOS2). Ce projet a été également possible grâce au support financier et logistique de nombreuses organisations (en ordre alphabétique):

- ArcticNet
- Centre d'Études Nordiques
- Conseil de Recherches en Sciences Naturelles et en Génie du Canada

- Environnement Canada
- Fonds de Recherche du Québec - Nature et Technologies
- the Kenneth M Molson Foundation
- Mittimatalik Hunters and Trappers Organization
- Northern Scientific Training Program
- Parcs Canada et spécialement le parc national Sirmilik
- Programme de Chaires de recherche du Canada
- Programme du plateau continental polaire
- Savoir Polaire Canada

Cette aventure des études doctorales aura été très enrichissante, tant sur le plan scientifique que personnel, et je termine en soulignant l'appui de ma famille, mon refuge primaire. Tout d'abord, mes parents, par votre amour et soutien inconditionnel, vous m'avez transmis un héritage inestimable. Merci aussi à Philippe et Guillaume, mes frérots d'amour! Guillaume a participé à la révision de mes équations. André, Joëlle, Raphael et Frédérique, vous m'avez accueillie chaleureusement parmi vous, aider à garder un bel équilibre tout en travaillant sur ma thèse et j'en suis vraiment reconnaissante. Mon dernier mot va à André, mon compagnon de vie, pour son soutien quotidien, son écoute et avec qui je partage beaucoup de passions.

TABLE DES MATIÈRES

LISTE DES TABLEAUX

LISTE DES FIGURES

Résumé

Comprendre comment et dans quelle mesure les interactions biotiques influencent l'abondance et la distribution des espèces est un défi majeur, notamment car la biodiversité est organisée en réseaux générant des interactions multiples liant les espèces entre elles. C'est d'autant plus difficile lorsque les interactions sont indirectes puisqu'elles peuvent emprunter des parcours complexes dans le réseau d'interactions impliquant plusieurs espèces. Les interactions indirectes, entre des proies partageant un prédateur, peuvent promouvoir la coexistence entre les proies ou dans certains contextes, entraîner l'exclusion locale d'une proie. Ces interactions sont largement répandues en milieu naturel et en dépit d'un nombre élevé de travaux s'y intéressant, il s'avère encore difficile de quantifier la force et déterminer la nature (p.ex., compétition apparente, mutualisme apparent) de l'interaction indirecte résultante entre des proies partageant un prédateur. Cela s'explique particulièrement par la difficulté de définir la réponse fonctionnelle et numérique du prédateur à ses proies.

Dans le but d'examiner les mécanismes qui modulent la force des interactions entre les espèces et d'améliorer notre capacité à quantifier la force de ces interactions dans les communautés naturelles, j'ai construit un modèle mécanistique des interactions prédateurs-proies. Ce modèle est basé sur les traits et le comportement des espèces et s'inspire d'une communauté de vertébrés de la toundra arctique, où les petits rongeurs cycliques (lemming) et les œufs d'oiseaux (bécasseaux, oies des neiges) partagent un prédateur (le renard arctique). Le modèle a été paramétré à partir de données issues de la littérature et du suivi écosystémique à long terme (>25 ans) de l'île Bylot (Nunavut).

Dans le premier chapitre, un modèle mécanistique de la réponse fonctionnelle du prédateur

à quatre de ses proies est dérivé en décomposant la séquence de la prédation (recherche, détection, attaque, capture et manipulation). Ce modèle est l'un des premiers modèles mécanistiques de la réponse fonctionnelle paramétré dans une communauté naturelle de vertébrés. Ce modèle servira de fondation à l'entièreté de la thèse. Dans le second chapitre, les mécanismes pouvant expliquer l'interaction indirecte positive entre des proies de la toundra arctique (les lemmings, les bécasseaux et les passereaux) sont examinés. Les résultats montrent que: (i) contrairement aux hypothèses classiques, le temps de manipulation des proies joue un rôle mineur dans notre système et (ii) des changements dans le comportement du renard (soit dans le budget d'activité quotidien et la distance parcourue) peuvent générer une interaction indirecte positive entre les lemmings et les oiseaux. Dans le dernier chapitre, j'évalue si la présence d'une proie (l'oie des neiges) peut mener à l'exclusion locale d'une autre proie (les bécasseaux) via des interactions trophiques indirectes. Les résultats montrent que les effets positifs de la présence d'une colonie d'oies sur le succès de la nidification des bécasseaux (via le temps de manipulation des œufs par les prédateurs) sont contrebalancés par l'effet négatif d'une augmentation de la densité des renards, causée par une réduction de la taille du domaine vital des renards dans la colonie d'oies. Ainsi, l'interaction nette résultant de la présence des oies était négative et cette interaction est suffisamment forte pour conduire à l'exclusion locale des bécasseaux. L'originalité de ce chapitre est d'identifier les mécanismes proximaux affectant la coexistence des proies dans une communauté naturelle de vertébrés en faisant le pont entre la taille du domaine vital du prédateur, le risque de prédation, jusqu'à la dynamique de populations.

Globalement, cette thèse illustre comment des modèles mécanistiques, basés sur des estimations empiriques des principales composantes de la prédation, peuvent améliorer notre capacité à quantifier la force de ces interactions dans les communautés naturelles. Cette thèse a permis d'identifier des mécanismes qui sous-tendent les interactions indirectes et propose un outil de modélisation pour quantifier les interactions indirectes dans les communautés naturelles.

Mots clés: interactions prédateurs-proies, réponse fonctionnelle, prédation, interactions indirectes, renard arctique (*Vulpes lagopus*), lemmings, passereaux, bécasseaux.

Abstract

Understanding how and to what extent biotic interactions influence the abundance and distribution of species is a major challenge, especially since biodiversity is organized in networks generating multiple interactions linking species together. This is particularly challenging when the interactions are indirect, since they can take complex paths through the network of interactions involving several species. Indirect interactions, between prey sharing a predator, can promote coexistence between prey or in some contexts, lead to the local exclusion of a prey. These interactions are widespread in the wild, and despite a large body of research on them, it is still difficult to quantify the strength and determine the nature (e.g. apparent competition, apparent mutualism) of the resulting indirect interaction between prey sharing a predator. This is particularly due to the difficulty of defining the functional and numerical response of the predator to its prey.

To examine the mechanisms that modulate the strength of interactions between species and to improve our ability to quantify the strength of these interactions in natural communities, I build a mechanistic model of predator-prey interactions. This model is based on species traits and behavior and was inspired by an Arctic tundra vertebrate community, where small cyclic rodents (lemmings) and bird eggs (sandpipers, snow geese) share a predator (the Arctic fox). The model was parameterized using data from the literature and long-term (>25 years) ecosystem monitoring on Bylot Island, Nunavut.

In the first chapter, a mechanistic model of the predator functional response to four of its prey was derived by breaking down the predation sequence (search, detection, attack, capture and manipulation). This model is the one of the first mechanistic model of the functional

response parameterized in a natural vertebrate community and highlights that the predator acquisition rate is not systematically limited to the highest prey densities observed in a natural system. This model will be the foundation for the entire thesis. In the second chapter, mechanisms that can explain the positive indirect interaction between Arctic tundra prey (lemmings, sandpipers and passerines) are examined. The results show that: (i) contrary to classical hypotheses, prey handling time plays a minor role in our system and (ii) changes in fox behavior (i.e., in daily activity budget and distance traveled) can generate a positive indirect interaction between lemmings and birds. In the last chapter, I evaluate whether the presence of one prey (snow geese) can lead to the local exclusion of another prey (sandpipers) through indirect trophic interactions. Results show that the positive effects of a goose colony on sandpiper nesting success (due to the handling time of goose eggs by the predator) were outweighed by the negative effect of an increase in fox density. The fox numerical response was driven by changes in home range size. As a result, the net interaction from the presence of geese was negative and could lead to local exclusion of sandpipers. The originality of this chapter is to identify proximal mechanisms affecting prey coexistence in a natural vertebrate community by linking predator home range size, predation risk, and population dynamics.

Overall, this thesis illustrates how mechanistic models, based on empirical estimates of key components of predation, can improve our ability to quantify the strength of predator-prey interactions in natural communities. The chapters together make theoretical contributions to ecology through the development and use of novel approaches to quantify predator-prey interactions.

Keywords: predator-prey interactions, functional response, predation, indirect interactions, arctic fox (*Vulpes lagopus*), lemmings, passerines, sandpipers.

CHAPITRE 1

Introduction générale et cadre théorique

Comprendre comment et dans quelle mesure les interactions biotiques influencent l'abondance et la distribution des espèces est un défi majeur notamment car la biodiversité est organisée en réseaux générant des interactions multiples liant les espèces entre elles(Godsoe et al., 2017). Les interactions biotiques indirectes sont particulièrement complexes car elles surviennent par le biais de chaînes d'interactions directes (Cazelles et al., 2016). En théorie, les interactions indirectes négatives entre les espèces qui partagent un ennemi commun peuvent modifier la composition de la communauté en excluant les espèces plus vulnérables à cet ennemi. Bien que ces interactions indirectes soient répandues (Holt and Bonsall, 2017), elles demeurent difficiles à quantifier dans les communautés naturelles.

1.1 Les interactions prédateurs-proies

Les interactions prédateurs-proies sont omniprésentes, gouvernent le flux d'énergie entre les niveaux trophiques et façonnent la structure des systèmes écologiques. Elles sont généralement quantifiées à l'aide de réponses fonctionnelles (c.-à-d. le taux d'acquisition de proies par un prédateur en fonction de la densité des proies; Solomon 1949) et numériques des prédateurs. Ces concepts sont au coeur du fonctionnement des communautés écologiques et influ-

encent l'abondance, la biodiversité et la dynamique des communautés (DeLong, 2021). Malgré plus de 70 ans de recherche (Solomon, 1949), modéliser les réponses fonctionnelles demeure un défi de taille, notamment puisque celles-ci sont modulées par de nombreux facteurs écologiques et environnementaux qui peuvent agir de manière concomitante et ainsi diminuer notre compréhension du fonctionnement des systèmes écologiques. Notre compréhension des réponses numériques des prédateurs est encore plus limitée que celle des réponses fonctionnelles (Abrams, 2022). Jusqu'à présent, la réponse numérique est généralement modélisée via la survie et la reproduction (avec ou sans délai) des prédateurs dans les modèles classiques d'interactions prédateurs-proies (voir les équations de MacArthur-Rosenzweig ; Rosenzweig and MacArthur 1963). Les applications de ces concepts se retrouvent notamment dans la lutte contre les parasites, la gestion des espèces envahissantes et la biologie de la conservation, et sont au coeur de la théorie de l'écologie des populations et des communautés.

1.1.1. La réponse fonctionnelle

Quantifier la réponse fonctionnelle d'un prédateur à sa proie requiert de connaître le taux d'acquisition de la proie par le prédateur selon la densité de la proie. La forme de la courbe obtenue est typiquement classée en trois catégories: Linéaire (type I), hyperbolique (type II), ou sigmoïdale (type III; Holling 1959*b*,*a*; Fig. 1.1A). La forme de type 1 est le plus simple: le taux d'acquisition augmente proportionnellement avec la densité des proies. La forme de type II est similaire dans la mesure où le taux d'acquisition augmente avec la densité des proies, mais atteint progressivement une asymptote. Cette asymptote est atteinte lorsque le prédateur est limité par le temps associé à la capture, à la consommation, au transport et à l'ingestion de la proie. La réponse fonctionnelle de type II est le modèle le plus souvent utilisé (Rall et al., 2012). La forme de type III est similaire à la type II, mais le taux d'acquisition augmente très lentement à faible densité, puis plus rapidement jusqu'à l'atteinte d'une asymptote. Cette classification est solidement ancrée en écologie et couramment utilisée par les écologistes lorsqu'ils intègrent la prédation dans les modèles de population et de communauté (Turchin and Hanski, 1997; Fryxell et al., 2007; Serrouya et al., 2015). Les variations de

la forme de la réponse fonctionnelle peuvent avoir d'importantes conséquences écologiques sur la structure et la dynamique des communautés en modifiant la force et la nature des interactions entre les espèces (Abrams et al., 1998; Abrams and Matsuda, 2004; Brose et al., 2006; Abrams and Cortez, 2015; Coblentz, 2020). Dans ce contexte, il est important de s'attarder à l'origine des modèles de réponses fonctionnelles et en quoi ils représentent une simplification du processus de quête alimentaire des prédateurs.

Les prochaines étapes décrivent la mécanique proposée par Holling (1959*a*) et illustrée dans un système prédateur-proie pour le contexte de cette thèse. L'aire recherchée (A; km^2) par un prédateur est exprimée par le produit de la vitesse du prédateur (s; km/day), la distance de réaction à une proie i (d_i; km) et du temps passé en recherche (T_s; day). Au sein de cette aire, une rencontre potentielle entre le prédateur et la proie se produit lorsque le prédateur arrive à une distance (d_i) à laquelle l'un peut détecter l'autre et réagir. Dans le cas où toutes les proies situées dans cette zone ne sont pas systématiquement détectées, attaquées et maîtrisées par le prédateur, la probabilité de détection ($f_{2,i}$), la probabilité d'attaque ($f_{3,i}$) et la probabilité de réussite d'une attaque ($f_{4,i}$) sont introduites (Fig. 1.1C). L'efficacité de capture d'une proie i (α_i; km^2/day) par le prédateur est exprimée par :

$$\alpha_i = s(2d_i) f_{2,i} f_{3,i} f_{4,i} \tag{1.1}$$

Le nombre de proies capturées ($V_{\alpha i}$) pendant un temps de recherche T_S pour une densité de proie N_i est exprimé par:

$$V_{\alpha i} = \alpha_i T_S N_i \tag{1.2}$$

Dans la dérivation initale du modèle, les prédateurs divisent leur temps entre la recherche et la manipulation des proies (T_h; day/prey item), de sorte que le temps disponible pour se nourrir T_t est soustrait par le temps de manipulation des proies:

$$T_S = T_t - (V_{\alpha i} T_h) \tag{1.3}$$

Le temps de manipulation comprend le temps nécessaire pour capturer, consommer, trans-

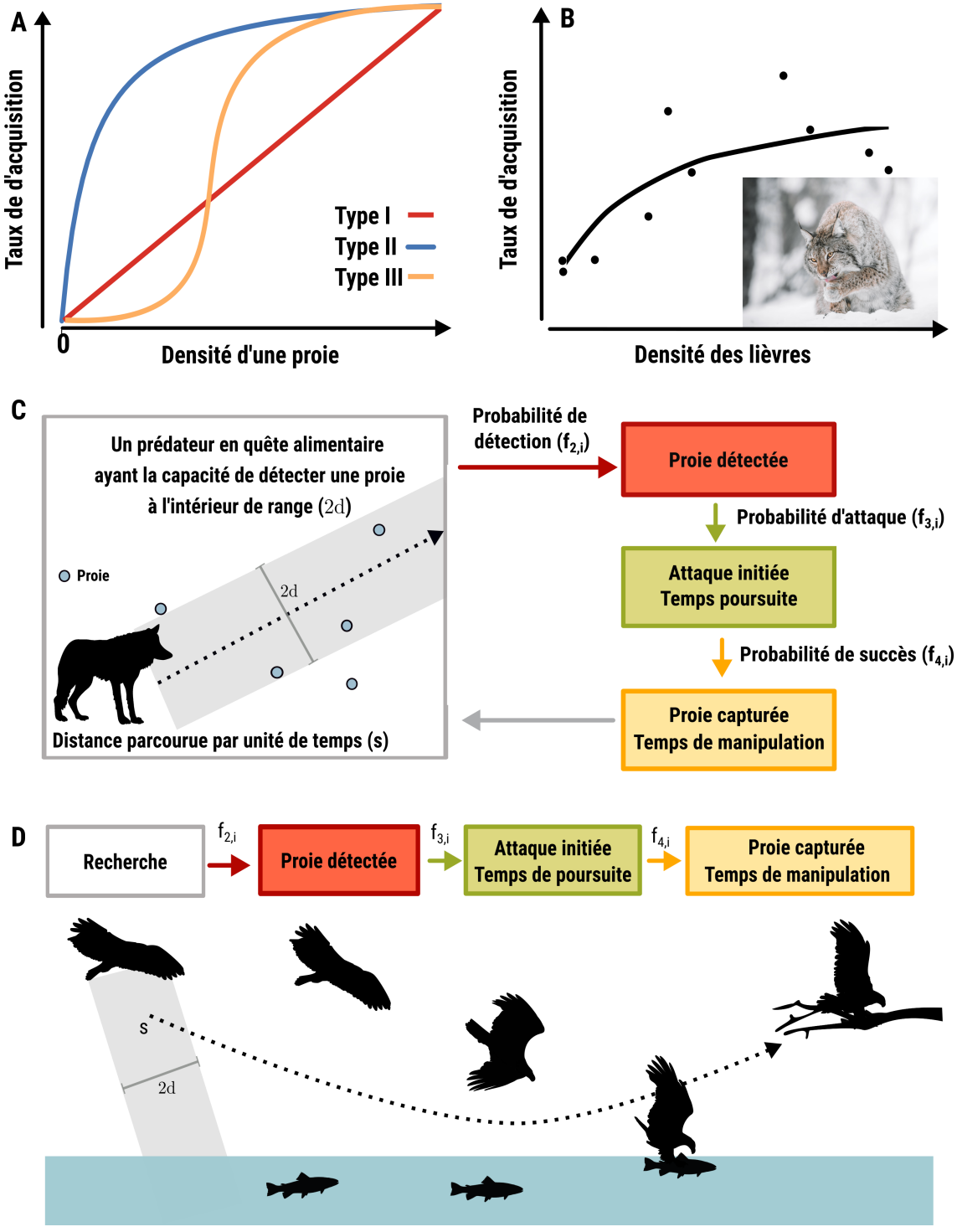

Figure 1.1. (**A**) Illustration des formes classiques de la réponse fonctionnelle des prédateurs catégorisées en trois types, (**B**) Réponse fonctionnelle du lynx à la densité de lièvres. Adaptée de Chan et al. 2017. Représentation schématique d'un modèle mécanistique de la réponse fonctionnelle pour un prédateur terrestre (**C**) et aviaire (**D**). La séquence de la prédation est décomposée en différentes étapes (e.g., la détection, l'attaque, la capture et la manipulation) qui définissent le comportement de quête alimentaire du prédateur et les comportements anti-prédateurs des proies. La figure (**D**) est inspirée de Pawar et al. 2012.

porter et digérer la proie. En substituant T_S de l'équation 1.3 dans l'équation 1.2 et en simplifiant, nous arrivons à:

$$V_{\alpha i} = \frac{\alpha_i N_i T_t}{1 + \alpha_i T_h N_i} \tag{1.4}$$

La réponse fonctionnelle d'un prédateur ($f(i)$) est le nombre de proies capturées par prédateur par unité de temps (taux d'acquisition). On l'exprime en divisant l'équation 1.4 par T_t :

$$f(i) = \frac{\alpha_i N_i}{1 + \alpha_i T_h N_i} \tag{1.5}$$

Cette équation correspond au modèle de type II. Lorsque la valeur de T_h est négligeable ou égale à 0, le modèle est équivalent à une réponse fonctionnelle de type I. Comparativement aux type I et II, l'équation de la réponse fonctionnelle de type III n'a pas, à ma connaissance, d'origine mécanistique. Ce modèle inclut de façon phénoménologique des effets non-linéaires simplement en ajoutant un exposant (θ) dans l'équation de type II:

$$f(i) = \frac{\alpha_i N_i^\theta}{1 + \alpha_i T_h N_i^\theta} \tag{1.6}$$

Ainsi, le paramètre θ génère des effets non-linéaires dans la courbe, mais n'est pas un paramètre biologiquement interprétable.

Depuis le travail fondateur de Holling (1959*a*), les écologistes ont développé de nombreux modèles mathématiques de réponses fonctionnelles (revus par Jeschke et al. 2002; Rall et al. 2012). Les différents modèles de réponses fonctionnelles sont souvent évalués avec des analyses statistiques. Bien que les données empiriques puissent être compatibles avec divers modèles de réponses fonctionnelles (p.ex., Gilg et al. 2006; Chan et al. 2017), la taille de l'échantillon est souvent insuffisante pour obtenir la puissance statistique nécessaire pour pouvoir faire la distinction entre les différentes formes de réponses fonctionnelles (Novak and Stouffer, 2020). De plus, cette approche ne permet pas d'identifier les mécanismes biologiques qui sous-tendent les forces d'interaction et les paramètres de la courbe (comme le temps de manipulation ou l'efficacité de capture d'une proie) doivent être interprétés avec prudence. Par exemple, Chan et al. (2017) concluent que le lynx est fortement limité par le temps de manip-

ulation (incluant la digestion) à haute densité de lièvres puisque le modèle de type II était le plus parcimonieux parmi 16 modèles candidats de réponses fonctionnelles (Fig. 1.1B). Bien que le temps de manipulation puisse être un mécanisme biologique important dans l'interaction lynx-lièvre, cette méthode ne permet pas de conclure sur les mécanismes impliqués et d'autres mécanismes mériteraient d'être explorés (Griffen, 2021). Cet exemple illustre comment l'idée que les prédateurs sont limités par le temps de manipulation est solidement ancrée en écologie et qu'elle influence notre interprétation des interactions prédateurs-proies.

À ce jour, les recherches théoriques et empiriques sur la réponse fonctionnelle ont porté principalement sur des systèmes à une proie, un prédateur (mais voir Smout et al. 2010; Serrouya et al. 2015; Baudrot et al. 2016; Chan et al. 2017). La version multi-espèces de l'équation de Holling (1959*b*) (Murdoch and Oaten, 1975) est largement utilisée pour modéliser la réponse fonctionnelle dans des systèmes impliquant plusieurs proies (Barraquand et al., 2015; Brose et al., 2005; McLellan et al., 2010; Serrouya et al., 2015). Ce modèle est aussi au cœur de modèles de réseaux alimentaires complexes (Schneider et al., 2016; Tyson and Lutscher, 2016) et le temps de manipulation est considéré comme un mécanisme dominant induisant des effets positifs à court terme sur les proies (Abrams, 1987; Abrams et al., 1998; Abrams and Matsuda, 1996). La somme des temps de manipulation des proies est une composante centrale à cette équation, où le temps passé à manipuler une proie i réduit le temps disponible pour la recherche d'autres proies. Ainsi, de par la structure des équations, les effets de la densité d'une proie sur les autres proies s'expriment uniquement via une modification du temps total disponible à la quête alimentaire du prédateur via le temps de manipulation. Cependant, il y a peu d'évidences que les prédateurs sont limités par les processus de manipulation aux densités de proies les plus élevées observées dans les systèmes naturels (Chan et al., 2017; Jeschke et al., 2002; Novak, 2010; Preston et al., 2018) et les évidences empiriques supportant ce modèle sont très rares (DeLong, 2021). Dans ce contexte, d'autres mécanismes mériteraient d'être étudiés.

La plupart des recherches empiriques sur les réponses fonctionnelles ont été menées dans

des conditions contrôlées en laboratoire ou dans des enclos (96 %, n = 116 études, revues par Pawar et al. 2012), témoignant de la difficulté de mesurer la réponse fonctionnelle en milieu naturel. La majorité des études utilise l'approche suivante: la densité des proies est estimée ou manipulée, la consommation des prédateurs est enregistrée et les modèles de réponse fonctionnelle sont évalués avec des analyses statistiques (revue de littérature par Rall et al. 2012). Intégrer des réponses fonctionnelles développées en milieu contrôlé pour comprendre la dynamique de populations en milieu naturel peut poser des problèmes. Par exemple, tel que souligné par Griffen (2021), alors qu'une étude réalisée en laboratoire sur les crabes de rivages (*Hemigrapsus sanguineus*) indiquait une consommation maximale de 125 moules par jour, des expériences réalisées sur le terrain ont révélées que les crabes ne consommaient qu'en moyenne 3.9 moules par jour. Basée sur la réponse fonctionnelle mesurée en laboratoire, Griffen et al. (2021) ont calculé que les crabes épuiseraient toute la population de moules en moins de 7h, prédisant un impact des crabes beaucoup plus élevé que celui observé en milieu naturel.

Mesurer la réponse fonctionnelle en milieu naturel est un défi de taille. Cela l'est particulièrement car la réponse fonctionnelle d'un prédateur à sa proie est hautement dynamique et elle varie en fonction d'une multitude de facteurs écologiques et environnementaux, comme la formation de groupes sociaux chez le prédateur (Fryxell et al., 2007), les conditions environnementales (Hone et al., 2011), la présence d'autres proies (Smout et al., 2010; Baudrot et al., 2016; Chan et al., 2017) et la présence de comportement de mise en réserve de nourriture chez le prédateur (Fletcher et al., 2010). Mesurer la réponse fonctionnelle est aussi difficile à cause d'une combinaison de facteurs, incluant une taille d'échantillon petite et qui ne couvre pas le gradient des densités de proies observées, la difficulté de suivre les interactions prédateurs-proies en continu et d'estimer la densité des proies et des prédateurs (Gilg et al., 2006; Therrien et al., 2014; Suryawanshi et al., 2017; Ellis et al., 2019). Enfin, la grande variabilité du taux d'acquisition des prédateurs observée dans la nature permet rarement aux modèles statistiques de pouvoir discriminer entre les différentes formes de réponses fonctionnelles (O'Donoghue et al., 1998; Vucetich et al., 2002; Chan et al., 2017).

Il y a aussi d'autres limites aux approches statistiques (mentionnées ci-haut). Ainsi, l'utilisation d'approches statistiques ne nous permet pas de modéliser avec précision les interactions prédateurs-proies dans les milieux naturels et d'autres approches doivent être utilisées.

Dériver la réponse fonctionnelle en utilisant une approche mécanistique consiste à décomposer la séquence de la prédation en différentes étapes (p.ex., la détection, l'attaque, la capture et la manipulation) qui définissent les stratégies de quête alimentaire du prédateur et les comportements anti-prédateurs des proies (Wootton et al. 2021; Figs. 1.1C et D). Ces étapes sont ensuite idéalement paramétrées avec des données empiriques. Chacune des étapes sera adaptée au système prédateur-proie étudié et certaines étapes seront pertinentes pour une interaction, mais non pertinentes pour une autre. Par exemple, l'inclusion de la probabilité de succès d'une attaque est pertinente si la proie est mobile et qu'elle a la capacité de fuir ou de se défendre, si la proie est sessile et sans mécanisme de défense, cette étape peut être omise. En comparaison aux approches statistiques, cette approche est basée sur des paramètres ayant une interprétation biologique et permet d'identifier les mécanismes modulant le taux d'acquisition des prédateurs et la forme de la réponse fonctionnelle. Cette approche permet ainsi d'identifier les moteurs proximaux des interactions prédateurs-proies ce qui améliorera notre capacité à modéliser des interactions écologiques. Cette approche fait aussi le pont entre la théorie et les données empiriques (Connolly et al., 2017). Malgré leurs avantages, les modèles mécanistiques de la réponse fonctionnelle sont très rares chez les vertébrés (Fryxell et al., 2007; Pawar et al., 2012).

1.1.2. La réponse numérique

La réponse numérique décrit la relation entre la densité de proies et le nombre de prédateurs. Dans la plupart des modèles prédateurs-proies, la réponse numérique est typiquement incorporée à travers des changements dans la survie ou la reproduction des prédateurs (Rosenzweig and MacArthur, 1963; Courchamp et al., 2003; Serrouya et al., 2015; Abrams, 2022). De façon générale, un simple facteur de conversion est utilisé pour traduire ce qui est

consommé par le prédateur (la réponse fonctionnelle) en nouveaux prédateurs (la réponse numérique; Fryxell et al. 2007; Pawar et al. 2012; Serrouya et al. 2015; Coblentz and DeLong 2020). Bien que l'application de cette simplification puisse être cohérente dans certaines situations, cela s'avère un raccourci qui ne représente probablement pas la dynamique observée dans plusieurs communautés naturelles (Abrams and Ginzburg, 2000).

Comme souligné récemment par Abrams (2022), notre compréhension de la réponse numérique est encore plus limitée que celle de la réponse fonctionnelle des prédateurs. Une augmentation de la densité de proies peut résulter en une plus grande densité de prédateurs à travers des processus divers, à la fois comportementaux et ou démographiques. Bien qu'un changement dans la densité de proies est susceptible de se réfléter dans dans la survie et/ou la reproduction du prédateur à large échelle spatiale (avec ou sans délai), des changements comportementaux peuvent aussi opérer et modifier la densité de prédateurs à l'échelle locale. S'intéresser à ces processus comportementaux devient encore plus pertinents chez des prédateurs mobiles (p.ex., loups, renards, harfangs, buses) pour comprendre les dynamiques prédateurs-proies locales. Par exemple, une augmentation de la densité des proies peut modifier les coûts/bénéfices des mouvements d'un prédateur se traduisant par un domaine vital plus petit et une augmentation de la densité de prédateurs. Alors que le lien entre la densité de proies et la taille des domaines vitaux des prédateurs a été documenté chez plusieurs espèces (Loveridge et al., 2009; Payne et al., 2022), ce processus comportemental est rarement inclut pour modéliser les interactions prédateurs-proies. Dans l'optique de comprendre les mécanismes qui modulent la force des interactions entre les espèces et de quantifier leur importance, il est nécessaire de se questionner sur les mécanismes qui façonnent la réponse numérique des prédateurs.

1.2 Interactions trophiques indirectes

La majorité des espèces ont un ou plusieurs ennemis naturels, tels que des prédateurs, des parasites ou des pathogènes. Ces ennemis naturels peuvent être spécialisés, mais généralement, ils exploitent plusieurs victimes. Cela conduit à la possibilité d'interactions indirectes, positives ou négatives, entre les espèces partageant le même ennemi. Ces interactions sont répandues au sein des communautés naturelles et peuvent influencer l'abondance et la coexistence des espèces (Holt, 1977; Holt and Lawton, 1994; Bonsall and Hassell, 1997; DeCesare et al., 2010). Elles prennent des formes qui s'étendent sur un gradient à partir des effets indirects réciproques (compétition et mutualisme apparent), aux interactions amensales et commensales (Fig. 1.2; Chaneton and Bonsall 2000).

Les fondements théoriques derrière les interactions indirectes ont été initialement proposé par Holt (1977) en utilisant un système simple à 2 proies et un prédateur. Au sein de ce système, une interaction indirecte survient lorsque l'effet de la densité d'une proie (R_1) sur la densité d'une autre (R_2) est modulé par des changements dans la réponse numérique et fonctionnelle du prédateur commun (P; Fig. 1.2). On peut quantifier la force et l'intensité de l'interaction indirecte par la somme des effets transmis par la réponse numérique et fonctionnelle du prédateur. Cependant, il y a un conflit potentiel, entre les effets indirects dus à la réponse fonctionnelle et numérique, reconnu depuis les travaux de Holt (1977) et qui n'a pas été résolu depuis (Holt and Bonsall, 2017). Pour illustrer ce conflit, considérons le même système à un prédateur et deux proies potentielles, R_1 et R_2. L'augmentation de la densité de la proie R_1 est susceptible de diminuer le taux d'acquisition du prédateur à la proie R_2, soit en raison du temps de manipulation de la proie R_1 ou d'un changement de comportement du prédateur, ce qui pourrait avoir un effet positif sur la proie R_2. Alternativement ou d'une façon additive, l'augmentation de la densité de la proie R_1 peut augmenter le nombre de prédateurs (réponse numérique aggrégative ou via la reproduction), ce qui pourrait avoir un effet négatif sur la proie R_2. À travers cet exemple, nous comprenons que l'interaction résultante entre les deux proies sera très sensible à la façon dont la réponse numérique et fonctionnelle du pré-

dateur sont définies (Oaten and Murdoch, 1975; Holt, 1977; Holt and Lawton, 1994; Abrams and Matsuda, 1996). La balance entre les effets liés à la réponse fonctionnelle et numérique a été beaucoup étudiée de façon théorique (Abrams and Matsuda, 1996) mais les prédictions des modèles ont rarement été testées en milieu naturel.

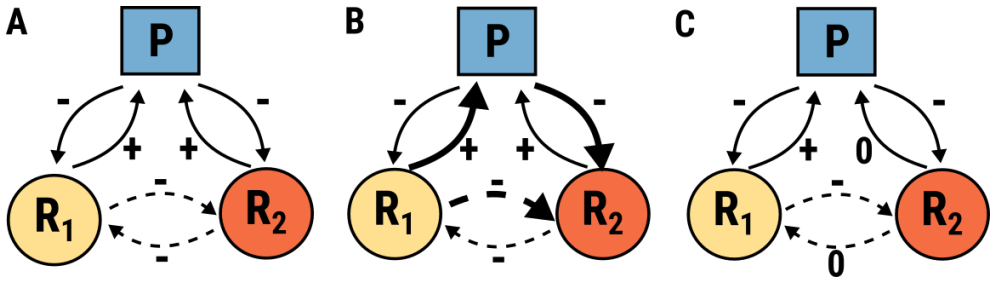

Figure 1.2. Schématisation des interactions directes (lignes pleines) et indirectes négatives (lignes pointillées)pouvant survenir entre deux proies (R_1 et R_2) partageant un prédateur (P). Les interactions indirectes s'étendent d'un gradient à partir de la compétition apparente symétrique **(A)**, de la compétition apparente asymétrique **(B)** à l'amensalisme indirect **(C)**. La largeur des lignes indique la force relative de l'interaction.

Le temps de manipulation des proies par un prédateur (ce qui inclut le temps à chasser, consommer ou à transporter une proie) est considéré comme un mécanisme dominant pouvant générer des interactions indirectes positives entre des proies partageant un prédateur (Abrams, 1987; Abrams and Matsuda, 1996; Abrams et al., 1998). Cependant, de plus en plus d'études indiquent que les prédateurs ne sont pas nécessairement limités par un tel mécanisme dans la nature (Chan et al., 2017; Preston et al., 2018). D'autres mécanismes peuvent également générer des effets indirects positifs, mais ils sont rarement inclus dans la modélisation des interactions prédateurs-proies (Stouffer and Novak, 2021). Par exemple, l'abondance d'une proie peut moduler le statut reproducteur et/ou le budget d'activité du prédateur ce qui aura en retour des impacts sur les autres proies consommées par le prédateur.

Une interaction indirecte négative peut survenir entre des espèces de proies partageant un prédateur (Holt, 1977). Par exemple, lorsqu'une proie est le principal déterminant de l'abondance du prédateur, une rétroaction faible peut être observée entre les autres proies et le pré-

dateur (Fig. 1.2B). Ultimement, cette asymétrie peut entraîner l'exclusion locale de ces proies et les mécanismes sous-jacents peuvent être liés à des différences dans les traits d'histoire de vie, comme la fécondité ou la vulnérabilité à la prédation (Roemer et al., 2002). C'est ce que Roemer et al. (2002) ont démontré dans un système insulaire impliquant une proie introduite abondante (le cochon sauvage (*Sus scrofa*)), une proie endémique (le renard insulaire (*Urocyon littoralis*)) et un prédateur commun (l'aigle royal (*Aquila chrysaetos*)). L'introduction du cochon sauvage a permis à l'aigle royal de coloniser les îles. Le renard étant plus vulnérable à la prédation et ayant une plus faible fécondité que le cochon sauvage, la prédation de l'aigle sur les renards a entraîné la population près de l'extinction. Ce phénomène est difficile à démontrer en observant une communauté établie puisque les espèces plus sensibles à la prédation sont absentes du système ou à de très faibles densités. L'exclusion n'est toutefois pas inévitable, une réponse numérique faible du prédateur commun (dans le cas où les sites de reproduction sont limitants par exemple), la présence de refuges spatiaux et temporels peuvent promouvoir la coexistence entre les proies (Holt and Lawton, 1994; Chivers et al., 2014).

1.3 Les interactions prédateurs-proies dans l'Arctique

La prédation joue un rôle central au sein des communautés terrestres arctiques et représente une force structurante du réseau trophique de la toundra arctique (Legagneux et al., 2012, 2014). Les lemmings sont au coeur du réseau trophique et connaissent des fluctuations marquées d'abondance ayant une périodicité de 3-4 ans (Gruyer et al., 2008). Le renard arctique (*Vulpes lagopus*), distribué à l'échelle circumpolaire, est le principal prédateur commun aux lemmings et aux oiseaux nichant au sol (McKinnon and Bêty 2009; Angerbjörn et al. 1999; Royer-Boutin 2015; Fig. 1.3). En conséquence, le succès de nidification des oiseaux (comme certaines espèces d'oies, de canards et de limicoles) fluctue de concert avec l'abondance des lemmings (Sittler et al., 2000; Bêty et al., 2002; McKinnon et al., 2014). Bien que ce phénomène soit connu depuis longtemps (Underhill et al., 1993; Summers et al., 1998; Nolet et al., 2013; McKinnon et al., 2014), les mécanismes sous-jacents demeurent mal compris.

Les communautés terrestres arctiques peuvent bénéficier d'un apport important de subsides allochtones telles que des carcasses de mammifères marins ou la présence de colonies d'oiseaux migrateurs (e.g. oies, fulmars, guillemots, eiders). Bien que les renards dépendent principalement des lemmings pour se reproduire, l'utilisation de ces subsides peut permettre aux renards d'atteindre des niveaux d'abondance supérieurs que ceux prédits par la productivité primaire de l'écosystème (Gauthier et al., 2004; Samelius et al., 2011; Giroux et al., 2012). Le renard démontre une forte réponse numérique à la fois démographique, à travers la reproduction, et agrégative à ces subsides (Roth, 2003; Giroux et al., 2012; McKinnon et al., 2013; Pivovaroff et al., 2017). La présence de colonies d'oies a le potentiel d'influencer la dynamique de populations des autres espèces nichant en Arctique par le biais d'interactions trophiques indirectes. Il a notamment été démontré que la probabilité d'occurrence de pluviers bronzés (*Pluvialis dominica*) nicheurs augmente avec la distance à la colonie d'oies sur l'île Bylot, au Nunavut (Lamarre et al., 2017). De même, l'exclusion locale du bécasseau semipalmé (*Calidris pusilla*) à La Pérouse, au Manitoba, a été observée en parallèle avec l'augmentation de la population d'oies des neiges (Jehl, 2007). Les mécanismes proximaux de cette interaction indirecte ne sont toutefois pas connus.

Les changements globaux se manifestent actuellement en Arctique par le biais d'une augmentation marquée des populations d'oies (Fox et al., 2005; Alisauskas et al., 2011), l'affaissement des cycles de lemmings (Ims et al., 2008) et des déclins marqués chez plusieurs espèces d'oiseaux de rivage (Baker et al., 2004; Deinet et al., 2015). L'augmentation des populations d'oies et des bernaches a été documentée notamment chez l'oie à bec court (*Anser brachyrhynchus*; Fox et al. 2005), la bernache cravant (*Branta bernicla*; Nolet et al. 2013), la petite et la grande oie des neiges (*Chen caerulescens*; Alisauskas et al. 2011; Lefebvre et al. 2017). Cette augmentation est attribuée à l'intensification de l'agriculture sur les aires d'hivernage et les haltes migratoires (Jefferies et al., 2004).

Figure 1.3. Renard Arctique (**A,D**), couple d'oies des neiges (**B**), bécasseau de Baid (**C**), interaction entre des oies des neiges et un renard en quête alimentaire (**E**) et lemming variable (**F**). Images prises sur le site d'étude de l'île Bylot, par Andréanne Beardsell.

Les limicoles représentent environ 30% de la biodiversité aviaire Arctique avec 59 espèces nichant dans la toundra (CAFF,2013). Plusieurs espèces ont subi des déclins marqués dans les dernières décennies (Deinet et al., 2015; Studds et al., 2017). C'est le cas notamment du bécasseau maubèche (Baker et al., 2004; Studds et al., 2017) et du bécasseau semipalmé (Jehl, 2007). Les causes responsables de ces déclins sont probablement multiples incluant notamment la perte d'habitat et les changements climatiques (CAFF,2013). L'impact de la prédation sur la dynamique des populations de limicoles nichant en Arctique n'a jamais été quantifié et pourrait être l'un des mécanismes contribuant au déclin des limicoles.

1.4 Objectifs de la thèse

Les objectifs généraux de cette thèse sont d'améliorer notre capacité à quantifier la force des interactions trophiques indirectes et d'examiner les mécanismes qui modulent la force de ces interactions dans les communautés naturelles. Ces objectifs généraux sont divisés en trois parties. Dans la première partie, je dérive un modèle mécanistique de la réponse fonctionnelle du prédateur à quatre de ses proies (lemmings, oies des neiges, bécasseaux et passereaux). Ce modèle servira de fondation à l'entièreté de la thèse. Dans la deuxième partie de ma thèse, j'examine les mécanismes potentiels pouvant expliquer l'interaction indirecte positive entre des proies de la toundra arctique (les lemmings, les bécasseaux et les passereaux). Dans la dernière partie, j'évalue si la présence d'une proie (l'oie des neiges) peut mener à l'exclusion locale d'une autre proie (les bécasseaux) via des interactions trophiques indirectes. En combinant une approche théorique et empirique, cette thèse aborde les interactions prédateurs-proies et leurs impacts indirects potentiels sur des espèces aviaires nichant dans la toundra arctique. L'ensemble des modèles présentés dans cette thèse ont été développés à partir de connaissances acquises d'une communauté de vertébrés de la toundra arctique.

1.5 Présentation du système d'étude

Les communautés terrestres arctiques offrent un contexte propice à l'étude des interactions de par la simplicité relative du réseau trophique et la capacité à observer directement les interactions prédateurs-proies. Pour développer les modèles mécanistiques de la prédation, j'ai eu l'opportunité d'utiliser un jeu de données exceptionnel et unique en écologie terrestre, soit le suivi écosystémique à long terme de l'île Bylot (Nunavut) où plus de 20 espèces de vertébrés (incluant le renard arctique, les lemmings, les oiseaux) sont suivies finement depuis plus de 25 ans, ce qui en fait l'une des communautés terrestres arctiques les plus étudiée au monde (Gauthier et al., 2013).

La zone d'étude ($\sim 500\,km^2$) comprend une colonie de grandes oies des neiges (*Anser caerulescens atlanticus*) de $\sim$ 20 000 couples, qui est concentrée dans une zone de 50-70 km^2 (McKinnon et al., 2014). L'emplacement du centre de la colonie d'oies est relativement stable au fil des années (Duchesne et al., 2021). Deux espèces cycliques de petits mammifères sont présentes : le lemming brun (*Lemmus trimucronatus*) et le lemming variable (*Dicrostonyx groenlandicus*) (Gauthier et al., 2013). Les espèces de bécasseaux qui nichent dans la zone d'étude incluent le bécasseau de Baird (*Calidris bairdii*) et à croupion blanc (*Calidris fuscicollis*). Le renard arctique est le principal prédateur commun aux lemmings et aux oiseaux nichant au sol (Bêty et al., 2002; McKinnon and Bêty, 2009). Dans la zone d'étude, les renards arctiques utilisent le même domaine vital pendant l'été faisant en moyenne 10 km^2 (Grenier-Potvin et al., 2021), et le degré de chevauchement est généralement faible dans la population étudiée (Clermont et al., 2021*b*). Comme plusieurs autres espèces (Oksanen et al., 1985), le renard arctique cache une grande proportion de la nourriture acquise pour consommation future (Careau et al., 2008). En présence d'une colonie d'oiseaux, entre 40 et 97% des oeufs acquis sont cachés (Stickney, 1991; Samelius and Alisauskas, 2000; Careau et al., 2008).

Les modèles ont été développés et évalués principalement à l'aide d'expériences sur le terrain

(à l'aide de nids artificiels), de données GPS précises et d'accéléromètrie de renards arctiques (depuis 2018), d'observations directes de renards en quête de nourriture (1996-2019) et de suivis de nids naturels et de la densité des lemmings (par capture-marquage-recapture).

CHAPITRE 2

Construction d'un modèle mécanistique de la réponse fonctionnelle d'un prédateur

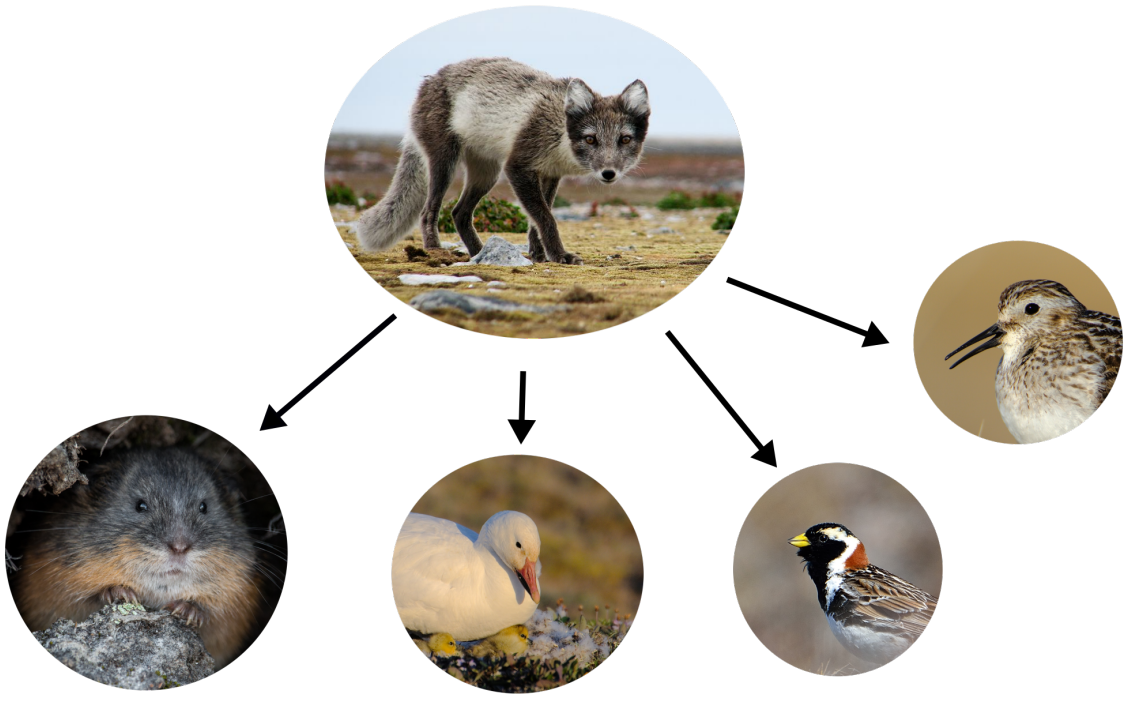

2.1 Contexte scientifique et publication associée

Cet article, intitulé « Derivation of predator functional responses using a mechanistic approach in a natural system » a été publié dans la revue *Frontiers in Ecology and Evolution* en 2021 dans le cadre d'un numéro spécial rassemblant des articles portant sur la réponse fonctionnelle (*New Perspectives and Emerging Directions in Predator-Prey Functional Response Research: Hommage to C.S. Holling (1930-2019)*). Cet article propose une méthode innovante pour quantifier la force des interactions prédateurs-proies et servira de fondation pour identifier les moteurs proximaux des interactions prédateurs-proies dans les communautés naturelles. En tant que première autrice, ma contribution à ce travail représente la revue de littérature, l'écriture du modèle mécanistique, la réalisation des simulations, la synthèse des données, la récolte d'une partie des données sur le terrain en 2019 et finalement la rédaction de l'article. Dominique Gravel, mon cosuperviseur de recherche, a contribué à de nombreuses réflexions sur le projet et au développement du modèle mécanistique. Dominique Berteaux, Joël Bêty et Gilles Gauthier ont contribué à la coordination du suivi à long terme de l'île Bylot et à la collecte de données. Jeanne Clermont a contribué à la récolte des données et à l'analyse de ces dernières, principalement en lien avec les données de mouvement des renards. Vincent Careau, Nicolas Lecomte et Claire-Cécile Juhasz ont grandement contribué à la récolte des données, particulièrement par les observations comportementales détaillées des renards. Pascal Royer-Boutin a contribué à la récolte, à la synthèse et à l'analyse des données du suivi à long terme de la nidification des oiseaux. Joël Bêty, mon superviseur de recherche, m'a épaulée et guidée tout au long du projet. Nous avons construit le modèle conjointement. Il a aussi grandement contribué à la révision de l'article. Finalement, l'ensemble des auteurs et autrices ont contribué à réviser l'article. Une version abrégée de cet article a été présentée sous forme d'une'affiche lors de la *Gordon Research Conference on Predator-Prey Interactions*, à Ventura (Californie, USA) en janvier 2020.

Les sections suivantes sont celles de l'article publié.

2.2 Title

Derivation of predator functional responses using a mechanistic approach in a natural system

2.3 Authors

Andréanne Beardsell, Dominique Gravel, Dominique Berteaux, Gilles Gauthier, Jeanne Clermont, Vincent Careau, Nicolas Lecomte, Claire-Cécile Juhasz, Pascal Royer-Boutin & Joël Bêty

2.4 Traduction du résumé de l'article publié

La réponse fonctionnelle est au cœur des interactions prédateur-proie en faisant le lien entre les niveaux trophiques. L'utilisation d'une réponse fonctionnelle innapropriée peut affecter profondément les résultats des modèles de population et de communauté. Pourtant, la plupart des réponses fonctionnelles sont évaluées à l'aide de modèles phénoménologiques qui, souvent, ne parviennent pas à distinguer les différentes formes de réponses fonctionnelles et ne peuvent pas identifier les mécanismes proximaux qui régulent les taux d'acquisition des prédateurs. En utilisant une combinaison de données comportementales, démographiques et expérimentales recueillies pendant 20 ans, nous développons un modèle mécanistique basé sur les traits et le comportement des espèces pour évaluer la réponse fonctionnelle d'un prédateur généraliste, le renard arctique (*Vulpes lagopus*), à diverses proies de la toundra (lemmings et nids d'oies, passereaux et bécasseaux). Les taux d'acquisition du renard à ses proies, dérivés à partir du modèle mécanistique, étaient cohérents avec les observations empiriques. Bien que les taux d'acquisition du renard diminuent légèrement lorsque les densités de nids d'oies et de lemmings sont élevées, aucune de nos simulations n'a donné lieu à une saturation du taux d'acquisition du prédateur pour toutes les espèces de proies. Nos résultats soulignent l'importance des composantes de la recherche du prédateur dans les interactions

prédateur-proie, en particulier la vitesse du prédateur, alors que les taux d'acquisition du prédateur n'étaient pas limités par les processus de manipulation. En combinant la théorie et les observations empiriques, cette étude souligne que le taux d'acquisition des prédateurs n'est pas systématiquement limité aux plus fortes densités de proies observées dans un système naturel. Cette étude illustre également comment des modèles mécanistiques peuvent générer des formes de réponses fonctionnelles spécifiques à la gamme de densités de proies observées dans la nature. De tels modèles sont nécessaires pour identifier les moteurs proximaux des interactions prédateur-proie et pour améliorer notre compréhension des interactions médiées par les prédateurs dans les communautés naturelles.

2.5 Abstract

The functional response is at the core of any predator-prey interactions as it establishes the link between trophic levels. The use of inaccurate functional response can profoundly affect the outcomes of population and community models. Yet most functional responses are evaluated using phenomenological models which often fail to discriminate among functional response shapes and cannot identify the proximate mechanisms regulating predator acquisition rates. Using a combination of behavioral, demographic and experimental data collected over 20 years, we develop a mechanistic model based on species traits and behavior to assess the functional response of a generalist mammalian predator, the arctic fox (*Vulpes lagopus*), to various tundra prey species (lemmings and the nests of geese, passerines and sandpipers). Predator acquisition rates derived from the mechanistic model were consistent with field observations. Although acquisition rates slightly decrease at high goose nest and lemming densities, none of our simulations resulted in a saturating response in all prey species. Our results highlight the importance of predator searching components in predator-prey interactions, especially predator speed, while predator acquisition rates were not limited by handling processes. By combining theory with field observations, our study provides support that the predator acquisition rate is not systematically limited at the highest prey densities observed in a natural system. Our study also illustrates how mechanistic models based on empirical es-

timates of the main components of predation can generate functional response shapes specific to the range of prey densities observed in the wild. Such models are needed to fully untangle proximate drivers of predator-prey population dynamics and to improve our understanding of predator-mediated interactions in natural communities.

Keywords: functional response, predation, trophic interactions, tundra, predator-prey interactions, arctic fox (*Vulpes lagopus*), Arctic

2.6 Introduction

A long-standing problem in ecology is to measure how the acquisition rate of a predator varies with prey availability, namely the functional response. Functional response shapes are typically categorised as linear (type I), hyperbolic (type II) or sigmoidal (type III; Holling 1959*b*,*a*). This classification is commonly used by ecologists when incorporating predation into population and community models (Turchin and Hanski, 1997; Fryxell et al., 2007; Serrouya et al., 2015), and type II is the most widely applied model (Rall et al., 2012). The shape of the functional response can have major consequences on the outcomes of population and community models. For instance, a type III promotes stability or coexistence whereas a type II destabilizes predator-prey dynamics (Murdoch, 1973; Sinclair et al., 1998). Describing the functional response of pairwise trophic interactions is also important to understand higher-order interactions. For instance, the shape of the functional response alone can profoundly change predictions about the outcome of predator-mediated trophic interactions (Abrams et al., 1998; Holt and Bonsall, 2017).

Although functional responses are at the core of predator-prey theory (Solomon, 1949), most empirical research on functional responses has been conducted under controlled laboratory or field enclosure conditions (96%, n = 116 studies, reviewed by Pawar et al. 2012) where prey density is manipulated, predator consumption is recorded, and the functional response models are compared through statistical analysis (referred to as phenomenological models). These approaches are not well suited for predators with relatively large home ranges and

may fail to reproduce foraging conditions encountered in the wild. Determining the shape of functional responses in natural systems is however often limited by a combination of factors, including small sample sizes, a relatively narrow gradient of observed prey densities, the difficulty to observe predator-prey interactions directly, or the difficulty to estimate predator and prey numbers (Gilg et al., 2006; Therrien et al., 2014; Suryawanshi et al., 2017; Ellis et al., 2019). The large variability around predator acquisition rates observed in the wild can also prevent us from discriminating among functional response shapes, and hence limit our ability to to accurately model predator-prey interactions in complex and natural ecosystems (O'Donoghue et al., 1998; Vucetich et al., 2002; Chan et al., 2017). Moreover, phenomenological models fail to identify the proximate mechanisms regulating predator acquisition rates. In this context, a mechanistically grounded approach to derive functional response is appealing.

Derivation of functional responses based on measurable features of species behavior (e.g. speed, attack and success probability) provides several advantages. Compared with phenomenological models, mechanistic models 1) allow assessing the shape of the functional response based on behavioral attributes of the predator, 2) are based on parameters with a direct biological interpretation, and hence have the potential to reinforce links between theory and data (Connolly et al., 2017). The number of mechanistic models of predator-prey interactions is growing, and most of them aim to predict trophic links based on species traits, especially body size (Gravel et al., 2013; Portalier et al., 2019; Ho et al., 2019). Mechanistic models of functional response further allow the integration of predator-prey pairs to describe trophic links, which can improve our ability to model complex ecological interactions. Despite their utility, mechanistic models based on the main components of predation in a natural system are, to our knowledge, virtually non-existent in vertebrate predators.

Using a combination of behavioral, demographic and experimental data collected over 20 years in a natural system, we develop a mechanistic model to assess the functional response of a generalist mammalian predator to various prey species (4 predator-prey pairs). The originality of our approach is to assess functional response i) by breaking down the components of predation (searching, chasing, capturing, and handling prey) and ii) by using field experiments and detailed behavioral observations to parameterize each component included in the mech-

anistic model. We focused on the derivation of functional response of predator-prey pairs. We evaluated the coherence of our models using data from a long-term field study that estimated prey densities and predator acquisition rates. We also performed sensitivity analyses to identify the main proximate drivers of change in predator acquisition rates. Finally, we modeled the potential effects of density dependence in components of predation on the shape of the functional responses within the range of prey densities observed in the field.

The mechanistic model was developed for the arctic fox (*Vulpes lagopus*), a generalist predator of the tundra ecosystem, using highly detailed empirical observations from a long-term ecological monitoring program in the Arctic (Gauthier et al., 2013). This system offers several benefits to study predator-prey interactions among vertebrates, including a relatively simple food web, an open landscape and the continuous summer daylight allowing direct behavioral observations. The arctic fox is an active hunting predator that travels extensive daily distances within its territory in summer (Poulin et al., 2021). Lemmings and birds (mostly eggs and juveniles) are the main components of the summer diet of arctic foxes in most tundra ecosystems (Angerbjörn et al., 1999; Giroux et al., 2012). Lemmings exhibit population cycles with peak density every 3-5 years (Fauteux et al., 2015), and the arctic fox predation pressure on tundra ground-nesting birds is typically released at high lemming density (Summers et al., 1998; Bêty et al., 2002; McKinnon et al., 2014). Surprisingly, the exact mechanisms driving this well-known short-term apparent mutualism between lemmings and birds are still unclear, but they likely involve fox functional responses (Summers et al., 1998; Bêty et al., 2002).

A few studies attempted to quantify the functional responses of arctic fox using phenomenological models (Angerbjörn et al., 1999; Eide et al., 2005; Gilg et al., 2006). Relatively low sample sizes reduced the ability of previous studies to fully distinguish between different shapes of functional responses. Moreover, the hoarding behavior of arctic foxes was not considered in previous estimations of functional responses (Angerbjörn et al., 1999; Eide et al., 2005; Gilg et al., 2006). Like many other animals (Vander Wall, 1990), arctic foxes can predate more prey than they consume on the short-term, and such behavior can strongly increase prey acquisition rates, e.g. foxes foraging in goose colonies can hoard between 40% and 97% of eggs acquired during the bird nesting period (Samelius and Alisauskas, 2000; Careau et al., 2008).

Although type III functional responses were previously used to model fox-prey population dynamics (Gilg et al., 2003, 2009), food hoarding may substantially reduce handling time and could therefore make the shape of the functional response linear or slightly convex (Oksanen et al., 1985).

2.7 Methods

2.7.1. Study system

During the summer, the southwest plain of Bylot Island, Nunavut, Canada (73° N; 80° W) harbors a large greater snow goose colony (*Anser caerulescens atlanticus*; ∼20,000 pairs). Insectivorous migratory birds are also nesting in the study area and include the lapland longspur (*Calcarius lapponicus*), a passerine, and several species of shorebirds (primarily *Calidris* spp. and *Pluvialis* spp.). Two species of small mammals are present, the brown (*Lemmus trimucronatus*) and collared (*Dicrostonyx groenlandicus*) lemmings. The brown lemming has high-amplitude cycles of abundance with a 3–5-year periodicity, whereas the collared has low-amplitude cycles (Gruyer et al., 2008). The mammalian predator guild is dominated by the arctic fox and the ermine (*Mustela erminea*). The arctic fox is the main nest predator of geese (Bêty et al., 2002; Lecomte et al., 2008), sandpipers (McKinnon and Bêty, 2009; Royer-Boutin, 2015) and passerines (Royer-Boutin, 2015). Additional details on plant communities and general landscape can be found in Gauthier et al. (2013).

The model was parametrized and evaluated using data from Bylot Island, where foxes and their prey have been monitored since 1993. We observed foraging foxes using binoculars and spotting scopes (20 x 60x) from one or two blinds located in the middle of the goose colony during 10 summers between 1996 and 2019.

2.7.2. Mechanistic model of functional responses

We used the Holling disk equation as a starting point to build the mechanistic model of functional response (Holling, 1959*a*) inspired by the general formalism of Pawar et al. (2012). Predation was broken down into four different components, which are searching, chasing, capturing, and handling of a prey item by a predator. Acquisition rate of a prey item (species i) by a predator ($f(i)$), namely the functional response, takes the following form:

$$f(i) = \frac{\alpha_i N_i}{1 + \alpha_i h_i N_i} \tag{2.1}$$

where α_i is the capture efficiency (km^2/h), N_i the prey density (number of i/km^2), and h_i the handling time of prey (h/i). Capture efficiency is obtained by the product of predator speed (s; km/h), reaction distance (d_i; km), detection (z_i) and attack probability (k_i) of the prey by the predator, and the success probability (p_i) of an attack (table 2.1):

$$\alpha_i = s(2d_i)z_i k_i p_i \tag{2.2}$$

The combination of the time spent chasing the prey once encountered ($\frac{T_{ci}}{p_i}$) and the time spent manipulating the prey once subdued (T_{mi}) define an overall prey handling time (h_i):

$$h_i = \frac{T_c i}{p_i} + T_m i \tag{2.3}$$

The time spent manipulating includes the time spent eating or hoarding the prey item.

α_i depends only on prey density, and we assumed that prey are randomly distributed. Satiety was not considered as a potential mechanism limiting acquisition rate. Indeed, foxes can predate more prey than they consume on the short-term; e.g. about 4% (n = 128) and 48% (n = 98) of predated eggs and lemmings are immediately eaten, respectively (Careau et al., 2007). Predator interference was not incorporated in the model as foxes rarely encounter and interact with other individuals while foraging within their summer territory (49 interactions,

which represents 0.9% of the time over 118 hours of direct observations of foxes foraging in the study area). The full model derivation is provided in supplementary material section 1.1.

The general model of functional response (Eq. 2.1) allows for a continuum between a linear (type 1) and a concave (type 2) functional response shape as a linear response can be elicited when handling time is negligible. In order to allow the mechanistic model to extend to a sigmoidal shape (type 3), we added density dependence in capture efficiency components that were expected to vary with prey density (i.e. reaction distance and detection and attack probabilities; see below).

Tableau 2.1. Definition of the parameters used in the functional response model.

Parameter name	**Symbol**	**Description**	**Unit**
Predator speed	s	Average speed at which the predator moves across the landscape (i.e. linear distance between successive locations). Implicitly, this parameter defines the time allocated to foraging.	km/h
Reaction distance	d	Maximum distance at which the predator and prey can detect or react to each other (in 2D, detection region = $2d$; Pawar et al. 2012).	km
Detection probability	z	Detection probability of the prey within d.	-
Attack probability	k	Attack probability, within d, once the prey is detected by the predator.	-
Chasing time	T_c	Average chase time per prey attacked. This parameter includes the duration of successful and unsuccessful chases.	h/i
Success probability	p	Success probability of an attack.	-
Complete predation probability	P_c	Complete predation probability of a nest.	-
Manipulation time	T_m	Average manipulation time per prey captured. This parameter includes the time spent eating or hoarding the prey item.	h/i
Nest attendance probability	w	Probability that a nest is attended by an incubating female.	-

2.7.3. Prey specific functional responses

We adapted the general model (eq. 2.1) to each prey species based on their traits and anti-predator behavior (figure 2.1). The specific models for each prey species are provided in table S2.

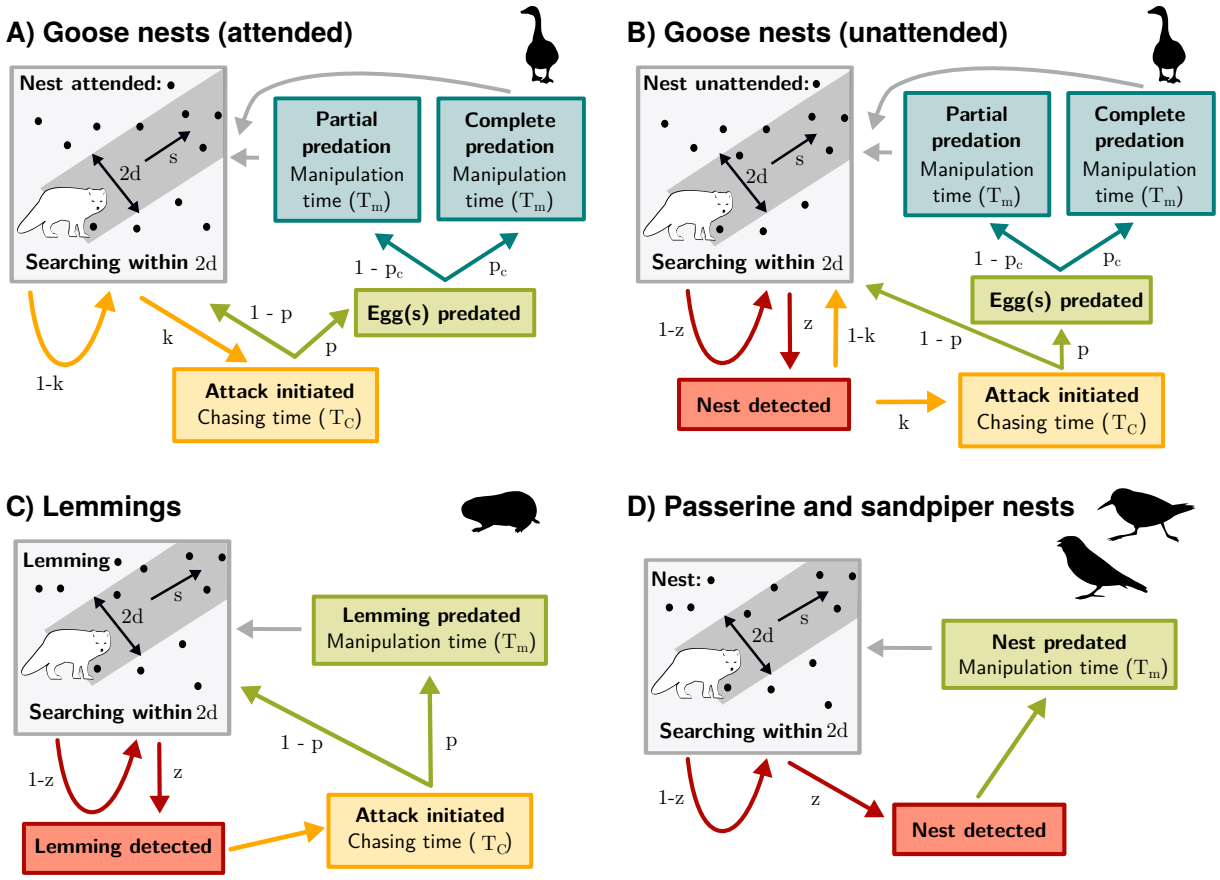

Figure 2.1. Conceptual mechanistic model of functional response of arctic fox to each prey species: attended (**A**) or unattended (**B**) goose nests, lemmings (**C**), and passerine and sandpiper nests (**D**). Predation was divided into four main components: search, detect, attack and handle (which includes eating and hoarding). Arrows illustrate the probability that the predator reaches the next component. When there is no parameter indicated beside the arrow, the probability is 1. Parameters are as follows : d is the reaction distance, s the predator speed, z the detection probability, k the attack probability, p the success probability, P_c the probability of complete nest predation, T_C the time spent chasing, and T_m the time spent manipulating the prey.

For goose nests, the first modification was to add a component for complete and partial nest

predation. This modification was necessary since a successful attack by the predator does not always result in complete clutch predation (Bêty et al., 2002), which can affect manipulation time and, ultimately, acquisition rates. The second modification was to split the general model into two components. A first component models acquisition rate of goose nests when the female is incubating or when one protecting adult is at $<$10 m from the nest (attended nest; figure 2.1A). A second component models acquisition rate of goose nests during incubation recesses when both adults are at $>$10 m from the nest (unattended nest; figure 2.1B). As geese can actively protect their nests against arctic foxes, their presence at the nest strongly influences fox foraging behavior (Samelius and Alisauskas, 2001; Bêty et al., 2002). This antipredator behavior translates into changes in capture efficiency components. Thus, parameter values of capture rates were estimated separately for goose nests that were attended or unattended (table S1). When a nest is attended by a highly conspicuous snow goose, we assumed that nest detection probability is 1 within d (figure 2.1A). For unattended nests, we used a detection probability function obtained from an artificial nests experiment (figure S1). Sometimes, unattended nests can be protected if parents detect a fox during an incubation recess and return quickly to their nest. Like attended nests, we thus estimated success probability (p) and complete clutch predation probability (P_c) for unattended nests (figure 2.1B). The third and last modification was to introduce the nest attendance probability (w). We estimated this parameter by combining information on the average time spent on the nest by females and on the average distance between females and their nest during the goose incubation period (Reed et al. 1995; Poussart et al. 2000; see supplementary material section 1.2).

The general model (eq. 2.1) was simplified for lemmings as we assumed that an attack is systematically initiated by the fox once a lemming is detected within d (figure 2.1C). Sandpipers and passerines exhibit a variety of antipredator behaviors (such as distraction displays) to avoid nest detection by the predator (Smith and Edwards, 2018). However, sandpipers and passerines cannot protect their nest once detected by a fox. Thus, we assumed that once a nest is detected, it is always predated (attack probability is 1 and no chasing time is included in the model; figure 2.1D).

We incorporated density dependence into the goose and the lemming models within the range

of densities observed in our study system. For each parameter in which density dependence was incorporated, the minimum and the maximum parameter values were associated respectively with the minimum and the maximum prey density to calculate the slope and the intercept of the density-dependence relationship. In the goose model, we modified attack and success probabilities for attended nests, and reaction distance and detection probability for unattended nests. In the lemming model, we added density dependence in reaction distance, detection and success probabilities. The rationale behind these additions is that predators may form search images for abundant prey, which can increase their ability to detect them (Nams, 1997; Ishii and Shimada, 2010). As predators could also increase their attack rate and success as prey density increases, we added density dependence in attack and success probabilities. We did not incorporate density dependence into the passerine and sandpiper nest models as the range of nest densities observed in our study system is likely too low to influence fox behavior (maximum of 12 nests/km^2 compared to a maximum of 926 goose nests and 414 lemmings per km^2). See supplementary material section 1.3 for more details on the incorporation of density dependence.

The model was implemented in R v. 3.6.0.

2.7.4. Parameter values

The model was parameterized mostly using data from Bylot Island but also from the literature when data were missing. Parameters were derived from field experiments using artificial nests or estimated using arctic fox GPS tracking data and direct observations of foraging foxes (table S1). See supplementary material section 1.2 for a detailed description of the method used to extract each parameter.

2.7.5. Evaluating the coherence between the mechanistic model and empirical predator acquisition rates

Predator acquisition rates at different prey densities were assessed in the field annually using two independent methods. These data did not allow validation of the shape of the functional responses, but they provided a way to evaluate the performance of the mechanistic model in estimating prey acquisition rates at the various prey densities observed in our study system.

First, we obtained goose eggs and lemming acquisition rates by conducting direct observations of foraging foxes for 10 summers between 1996 and 2019 during the goose incubation period (details on behavorial observations can be found in Bêty et al. (2002) and Careau et al. (2008)). For each year, the acquisition rate was calculated as the total number of prey acquired (goose eggs or lemmings) divided by the total length of the observation bouts of individual foxes. The acquisition rate of a clutch of eggs was estimated by dividing the acquisition rate of goose eggs by the annual average clutch size. For the years where information was available, we also calculated the acquisition rate for attended and unattended nests. We estimated annual goose nest density either by visual counts of the nests located in the observation zone (range: 0.5-3 km^2) during the incubation period (1996-1999, 2019) or over a fixed 0.2 km^2 plot within the intensively monitored core area of the goose colony (2004-2005, 2015-2016). We estimated lemming density annually with snap traps from 1994 to 2009 and with live traps from 2004 to 2019 (see Fauteux et al. 2018 for methods). We summed the density estimate of brown and collared lemming.

Second, we obtained passerine and sandpiper nest acquisition rates by monitoring annually (2005 to 2013) the fate of passerine and sandpiper nests (Gauthier et al., 2013; McKinnon et al., 2014). Nest density was estimated as the number of passerine and sandpiper nests found in a 8 km^2 plot systematically searched throughout the breeding season. We estimated acquisition rate of nest content (eggs or chicks) by using the daily survival rate of nests (dsr), the total number of nests found in the study plot (N_{tot}), the number of foxes foraging in the plot (N_{fox}) and the proportion of nests predated by foxes (P_{fox}). Since foxes establish territorial pairs on Bylot (Rioux et al., 2017), we assumed that 2 foxes were foraging in the study plot. We

also considered that foxes were responsible for 100% (n = 19) and 81% (n = 25) of the failed sandpiper and passerine nests, respectively, as indicated by camera monitoring (McKinnon and Bêty, 2009; Royer-Boutin, 2015). An estimation of the acquisition rate is obtained by:

The daily nest survival rate was modeled using the logistic exposure method (Shaffer, 2004). Additional details on daily nest survival rate calculations and nest monitoring methods can be found in Royer-Boutin (2015). Density estimates for all prey species were standardized as the number of nests per km^2.

2.7.6. Uncertainty and sensitivity analysis

We quantified how uncertainty in parameter values affected estimation of predator acquisition rates by using the Latin hypercube sampling technique (an efficient implementation of the Monte Carlo methods; Marino et al. 2008). This analysis allowed us to investigate the uncertainty in the model output generated by the uncertainty in parameter inputs. Each parameter was represented by a probability distribution (uniform or normal truncated) based on the distribution of empirical data (table S1). For some parameters, the biological information was limited, so we assigned a uniform distribution allowing for a large range bounded by minimum and maximum values. Latin hypercube sampling was then applied to each distribution (N = 1000 iterations). This method involved dividing a probability distribution into N equal probability intervals that were then sampled without replacement, resulting in N iterations of the model using each combination of parameters values. This method allowed us to explore the entire range of each parameter and most of them encompass various environmental conditions (e.g. weather conditions, prey availability). We computed the median, the 90th, 95th and 99th percentiles of the model output by using the empirical cumulative distribution.

We also conducted a local sensitivity analysis to identify key parameters of the mechanistic models within the range of prey densities observed in our study system. We modified each parameter value by $\pm$ 100% while holding others constant, and we assessed how this variation affected the predator acquisition rate (expressed as % of change).

2.8 Results

From 1996 to 2019, we observed foraging foxes in the goose colony for 124 hours. Average goose nest density was 409 nests/km^2 (range: 100-926 nests/km^2) and lemming density was 193 ind./km^2 (range: 11-414 ind./km^2; table S3). Based on direct observations of foraging foxes, average acquisition rates were 0.61 nest/fox/h (range: 0.19-1.82 nest/fox/h) for goose nests and 0.94 ind./fox/h (range: 0-2.85 ind./fox/h) for lemmings (table S3). The majority of eggs acquired (67%) were from unattended goose nests, while 33% were from attended nests (n = 218). Average passerine nest density was 7.7 nests/km^2 (range: 6.1-12.3 nests/km^2), and sandpiper density was 2.5 nests/km^2 (range: 1.0-5.9 nests/km^2; table S4). Based on nest monitoring, average acquisition rates were 0.10 nest/fox/h (range: 0.03-0.28 nest/fox/h) and 0.04 nest/fox/h (range: 0.002-0.169 nest/fox/h) for passerine and sandpiper nests, respectively (table S4).

The uncertainty analysis revealed that varying simultaneously all parameters used in the mechanistic model generated considerable variation in fox acquisition rates (figure 2.2). Nonetheless, no parameter combinations resulted in a saturating functional response for all prey species within the range of prey densities observed in our study system: the acquisition rate at maximal prey density was below the saturation point in all simulations (see histograms in figure 2.2 and figure S5). Based on the value of the parameters estimated within the observed prey densities, acquisition rate at saturation was 8 nests/fox/h for goose nests, 17 ind./fox/h for lemmings, 166 nests/fox/h for passerine and 26 nests/fox/h sandpiper nests. Depending on the prey species, most or all fox acquisition rates observed in the field fell within the 99th percentile of the values derived from the mechanistic models (figure 2.2). The highest acquisition rates observed in the field were also much below the estimated saturation point in all prey species (figure 2.2). As the goose nest model was split for attended and unattended goose nests, we also computed acquisition rates separately for each of these situations. Goose nest acquisition rate derived from the mechanistic model was higher for unattended nests than attended nests, which is consistent with empirical estimations (figure S6). Although most (66%) field estimates of acquisition rates fell within the 95th percentiles of the model output

for unattented goose nests, all values were under the model median at nest densities above 200 nests/km^2 (figure S6). This may indicate a slight overestimation of the proportion of unattended nests at relatively high densities.

Sensitivity analyses indicated that predator speed was an influential parameter of the functional response of all prey species (figure 2.3). Goose nest acquisition rate was generally more affected by parameters associated with unattended nests than attended nests (figure 2.3A). The magnitude of change in goose nest acquisition rate related to the changes in manipulation time increased slightly with nest density. Lemming acquisition rate was not affected by chasing and manipulation time, whereas detection distance, and detection and success probability had an influence equivalent to predator speed (figure 2.3B). Similarly, functional response models of passerine and sandpiper nests were not sensitive to change in manipulation time, whereas detection distance and detection probability had an influence equivalent to predator speed (figure 2.3C).

Adding density dependence into the goose and the lemming models had relatively minor effects on acquisition rates derived for low to moderate densities observed in our study system. The shape of the functional response changed slightly between models without or with density dependence in capture efficiency components (allowing for a gradient between type I and type III). At high densities, acquisition rates remained much below saturation points, and a maximum difference of 1.4 nests/fox/h at 1000 goose nests/km^2 and 2.1 lemmings/fox/h at 450 lemmings/km^2 were found between models (figure 2.4).

2.9 Discussion

Benefiting from a combination of behavioral, demographic and experimental data collected over the past 20 years, we developed a mechanistic model of arctic fox functional response to four prey species. Our model derives the shape of the functional response of each predator-prey pair along a gradient from linear to sigmoidal. Predator acquisition rates derived from the mechanistic model were consistent with field observations, and the main proximate mech-

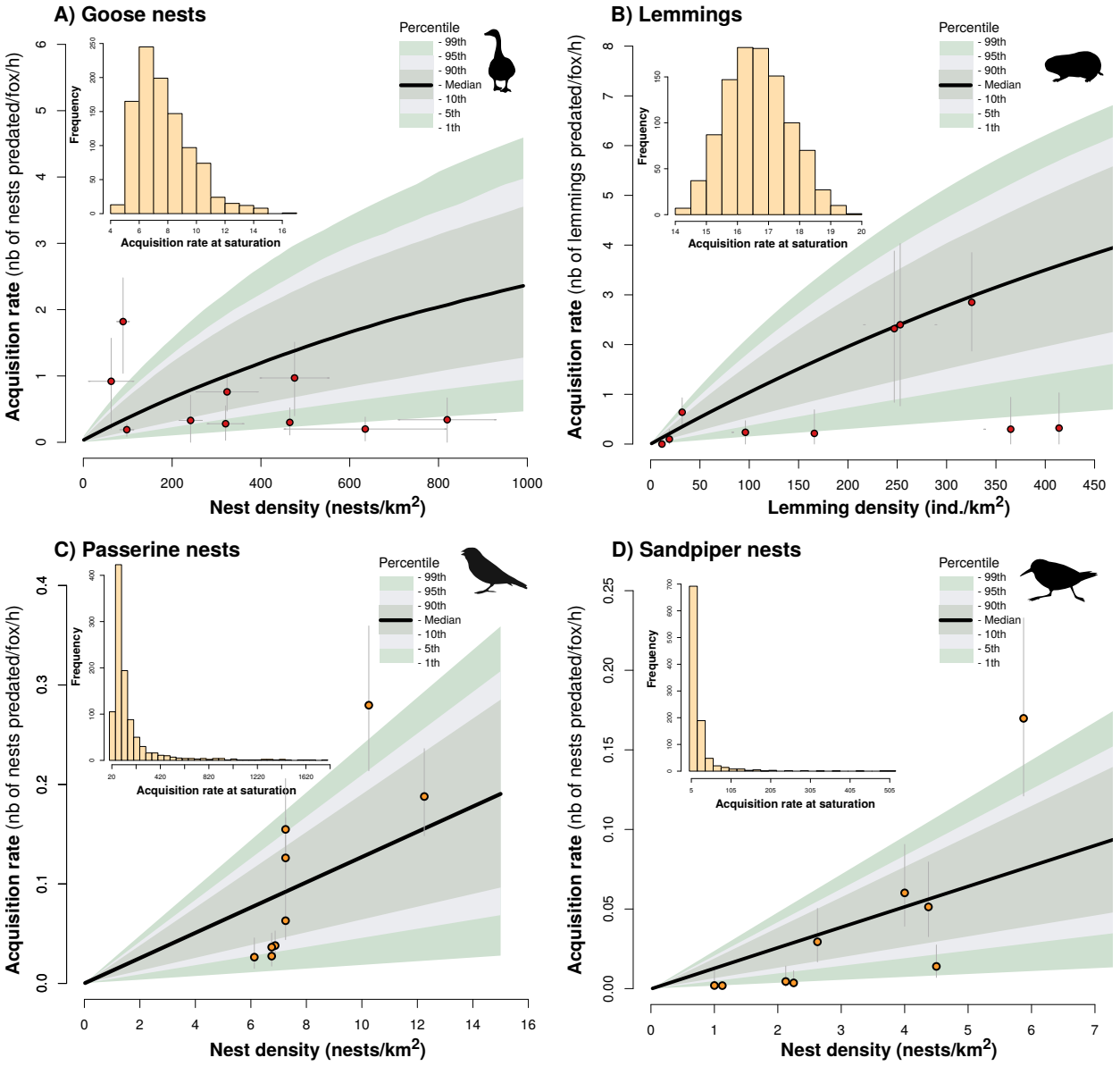

Figure 2.2. Functional response of arctic fox to density of goose nests (**A**), lemmings (**B**), passerine nests (**C**), and sandpiper nests (**D**). Black lines represent the median of the mechanistic model and the color bands represent the 90th, 95th, and 99th percentiles based on 1000 simulations. Empirical data are represented by red and yellow dots respectively. Histograms in the inset show the distributions of acquisition rate at saturation for each simulation. Horizontal error bars in (**A**) indicate the range of nest density during the incubation period. Vertical errors bars in (**A**) and (**B**) represent standard errors calculated using bootstrapping. Errors bars in (**C**) and (**D**) represent 95% confidence intervals from daily survival rate estimates.

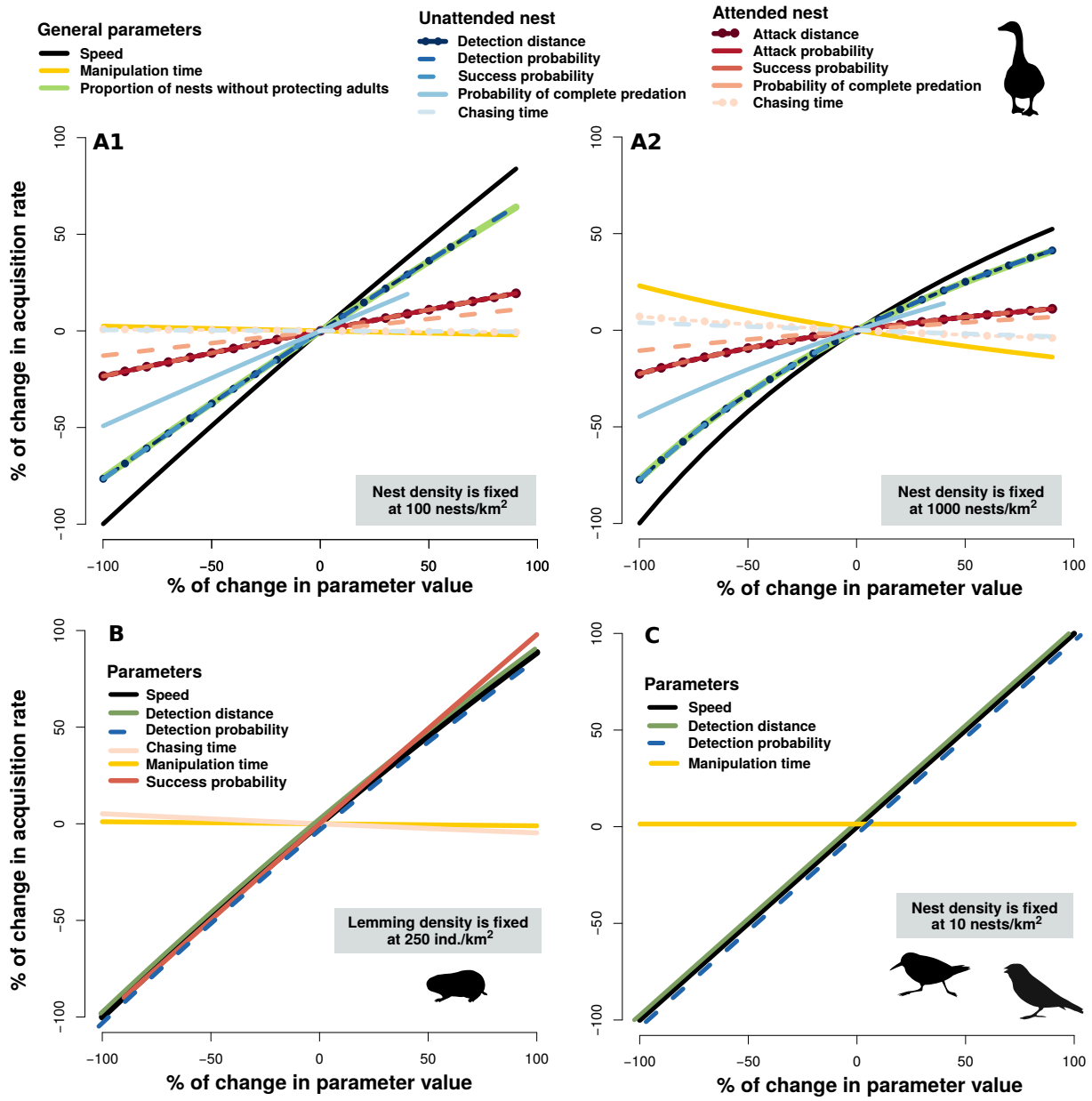

Figure 2.3. Sensitivity of predator acquisition rates to changes in parameter values of the mechanistic models used to assess the functional response of arctic fox to goose nests (at 100 (**A1**), and 1000 nests/km^2 (**A2**)), to lemmings at 250 ind./km^2 (**B**) and to passerine and sandpiper nests at 10 nests/km^2 (**C**). Sensitivity analyses are presented at intermediate densities for lemmings and passerine and sandpiper nests, since the results were very similar within the range of densities observed in our study system.

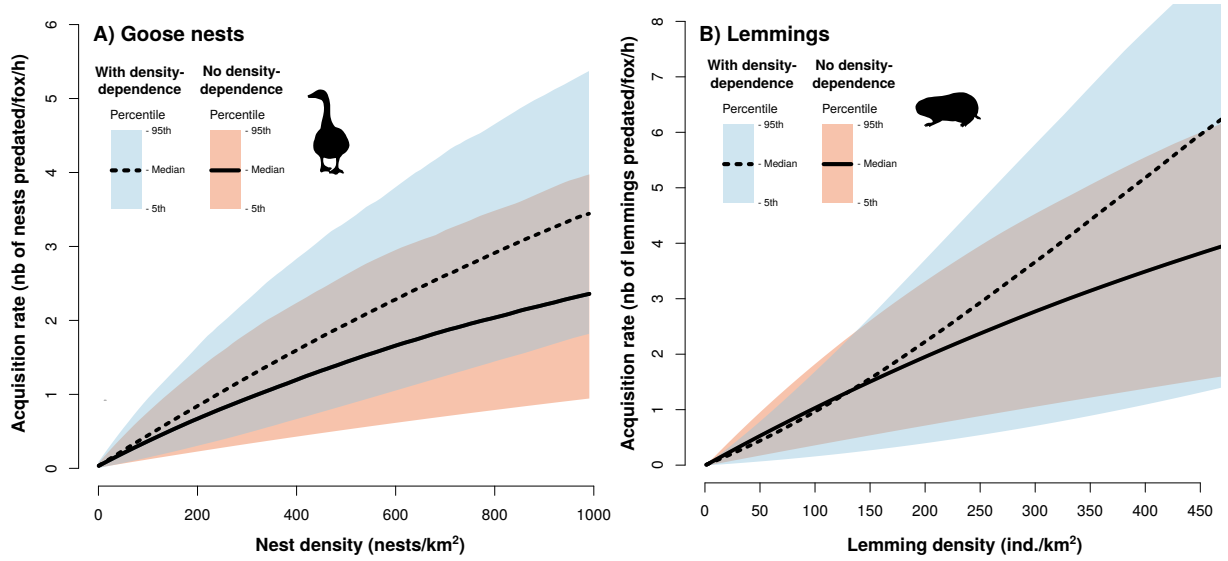

Figure 2.4. Functional response models of arctic fox to goose nests (**A**) and lemmings (**B**) with and without density dependence on capture efficiency components, within the range of densities observed in the field. Black lines represent the median of the mechanistic model and the color bands represent the 95th percentiles based on 1000 simulations.

anisms driving predator acquisition rates were also identified. In all prey species, predator speed was an influential parameter, while handling time had a limited influence on acquisition rates. Although type III functional responses were previously used to model fox-prey population dynamics (Gilg et al., 2003, 2009), our simulations indicate that predator acquisition rate was not systematically limited at the highest prey densities observed in our study system. Our model allows for a mechanistic interpretation of the functional response of predator-prey pair and could be extended to more complex modules involving multiple predators and prey species.

Our results add to a growing body of research indicating that predators may not become systematically satiated or saturated at the highest densities of prey observed in nature (Novak, 2010; Chan et al., 2017; Preston et al., 2018). Holling's functional response models (type II and III), which are commonly used in population dynamics models (Turchin and Hanski, 1997; Gervasi et al., 2012; Serrouya et al., 2015), predict that predator acquisition rates should eventually saturate at high prey densities. Based on mechanistic models, which allowed us to vary simultaneously all components of predation, we found no evidence of arctic fox saturation at

the highest prey densities observed in a natural system. Several factors may explain this result. First, the hoarding behavior of arctic foxes may substantially reduce handling time by limiting the constraints associated with digestion and satiety, which can make the functional response shape linear or slightly convex even at high prey densities (Oksanen et al., 1985). Second, while predator acquisition rates must theoretically become constrained by handling and/or digestion at high prey densities, the prey densities required to reach a saturation point could be rarely observed in natural systems. Indeed, empirical support for saturating functional response in the wild is relatively rare and comes mostly from controlled laboratory experiments in which the range of prey densities may exceed the range observed in nature (99% of all type II functional response were derived from controlled laboratory experiments (n = 61 studies); reviewed by Rall et al. 2012). Such an issue can be avoided when mechanistic approaches are used to derive functional responses. One particularity of our system is the presence of a large goose colony where prey density can be quite high (up to $\sim$900 nests/km^2). Interestingly, even in this context, we found no evidence of predator saturation.

Historically, a categorical approach was adopted by ecologists to define functional responses. A linear functional response was traditionally attributed to filter feeders (Jeschke et al., 2004), a hyperbolic shape (type II) to invertebrates and a sigmoidal shape (type III) to vertebrate predators (Holling 1965, but see Hassell et al. 1977). Although, this categorization has some heuristic value in introductory texts and can be useful in some aspects of research where categorization is necessary, types I, II, and III should be considered simply as particular cases along a continuum. Instead of using a priori shapes to describe functional responses, our study illustrates how mechanistic models can generate functions linking prey density and predator acquisition rates that are specific, and hence more relevant, to the range of densities observed in a food web. Considering the strong effect of functional responses on the outcome of predator-prey models (Abrams et al., 1998; Sinclair et al., 1998), such specific functions should improve our ability to adequately simulate and quantify the strength of species interactions in natural communities.

We did not incorporate predator dependence in the functional response model, despite a growing body of studies indicating that some mechanisms (e.g. facilitation, interference) are

likely to occur in functional responses (Novak et al., 2017). However, arctic foxes maintained summer territories (averaging 9.6 km^2) with low overlap (A. Grenier-Potvin and D. Berteaux, submitted manuscript), which prevents potential interference within territories. We are thus confident that variation in predator density should not affect our main conclusions. Nonetheless, the mechanistic model could be extended to more complex predator-prey systems, including predator interference.

Habitat characteristics could affect several parameters of the mechanistic model, hence the functional response shape and magnitude could be modulated by the structural complexity of the landscape (Toscano and Griffen, 2013; Barrios-O'Neill et al., 2015). For instance, the detection distance of a nest by arctic foxes could be lower in dense vegetation (Flemming et al., 2016), the attack probability could be lower for nests located in wetlands and islets only accessible by swimming (Lecomte et al., 2008; Gauthier et al., 2015), and the success probability of an attack could be modulated by the presence of complex networks of lemming tunnels offering refuges. Exploration of the effects of structural complexity on functional responses remains rare (but see Lipcius and Hines 1986; Toscano and Griffen 2013; Barrios-O'Neill et al. 2015), and more empirical research is needed to integrate these sources of variation in mechanistic models.

The outputs of the mechanistic model were generally consistent with field observations. However, adding more complexity could improve its performance and our ability to identify the main drivers of predator acquisition rates. For instance, group defence and mutual vigilance are additional factors that may reduce predator acquisition rates at high prey density (Clark and Robertson, 1979). Although there is no evidence of group defence in geese (Bêty et al., 2001), the snow goose could benefit from the vigilance and early warning provided by neighbors nesting nearby (Samelius and Alisauskas, 2001). Beyond a threshold of goose nest density, such anti-predator behavior could reduce the proportion of unattended nests with increasing nest densities. Nest attendance probability was an influential parameter of the goose model and mutual vigilance may partly explain why acquisition rates observed in the field at moderate-high nest densities were under the model median (figure 2.2A).

One mechanism often advanced for explaining the apparent mutualism between two prey sharing a common predator is predator saturation or satiation (Holt, 1977; Abrams and Matsuda, 1996). Our results showed that the arctic fox doesn't reach saturation at the highest lemming densities observed in our study system. This suggests that the underlying mechanism for the short-term positive effect of high lemming density on arctic bird reproductive success (Blomqvist et al., 2002; Bêty et al., 2002) is likely not predator satiation nor saturation. Instead, the apparent mutualism between birds and lemmings could arise from changes in other components of the functional response. For instance, the attack probability of an attended goose nest could be inversely dependent of lemming density, or daily distance traveled by the predator (speed) could be dependent of lemming density. As indicated by our sensitivity analyses, attack probability was not a strong driver of prey acquisition rates while predator speed was an influential parameter in all prey species. Hence, lemming-induced changes in predator speed through changes in predator activity budget (e.g. due to predator reproductive status or hunger level) could be an alternative hypothesis explaining the apparent mutualism between lemmings and arctic birds. Density dependent changes in components of the functional response have been observed in other systems and can generate nonlinearities in the functional response (Hassell et al., 1977; Abrams, 1982). The integration of all prey species into a mechanistic multi-species functional response model is the next step to fully identify the main proximate drivers of indirect interactions in natural communities.

2.10 Conclusion

Previous studies of functional responses typically tried to discriminate between predetermined shapes of functional responses. Our study illustrates how mechanistic models based on empirical estimates of the main components of predation can generate functional responses specific to a range of prey densities relevant to a given food web. Such mechanistically derived functional responses are needed to untangle proximate drivers of predator-prey population dynamics and to improve our understanding of predator-mediated interactions in natural communities. Although it would be unrealistic to resolve every pairwise interaction within

ecological networks, our mechanistic model provides a starting point for studying higher-order effects such as indirect interactions that can emerge among prey species.

2.11 Acknowledgments

The research relied on the logistic assistance of the Polar Continental Shelf Program (Natural Resources Canada) and of Sirmilik National Park of Canada. The research was funded by (alphabetical order): Arctic Goose Joint Venture, the Canada Foundation for Innovation, the Canada Research Chairs Program, the Canadian Wildlife Service, the Fonds de recherche du Québec-Nature et technologies, the International Polar Year program of Indian and Northern Affairs Canada, the Natural Sciences and Engineering Research Council of Canada, the ArcticNet Network of Centers of Excellence, the Northern Ecosystem Initiative Program (Environment Canada), the Northern Scientific Training Program, the Nunavut Wildlife Management Board, Polar Knowledge Canada, Université du Québec à Rimouski, Université Laval and the W. Garfield Weston Foundation. We are especially grateful to the many people who helped us with field work over many years, the Mittimatalik Hunters and Trappers Organization and Park Canada's staff for their assistance. We sincerely thank both reviewers for their constructive and relevant comments. The article was published on BioRxiv (Beardsell et al., 2020).

2.12 Supplementary Methods

2.12.1. Derivation of the mechanistic model of functional response

The area searched (A; km^2) by a predator is expressed by the product of predator speed (s, km/h), the reaction distance to a prey item i (d_i, km), and the time spend searching (T_s, h):

$$A = s(2d_i)T_s \tag{2.4}$$

A potential encounter occurs when the predator comes within the distance (d_i) at which one can detect and react to the other. As not all prey within this area may be detected, attacked and subdued by the predator, we introduced the detection probability (z_i), the attack probability (k_i), and the success probability of an attack (p_i). Capture efficiency of a prey item i by the predator is expressed by:

$$\alpha_i = s(2d_i)z_i k_i p_i \tag{2.5}$$

The number of prey captured ($V_{\alpha i}$) during a search duration T_S for a density N_i is:

$$V_{\alpha i} = \alpha_i T_s N_i \tag{2.6}$$

The time spent searching (T_S) is defined as:

$$T_S = T_t - \frac{T_{ci} V_{\alpha i}}{p_i} - T_{mi} V_{\alpha i} \tag{2.7}$$

where T_t is the time available for feeding; $\frac{T_{ci} V_{\alpha i}}{p_i}$ is the time spent chasing prey once they are encountered (which includes successful and unsuccessful chases); and $T_{mi} V_{\alpha i}$ is the time spent manipulating prey if they are subdued (which includes time spent eating or hoarding the prey

item).

By simplifying Eq. 2.7 we have:

$$T_S = T_t - V_{\alpha i}(\frac{T_{ci}}{p_i} + T_{mi}) \tag{2.8}$$

We can combine the chasing and manipulation time to produce an overall prey handling time (h_i):

$$h_i = \frac{T_{ci}}{p_i} + T_{mi} \tag{2.9}$$

Substituting T_s from Eq. 2.8 into Eq. 2.6, we arrive at:

$$V_{\alpha i} = \frac{\alpha_i N_i T_t}{1 + \alpha_i h_i N_i} \tag{2.10}$$

The functional response of a predator ($f(i)$) is the number of prey captured per predator per unit of time (acquisition rate). This is expressed by dividing Eq. 2.10 by T_t:

$$f(i) = \frac{\alpha_i N_i}{1 + \alpha_i h_i N_i} \tag{2.11}$$

2.12.2. Estimation of parameter values

Predator speed

A total of 16 foxes (7 females and 9 males) were equipped with a GPS collar (Radio Tag-14, Milsar, Poland) during the summers of 2018 and 2019. Of those, 7 were equipped during both years giving us a total of 23 fox-summers (8 foxes in 2018 and 15 in 2019). Reproductive fe-

males (2 out of 4 in 2018 and 6 out of 7 in 2019) spent substantial time nursing the pups in the den. Foxes were captured using Tomahawk cage traps #205 (Tomahawk Live Trap Company, Tomakawk, WI, USA) or Softcatch #1 padded leghold traps (Oneida Victor Inc. Ltd., Cleveland, OH, USA) as described in (Rioux et al., 2017). GPS fix intervals were fixed at 4 minutes (360 fixes per day), and data were downloaded to a hand-held receiver using UHF transmission. GPS location error was of 11 m (Poulin et al., 2021).

Average predator speed (km/day) was estimated by adding linear distances between successive locations, using the *adehabitatLT* library in R. Predator speed was extracted from June 5 to July 9 to focus on the incubation period of most birds. We removed from analyses all fixes obtained $<$48 hours after capture and days where the number of fixes was insufficient ($<$75% of all fixes). Predator speed was converted per hour and average speed was 1.52 km/h (sd = 0.59 km/h, n = 123 fox-days).

Nest attendance probability - During goose incubation period, the time spent on the nest by females average 93% (μ = 93.6, se = 1.6%, n = 7 females; Poussart et al. 2000 and μ = 93, n = 41 females; Reed et al. 1995). During incubation recesses females usually remained close to their nests, and 90% of all records (n = 183) were within 20 m (Reed et al., 1995). Since there is uncertainty in the proportion of females within 10 m, we used 90% as the maximum and 50% as the minimum. By combining this information, we can estimate a minimum probability of nest attendance at 96.5.% and a maximum probability of nest attendance at 99.3%.

Detection probability - We used artificial nests to assess experimentally the detection probability of unattended goose nests in summer 2019. Goose eggs were simulated with domestic hen eggs. Two eggs were placed in each artificial nest and covered with goose down collected from old goose nests. A total of 24 paired artificial nests were deployed randomly in the goose colony. The two paired nests were separated either by 10, 30, 60, 80 or 100 m. Movement-triggered cameras (model PM35T25, Reconyx) were set directly on the ground 5 m from each nest allowing to identify nest predators and to determine the exact time of nest predation. A successful detection was considered to have occurred when the two paired nests were pre-

dated by a fox in the same time interval (n = 9 cases). An unsuccessful detection occurred when only one nest of the pair was depredated by a fox (n = 6 cases). When a nest was predated by another species (e.g. gulls, ravens) or the event of predation was undetected by the camera, the pair was excluded from the analysis (n = 9 cases). We used a linear model with a binomial distribution to model detection probability in relation to detection distance (figure 2.5).

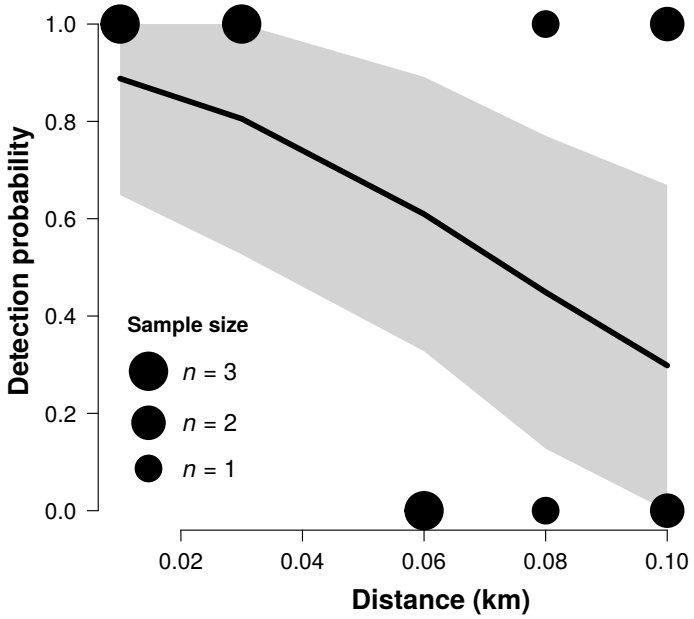

Figure 2.5. Probability that an artificial (unattended) goose nest was detected and depredated by an arctic fox as a function of the distance between paired nests. Each circle represents observed values and circle size is proportional to the number of observations. The curve represents the average detection probability and the gray band represents the 95% confidence interval of the regression.

Reaction distance - The reaction distance on attended nests was defined as the distance at which an attack can be initiated by the predator. This parameter was estimated with direct observations of foraging foxes in summer 2019 (μ = 0.0328, se = 0.007, n = 25 attacks). On unattended nests, the reaction distance was defined as the maximum distance at which the predator can detect an unattended nest. We used a combination of direct observations combined with artificial nests (same experience as for the detection probability) to estimate the reaction distance on unattended nests (μ = 0.0365 km, se = 0.009, max = 0.1 km, n = 13). We used 0.1 to 0.12 km as a range of maximum distance as the detection probability was still

around 30% at 0.1 km (figure 2.5). As our sample size was limited for attended and unattended nests, we assigned a uniform distribution for both parameters.

Chasing time- By conducting direct observations of foraging foxes from a blind, we obtained the average chase time per egg attacked from a nest (μ = 23 sec/egg, sd = 29, n = 148 attacks). To convert per nest, we subsampled the data set and summed up 4 individual values. This total was then adjusted to the average clutch size of 3.7 (μ = 0.02 , se = 0.0024 h per nest).

Manipulation time- By conducting direct observations of foraging foxes from a blind, we obtained the time required by the predator to manipulate one egg, which includes consumption or hoarding time (μ = 136 sec/egg, sd = 127, n = 207). To convert per nest, we subsampled the data set and summed up 4 individual values. This total was then adjusted to the average clutch size of 3.7 (μ = 0.14 , se = 0.009 h per nest).

Attack probability of attended nests- Based on direct observations of foraging foxes from a blind, we estimated attack probability at 22% by using the proportion of attended nests attacked by a fox divided by the total number of possible attacks (n = 215). The total number of possible attacks is obtained by adding the number of attacks towards attended nests and the number of times the foxes are chased by the geese without having initiated an attack. The latter gives us an estimation of the number of opportunities to initiate an attack. This estimation of attack probability gives us the upper limit of attack probability as the total number of possible attacks is most likely underestimated. Thus, we used a wide range of values (from 0.01 to 0.22) and a uniform distribution for this parameter.

Success probability- Based on direct observations of foraging foxes from a blind, the probability of a successful attack was 93.4% on unattended nests (se = 0.022, n = 137 attacks) and 9.8% on attended nests (se = 0.011, n = 701 attacks).

Complete predation probability- Based on direct observations of foraging foxes from a blind, the probability of a complete clutch predation once an egg is subdued on unattended nests was 69% (se = 0.12, n = 16) and was 47% (se = 0.13, n = 15) on attended nests. The probability of complete clutch predation for an unattended nest is not 1 since a parent may detect a fox

during incubation recess and return quickly to protect the nest.

Lemming parameters

Reaction distance and detection probability Based on direct observations, foxes generally initiate their attacks on lemmings within 5 m (on 29 attacks recorded in 1996-1999 and 2019). We assumed that the maximum reaction distance was twice that distance (10 m) and that detection probability followed a decreasing sigmoid function. Hence, detection probability was considered fairly high within 5 m radius (100-80%) and declined sharply between 5 and 10 m.

Chasing time By conducting direct observations of foraging foxes, we estimated the average chase time per lemming attacked (μ = 88 sec, se = 7.1, n = 246 attacks).

Success probability By conducting direct observations of foraging foxes, we estimated the probability of a successful attack on a lemming at 51% (se = 0.03, n = 268 attacks).

Manipulation time Based on direct observations of foraging foxes, we estimated the average manipulation time per lemming captured, which includes consumption and hoarding time (μ = 37 sec, se = 3.0, n = 93).

Passerine parameters

Reaction distance The reaction distance was defined as the maximum distance between an observer (a simulated predator) and the nest when the bird flushes the nest. To measure the reaction distance, a human observer approached nests from a random bearing at normal walking speed ($\sim$4 km/h). The observer made several approaches until the bird leaves the nest. At each approach the distance between the observer and the nest was noted. Flush

distance was recorded for 45 different nests in summer 2019 and ranged from 0 to 20 m (μ = 2.8 m, sd = 3.6 m, n = 77) The distance was measured either by pacing or with a GPS unit.

Detection probability Detection probability was estimated by following the same method as reaction distance. Besides recording flush distances, the distance between the observer and the nest was noted even if the bird didn't flush. We used a linear model with a binomial distribution to model detection probability (0; the bird didn't flush, 1; the bird flushed) in relation to the minimum distance between the observer and the nest (n = 167, figure 2.6).

Manipulation time By using movement-triggered cameras near the nest, we extracted manipulation time from 17 passerine nests monitored between 2006 and 2014. The average manipulation time was 31 sec (sd = 30 sec) and included consumption and hoarding time. Cameras (PM35T25 model) were set directly on the ground 5 m from the nest (for more details about camera features see McKinnon and Bêty (2009)).

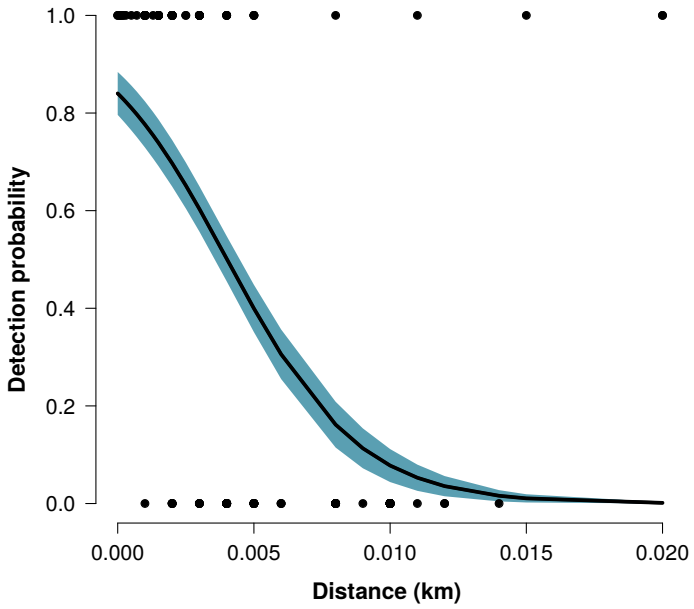

Figure 2.6. Detection probability of a passerine nest in relation to the distance between the observer and the nest. The gray band represents the $\pm$ standard error of the regression.

Sandpiper parameters

Reaction distance and detection probability Reaction distance was estimated by Smith and Edwards (2018) following the same method as described for passerines reaction distance. The mean reaction distance was 15.3 m (sd = 18.8 m, n = 104 nests, max = 85 m) for White-rumped Sandpiper (*Calidris fuscicollis*; Smith and Edwards (2018)). We used the same detection probability function as for passerines (figure 2.6).

Manipulation time By using movement-triggered cameras near real and artificial sandpiper nests, we extracted manipulation time from 5 sandpiper and 18 artificial nests monitored between 2006 and 2016. An artificial nest consisted of four Japanese quail (*Coturnix japonica*) eggs placed in a small depression made in the ground, similar to the simple nest scrapes used by sandpipers. Quail eggs resemble those of sandpipers in colouration and size. The average manipulation time was 250 sec (sd = 189 sec) and includes consumption and hoarding time. Cameras (PM35T25 model) were set directly on the ground 5 m from the nest (for more details about camera features see McKinnon and Bêty (2009)).

Tableau 2.2. Parameter values and distribution used in the functional response model of arctic fox to goose nests, lemmings, passerine and sandpiper nests.

Parameter name	Value	Distribution
Predator speed	μ = 1.52 km/h, sd = 0.59, n = 123 fox-days	Normal-truncated
Goose nests		
Nest attendance probability	min = 0.965, max = 0.993	Uniform
Chasing time	μ = 0.02, se = 0.0024 h per nest	Normal-truncated
Manipulation time	μ = 0.14 , se = 0.009 h per nest	Normal-truncated
Goose attended nests		
Reaction distance	min = 0.026, max = 0.040 km	Uniform
Attack probability	min = 0.01, max = 0.22	Uniform
Success probability	p = 0.098, se = 0.011	Normal-truncated
Complete predation probability	p = 0.47, se = 0.13	Normal-truncated
Goose unattended nests		
Reaction distance	min = 0.10, max = 0.12 km	Uniform
Detection probability	Cumulative detection probability at the reaction distance. See figure 2.5	NA
Success probability	p = 0.934, se = 0.022	Normal-truncated
Complete predation probability	p = 0.69, se = 0.12	Normal-truncated
Lemmings		
Reaction distance	min = 0.005, max = 0.010 km	Uniform
Detection probability	Cumulative detection probability at the reaction distance. See figure 2.8	NA
Chasing time	μ = 0.024, se = 0.0019 h per ind.	Normal-truncated
Success probability	p = 0.51, se = 0.03	Normal-truncated
Manipulation time	μ = 0.010 , se = 0.0008 h per ind.	Normal-truncated
Passerine nests		
Reaction distance	0.02 km	NA
Detection probability	Cumulative detection probability at 0.02 km (0.24). See figure 2.6	NA
Manipulation time	μ = 0.0086, se = 0.0005 h/nest	Normal-truncated
Sandpiper nests		
Reaction distance	0.085 km	NA
Detection probability	Cumulative detection probability at 0.085 km (0.059). See figure 2.6	NA
Manipulation time	μ = 0.069, se = 0.0023 h/nest	Normal-truncated

Note: Reaction distance refers to the detection distance for all prey, except for attended goose nests, where reaction distance refers to the attack distance.

Tableau 2.3. List of equations to derive the functional response of arctic fox to each prey species.

Model	Form
Goose nests (G)	
Acquisition rate	$f(G) = f(G_a) + f(G_{ua})$
Goose attended nests (Ga)	
Capture efficiency - Complete predation	$\alpha_{Gac} = s \cdot (2d_{Ga}) \cdot k_{Ga} \cdot p_{Ga} \cdot P_{cGa}$
Capture efficiency - Partial predation	$\alpha_{Gap} = \frac{s \cdot (2d_{Ga}) \cdot k_{Ga} \cdot p_{Ga} \cdot (1 - P_{cGa})}{3.7*}$
Handling time	$h_{Ga} = \frac{T_{cG}}{p_{Ga} \cdot P_{cGa}} + T_{mG}$
Acquisition rate	$f(G_a) = \frac{(\alpha_{Gac} + \alpha_{Gap}) \cdot w \cdot N_G}{1 + (\alpha_{Gac} + \alpha_{Gap}) \cdot h_{Ga} \cdot w \cdot N_G}$
Goose unattended nests (G_{ua})	
Capture efficiency - Complete predation	$\alpha_{Guac} = s \cdot (2d_{Gua}) \cdot z_{Gua} \cdot p_{Gua} \cdot P_{cGua}$
Capture efficiency - Partial predation	$\alpha_{Guap} = \frac{s \cdot (2d_{Gua}) \cdot z_{Gua} \cdot p_{Gua} \cdot (1 - P_{cGua})}{3.7*}$
Handling time	$h_{Gua} = \frac{T_{cG}}{P_{cGua} \cdot p_{Gua}} + T_{mG}$
Acquisition rate	$f(G_{ua}) = \frac{(\alpha_{Guac} + \alpha_{Guap}) \cdot (1 - w) \cdot N_G}{1 + (\alpha_{Guac} + \alpha_{Guap}) \cdot h_{Gua} \cdot (1 - w) \cdot N_G}$
Lemmings (L)	
Capture efficiency	$\alpha_L = s \cdot (2d_L) \cdot z_L \cdot p_L$
Handling time	$h_L = \frac{T_{cL}}{p_L} + T_{mL}$
Acquisition rate	$f(L) = \frac{\alpha_L \cdot N_L}{1 + \alpha_L \cdot h_L \cdot N_L}$
Passerine nests (P)	
Capture efficiency	$\alpha_P = s \cdot (2d_P) \cdot z_P$
Handling time	$h_P = T_{mP}$
Acquisition rate	$f(P) = \frac{\alpha_P \cdot N_P}{1 + \alpha_P \cdot h_P \cdot N_P}$
Sandpiper nests (S)	
Capture efficiency	$\alpha_S = s \cdot (2d_S) \cdot z_S$
Handling time	$h_S = T_{mS}$
Acquisition rate	$f(S) = \frac{\alpha_S \cdot N_S}{1 + \alpha_S \cdot h_S \cdot N_S}$

Note: *This value refers to the average clutch size of the greater snow goose (Gauthier et al., 2013).

2.12.3. Exploration of density dependence in capture efficiency components

We incorporated density dependence into the goose and the lemming models within the range of densities observed in our study system. For each parameter in which density dependence was incorporated, the minimum (p_{min}) and the maximum (p_{max}) parameter values were associated respectively with the minimum (N_{min}) and the maximum (N_{max}) prey density in order to calculate the slope and the intercept of the density-dependence relationship:

$$slope = (p_{max} - p_{min})/(N_{max} - N_{min}) \tag{2.12}$$

$$intercept = p_{max} - (slope * N_{max}) \tag{2.13}$$

In the goose model, we modified attack and success probabilities for nests attended, and reaction distance and detection probability for nests unattended (e.g. figure 2.7). In the lemming model, we added density dependence in reaction distance, detection and success probabilities (e.g. figure 2.8).

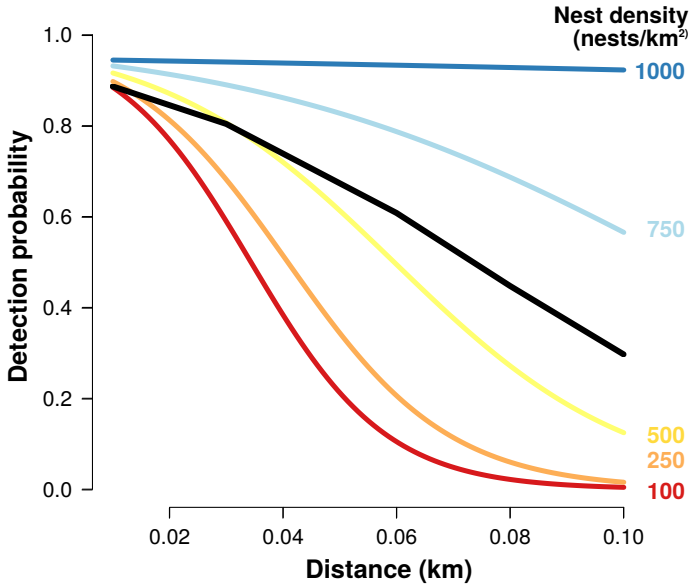

Figure 2.7. Probability that an artificial (unattended) goose nest was detected and depredated by the arctic fox as a function of distance along a gradient of goose nest density. The color gradient indicates the range of detection functions used to explore density dependence in detection probability.

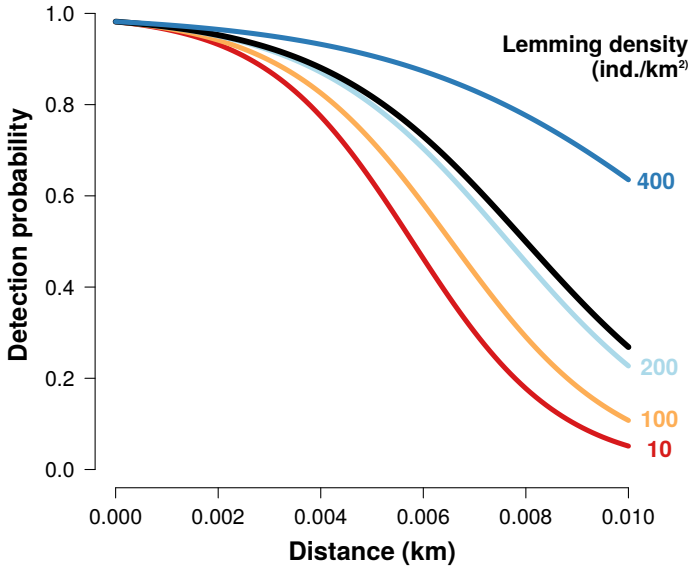

Figure 2.8. Probability that a lemming is detected by an arctic fox along a gradient of lemming density. The black line represents the average detection probability. The color gradient indicates the range of detection functions used to explore density dependence in detection probability.

2.13 Supplementary Tables

Tableau 2.4. Empirical data used to evaluate the performance of the mechanistic model of functional response of arctic fox to goose nests and lemmings on Bylot Island, Nunavut. Data are listed by year.

Year	**Observation length** (h)	**Average clutch size**	**Goose density range** (nests/km^2)	**Goose nest acquisition rate** (nests/fox/h)	**Lemming density** (ind./km^2)	**Lemming acquisition rate** (ind./fox/h)
1996	3.1	3.7	79-100	1.82	414	0.32
1997	4.7	3.9	219-264	0.33	166	0.21
1998	9.5	3.8	283-358	0.28	247	2.32
1999	4.2	3.1	15-110	0.92	11	0
2004	29.8	3.6	85-110	0.19	325	2.85
2005	43.6	3.6	257-390	0.76	32	0.64
2015	3.4	3.5	713-926	0.34	365	0.30
2016	3.3	3.4	401-550	0.97	253	2.40
2017	10.1	3.5	456-814	0.20	19	0.10
2019	12.7	4.0	381-465	0.30	137	0.24

Tableau 2.5. Empirical data used to evaluate the performance of the mechanistic model of functional response of arctic fox to passerine and sandpiper nests on Bylot Island, Nunavut. Data are listed by year.

Year	**Passerine nes density** (nests/km^2)	**Passerine nest acquisition rate** (nests/fox/h)	**Sandpiper nest density** (nests/km^2)	**Sandpiper acquisition rate** (nests/fox/h)
2005	7.3	0.15	4.4	0.051
2006	10.3	0.28	5.9	0.169
2007	6.1	0.03	2.1	0.004
2008	7.3	0.06	1.0	0.002
2009	6.9	0.04	1.1	0.002
2010	6.8	0.04	4.5	0.014
2011	6.8	0.03	2.3	0.004
2012	12.3	0.19	4.0	0.060
2013	7.3	0.13	2.6	0.029

2.14 Supplementary Figures

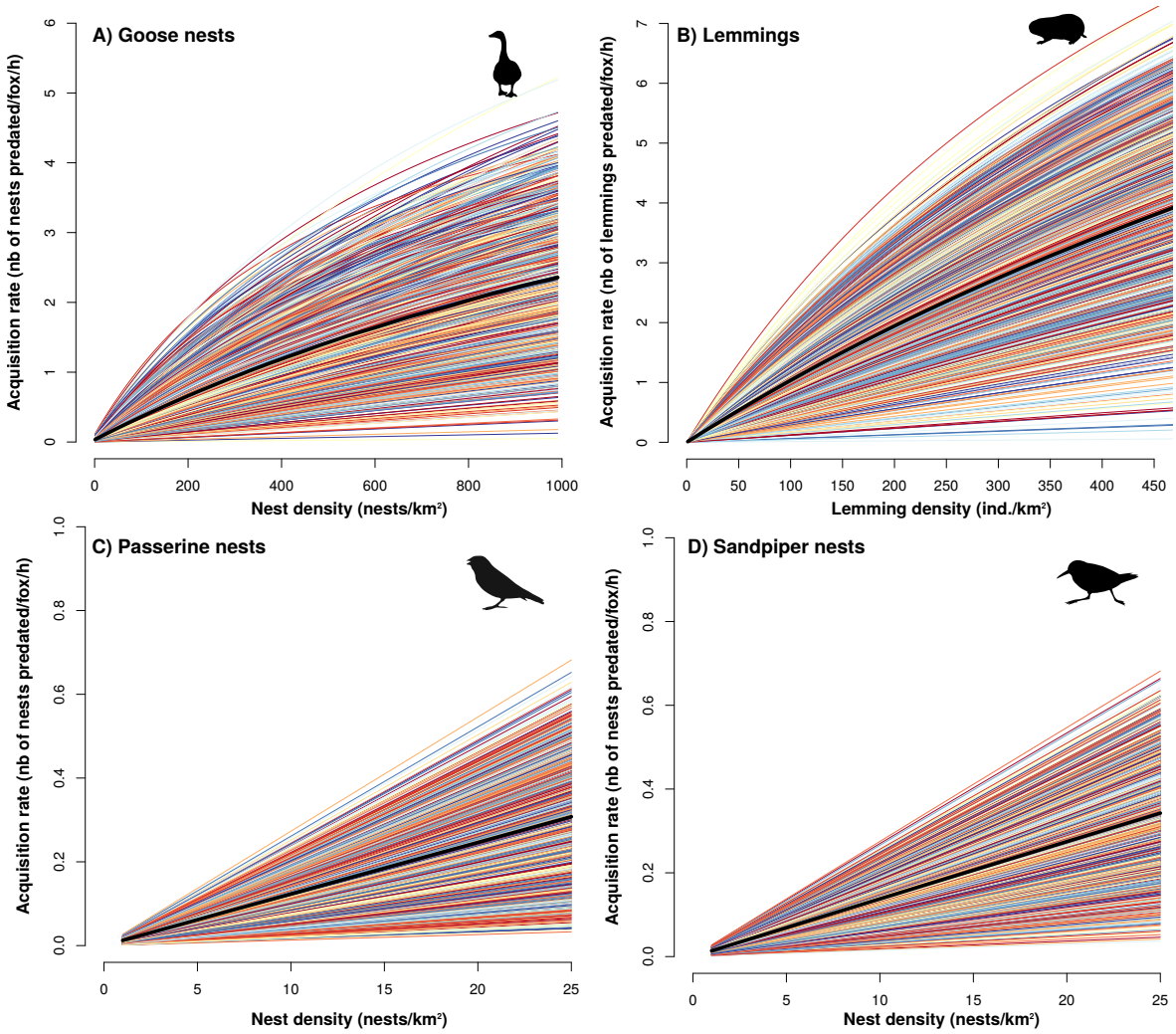

Figure 2.9. Functional response of arctic fox to density of goose nests (**A**), lemmings (**B**), passerine nests (**C**), and sandpiper nests (**D**). Each line reprents a simulation and the solid black line represents the model median (N = 1000 simulations).

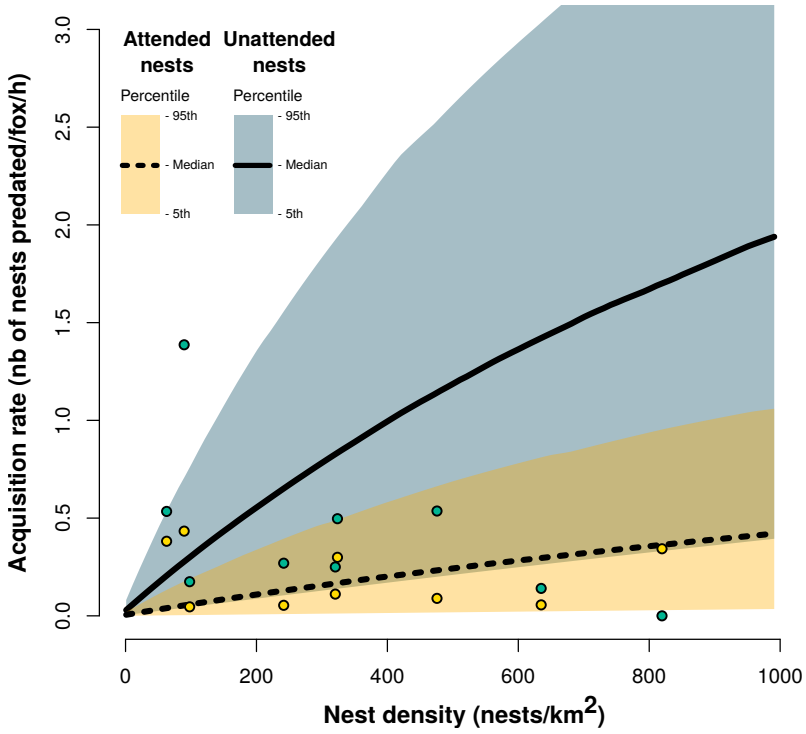

Figure 2.10. Functional response of arctic fox to density of goose nests for attended and unattended nests. The black lines represent the model median and the color bands represent the 95th percentiles based on 1000 simulations. Empirical data for attended and unattended nests obtained from direct observations of foraging foxes are represented by yellow and blue dots respectively.

CHAPITRE 3

Vers une compréhension mécanistique des interactions indirectes entre les proies de la toundra arctique

3.1 Contexte scientifique et publication associée

Cet article, intitulé « A mechanistic model of functional response provides new insights into indirect interactions among arctic tundra prey » a été publié dans la revue *Ecology* en 2022. Ce chapitre est ancré dans l'approche développée au chapitre précédent et intègre plusieurs proies au sein du modèle mécanistique et des données fines des mouvements des renards (GPS et accélérométrie). Cette étude se démarque aussi en alliant de la modélisation, observations empiriques détaillées et expériences en milieu naturel pour construire et évaluer le modèle. Cet article améliore notre capacité à quantifier la force des interactions entre les espèces en milieu naturel. Cet article a été corédigé par moi-même, Dominique Gravel, Jeanne Clermont, Dominique Berteaux, Gilles Gauthier et Joël Bêty. D'une façon similaire au chapitre précédent, cet article est le fruit de données écologiques récoltées à l'île Bylot depuis 1996 et du travail (colossal) de Gilles Gauthier, Dominique Berteaux et Joël Bêty dans la coordination de ce suivi écosystémique. J'ai structuré et établi les objectifs de cet article conjointement avec Dominique Gravel et Joël Bêty. J'ai réalisé les simulations, les analyses et dirigé la rédaction de l'article. Jeanne Clermont a extrait les données provenant de l'accélérométrie et des colliers GPS des renards. L'ensemble des co-auteurs.trices ont contribué à la rédaction et aux révisions de l'article. Une version abrégée de cet article a été présentée sous forme d'une présentation orale lors du *Annual meeting of the Ecological Society of America*, en format virtuel, en août 2021.

Les sections suivantes sont celles de l'article publié.

3.2 Title

A mechanistic model of functional response provides new insights into indirect interactions among arctic tundra prey

3.3 Authors

Andréanne Beardsell, Dominique Gravel, Jeanne Clermont, Dominique Berteaux, Gilles Gauthier, Joël Bêty

3.4 Traduction du résumé de l'article publié

Ancré au coeur de l'écologie, le temps de manipulation des proies par un prédateur est considéré comme un mécanisme dominant pouvant générer des interactions indirectes positives entre des proies partageant un prédateur. Cependant, de plus en plus d'études indiquent que les prédateurs ne sont pas nécessairement limités par un tel mécanisme dans la nature. Des changements dans le comportement de quête alimentaire des prédateurs peuvent également générer des effets indirects positifs, mais ils sont rarement inclus dans les modèles de réponse fonctionnelle. Dans le but de décortiquer les mécanismes proximaux des interactions entre les espèces dans les communautés naturelles et d'améliorer notre capacité à quantifier la force de ces interactions, nous avons modifié la version multi-proies de l'équation de Holling en incluant des changements dans le comportement de recherche de nourriture des prédateurs. Notre modèle, basé sur les traits et le comportement des espèces, s'inspire de la communauté de vertébrés de la toundra arctique, où le principal prédateur (le renard arctique) est un prédateur actif se nourrissant principalement de petits rongeurs cycliques (lemming) et d'œufs de diverses espèces d'oiseaux nichant dans la toundra. Bien que les effets positifs indirects à court terme des lemmings sur les oiseaux ont été documentés dans l'Arctique circumpolaire, les mécanismes sous-jacents demeurent mal compris. Nous avons bénéficié de données empiriques détaillées provenant du suivi écologique à long terme (>25 ans) de l'île Bylot (Nunavut) pour paramétrer le modèle mécanistique et d'une série temporelle de 15 ans de la densité des proies et du succès de nidification des oiseaux pour évaluer la force d'interaction entre les espèces. Nous avons constaté que: (i) contrairement aux hypothèses classiques, le temps de manipulation des proies joue un rôle mineur dans notre système et (ii)

des changements dans le comportement du renard (soit dans le budget d'activité quotidien et la distance parcourue) peuvent générer une interaction indirecte positive entre les lemmings et les oiseaux. Ces ajustements du comportement de quête alimentaire des renards semblent être le mécanisme dominant des effets indirects positifs observés entre les proies de la toundra arctique. Ces ajustements sont rarements intégrés dans les composantes de la réponse fonctionnelle et ont été peu étudiés dans les communautés naturelles de vertébrés. Ils méritent plus d'attention pour améliorer notre capacité à quantifier la force des interactions entre les espèces.

3.5 Abstract

Prey handling processes are considered a dominant mechanism leading to short-term positive indirect effects between prey that share a predator. However, a growing body of research indicates that predators are not necessarily limited by such processes in the wild. Density-dependent changes in predator foraging behavior can also generate positive indirect effects but they are rarely included as explicit functions of prey densities in functional response models. With the aim of untangling proximate mechanisms of species interactions in natural communities and improving our ability to quantify interaction strength, we extended the multi-prey version of the Holling disk equation by including density-dependent changes in predator foraging behavior. Our model, based on species traits and behavior, was inspired by the vertebrate community of the arctic tundra, where the main predator (the arctic fox) is an active forager feeding primarily on cyclic small rodent (lemming) and eggs of various tundra-nesting bird species. Short-term positive indirect effects of lemmings on birds have been documented over the circumpolar Arctic but the underlying mechanisms remain poorly understood. We used a unique data set, containing high-frequency GPS tracking, accelerometer, behavioral, and experimental data to parameterize the multi-prey model, and a 15-year time series of prey densities and bird nesting success to evaluate interaction strength between species. We found that: (i) prey handling processes play a minor role in our system and (ii) changes in arctic fox daily activity budget and distance traveled can partly explain the predation release on

birds observed during lemming peaks. These adjustments in predator foraging behavior with respect to the main prey density thus appear as the dominant mechanism leading to positive indirect effects commonly reported among arctic tundra prey. Density-dependent changes in functional response components have been little studied in natural vertebrate communities and deserve more attention to improve our ability to quantify the strength of species interactions.

Keywords: arctic fox (*Vulpes lagopus*), indirect effects, lemmings, multi-prey, nonlinear species interactions, passerines, predation, predator-prey interactions, sandpipers.

3.6 Introduction

Interactions between predator and prey in natural communities are difficult to describe quantitatively. Various mathematical models have been used to quantify prey acquisition by the predator and to investigate the nature and the strength of species interactions within food webs (Abrams et al., 1998; Pawar et al., 2012; Baudrot et al., 2016; Chan et al., 2017). Several studies have compared how a predator acquisition rate varies with prey density using statistical approaches (reviewed by Novak and Stouffer (2020)), but few of them explicitly tackled the underlying mechanisms. Although empirical data may be consistent with various functional response models, this does not provide clear insight into the mechanisms underpinning interaction strengths. Moreover, the sample size is often insufficient to obtain the statistical power needed to properly discriminate between different models (Novak and Stouffer, 2020). Process-based mechanistic models (hereafter referred to as mechanistic models) may help in untangling proximate mechanisms of species interactions (Connolly et al., 2017; Griffen, 2021) and can improve our ability to adequately quantify the strength of interactions in natural communities (Spalinger and Hobbs, 1992; Beardsell et al., 2021; DeLong, 2021).

The multi-species version of the Holling (1959*b*) disk equation (Murdoch and Oaten, 1975) is widely used to model predation rates in multi-prey systems and assumes a saturation of predator acquisition rates with increasing prey availability due to rate-limiting handling pro-

cesses (Brose et al., 2005; McLellan et al., 2010; Barraquand et al., 2015; Serrouya et al., 2015). The summation of the handling time of all prey items is a critical component of this equation and can generate indirect interactions among prey. Increasing abundance of one species saturates the predator because of its limited prey handling capacities (which includes the time needed to pursue, catch and manipulate a prey item; Jeschke et al. (2002)) and thereby indirectly releases predation pressure on other prey. This equation is often at the core of more complex food web models (Schneider et al., 2016; Tyson and Lutscher, 2016; Barrios O'Neill et al., 2019) and handling time is considered a dominant mechanism inducing short-term positive effects among prey (Abrams, 1987; Abrams and Matsuda, 1996; Abrams et al., 1998). However, the role of handling processes in predator-mediated interactions lacks definitive evidence in the wild and a growing body of research indicates that predators are not necessarily limited by handling processes at the highest prey densities observed in natural systems (Jeschke et al., 2002; Novak, 2010; Chan et al., 2017; Preston et al., 2018; Beardsell et al., 2021).

It is unlikely that predators simply acquire more prey at a rate proportional to their abundance. Non-linearities in functional responses are capable of influencing predation rates via several mechanisms. For instance, the density of a prey may modulate the predator state (e.g., hunger level, reproductive status), which in turn could have an impact on other prey consumed by that predator. Although a dependence of some components of the functional response to prey density have long been recognized as biologically plausible (Hassell et al., 1977; Abrams, 1982), its potential importance for predator acquisition rates has been little studied empirically (but see Okuyama (2010, 2012)), and it is rarely included as explicit functions of prey density in functional response models (Stouffer and Novak, 2021). Yet, changes in predator foraging behavior according to prey density can generate positive effects between prey species (Abrams and Matsuda, 1996, 1993) and warrant additional attention in natural predator-prey systems (Stouffer and Novak, 2021).

Our objectives were twofold. First, we developed a mechanistic model of acquisition rates that includes a dependence in both predator handling time and foraging behavior on the main prey density. Second, we illustrated this model using the predator-prey dynamics of a multi-prey system in the arctic tundra to identify the proximate mechanisms of the well-known

short-term positive indirect effects of cyclic rodents on nesting birds (see below). This type of predator-mediated effect is widespread between prey sharing a predator and can affect species abundance and coexistence in various ecosystems (Bonsall and Hassell, 1997; Duchesne et al., 2021). We evaluated three hypotheses that could explain such indirect interactions (Table 3.1 and Fig. 3.1). The first hypothesis was based on the multi-prey version of the Holling (1959*b*) disk equation, in which prey handling processes reduce the time available to search for other prey and result in positive indirect effects between prey. The second and the third hypotheses extended the multi-prey model to include prey density-dependent effect on prey handling time and on predator foraging behavior, respectively (Table 3.1).

We developed the multi-prey mechanistic model for the arctic fox, an active-searching top predator of the arctic tundra that feeds primarily on lemmings, as well as on bird eggs during the summer (Angerbjörn et al., 1999; Giroux et al., 2012). Within this predator-prey system, lemmings are the most abundant prey and show population cycles with a maximum density occurring every 3-5 years (Fauteux et al., 2015). Fox predation pressure on eggs of ground-nesting birds is generally released when lemming density is high, leading to short-term positive indirect effects of lemmings on bird nesting success (Summers et al., 1998; Nolet et al., 2013; McKinnon et al., 2014). This classic example of predator-mediated effects among vertebrates was studied across the circumpolar arctic but the underlying proximate mechanisms remain unclear (Underhill et al., 1993; Summers et al., 1998; Nolet et al., 2013; McKinnon et al., 2014). We parameterized the model using a combination of behavioral, demographic, and experimental data acquired over 20 years in the high-arctic tundra. As a previous mechanistic single-prey model indicated that the arctic fox is not limited by handling processes at the highest lemming densities observed in our study system (Beardsell et al., 2021), we expected changes in the predator foraging behavior in relation to lemming density to be the dominant mechanism of the short-term positive effects of lemmings on arctic bird nesting success.

Tableau 3.1. Three hypothesized mechanisms underlying the short-term positive effects of a cyclic prey (prey 1; lemmings) on two prey species (prey 2 and 3; passerine and sandpiper nests, respectively) through a common predator (arctic fox).

Predation component	**Density-dependent component**	**Hypothesized mechanism**	**Application to a multi-prey community in the Arctic**
Prey handling time	None	Constraints on predator foraging such as the time required to handle (chasing, manipulating) prey may lead to positive indirect effects because time spent handling one prey reduces the time available for searching other prey (Holt, 1977). The average handling time per prey is independent of prey density.	As lemming density increases, foxes spend more time handling lemmings, reducing the time available to search for passerine and sandpiper nests.
Prey handling time through prey delivery	Positively related to prey density	Prey density commonly influences predator investment in reproduction (Gilg et al., 2003; Terraube et al., 2015). Central place foragers must often return to a specific location (e.g., nest, den) to feed their offspring. Prey delivery is therefore part of handling time, and as investment in reproduction increases (e.g., litter size, which may depend on prey abundance), the probability of prey delivery increases. This process results in a relationship between prey handling time and prey density.	The breeding probability of a fox pair increases with summer lemming density (Juhasz et al., 2020). During breeding, which overlaps with the nesting period of birds, foxes primarily bring lemmings back to their dens, which increases the time spent handling the retrieved prey. Thus, the time foxes spent handling lemmings increases with lemming density through prey delivery.
Predator activity time and distance traveled	Both parameters negatively related to prey density	Predators adjust the amount of time devoted to foraging, resting, and reproductive behaviors with prey availability (Harding et al., 2007; Busdieker et al., 2019). This behavioral flexibility may result in reduced foraging effort as prey density increases (Harding et al., 2007) or in increased time-consuming behaviors associated with reproduction (e.g., parental care).	There are two non-exclusive processes. First, when lemming densities increase, foxes can decrease their foraging effort. Second, when lemming densities are high enough, foxes breed and females can increase time spent near the den (for lactation/parental care before cubs emerge). This period overlaps with the nesting period of birds. At high lemming densities, those processes can translate into a decrease in fox distance traveled and activity time during the bird nesting period.

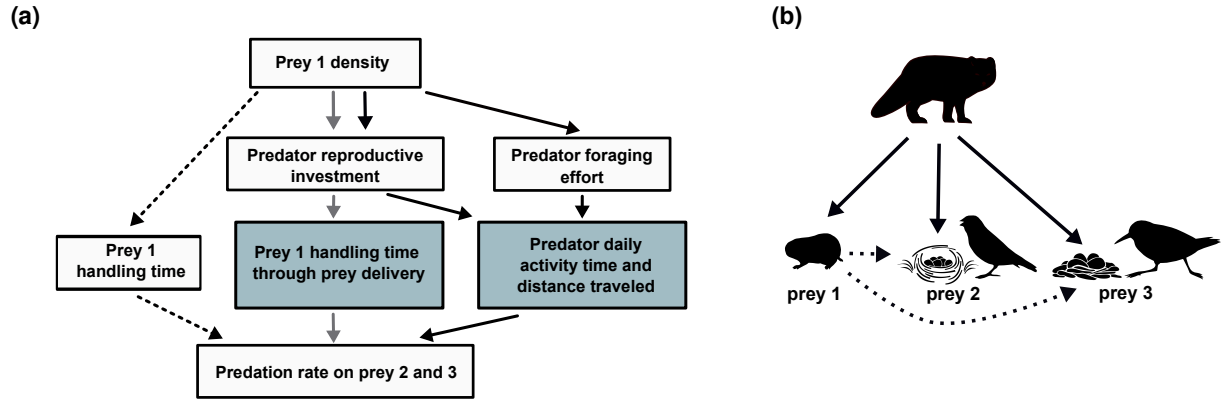

Figure 3.1. **(a)** Schematic representation of three hypothesized mechanisms underlying the short-term positive effect of a cyclic prey (prey 1, lemmings) on two prey species (prey 2 and 3, passerine and sandpiper nests, respectively) through a common predator (arctic fox). Different arrows (dotted, grey and black) correspond to each hypothesis described in Table 3.1. The blue boxes indicate the parameters where prey density-dependence was included. **(b)** Diagram of a simplified arctic food web indicating the direct (solid arrows) and indirect (dotted arrows) links between the predator (arctic fox), prey 1 (lemmings), prey 2 (passerine nests) and 3 (sandpiper nests).

3.7 Methods

3.7.1. Study system

The mechanistic model of multi-prey functional response was developed using data from a long-term ecological monitoring on Bylot Island, Nunavut, Canada (73° N; 80° W). Two cyclic species of small mammals are present, the brown (*Lemmus trimucronatus*) and collared (*Dicrostonyx groenlandicus*) lemmings. Ground-nesting birds present include passerines (mostly Lapland longspur, *Calcarius lapponicus*) and sandpipers (primarily Baird's Sandpiper (*Calidris bairdii*) and White-rumped Sandpiper (*Calidris fuscicollis*)). The monitoring area of lemmings, and passerine and sandpiper nests is located within the Qarlikturvik Valley (72°85'N, 78°85'W). Sandpipers and passerines nest at relatively low densities (2 and 7 nests km^{-2} on average, respectively). During the breeding season (June until July) passerines and sandpipers lay an average of 5 and 4 eggs, which they incubate for 12 and 21 days, respectively (Gauthier et al.,

2013; McKinnon et al., 2014; Hussell and Montgomerie, 2020). Sandpiper chicks typically leave the nest within 24 hours of hatching (McKinnon et al., 2014), while passerine chicks remain in the nest for 9-10 days (Hussell and Montgomerie, 2020).

The arctic fox is the main egg predator of ground-nesting birds on Bylot Island (McKinnon and Bêty, 2009; Royer-Boutin, 2015). The nesting period for birds (typically mid-June to early mid-July) overlaps with the lactation period for foxes. Fox gestation period is around 52 days and births usually occur in late May on Bylot Island (Audet et al., 2002; Morin, 2015). Fox cubs are weaned after 6-7 weeks (Audet et al., 2002). Arctic foxes maintain summer territories (averaging 10 km^2) with little overlap (Grenier-Potvin et al., 2021), which limits interference between foxes within territories. Also, foxes rarely encounter and interact with other individuals while foraging within their summer territory (Beardsell et al., 2021). The number of territorial adult foxes remains relatively constant between summers, even if the breeding success of foxes is strongly influenced by lemming cycles (Royer-Boutin, 2015; Juhasz et al., 2020). Like many other animals (Vander Wall, 1990), arctic foxes generally predate more prey than they immediately consume (with associated food hoarding behavior) and thus hide a large proportion of the prey they capture (Samelius and Alisauskas, 2000; Careau et al., 2007).

The monitoring area of passerine and sandpiper nests is located ∼30 km away from a colony of greater snow geese (*Anser caerulescens atlanticus*). We excluded geese from the model since they are virtually absent and isotopic studies confirmed that the contribution of goose eggs to the fox diet was limited in the monitoring area (Giroux et al., 2012). However, fox movement data (GPS and accelerometer; see details below) used to parameterize the model were collected within the goose colony. Snow geese can influence fox habitat selection and diet within the colony (Giroux et al., 2012; Grenier-Potvin et al., 2021). Such effects could slightly bias the average values of a few parameters used in our models (e.g., daily distance traveled, time spent active). However, we are highly confident that the effect of lemming fluctuations on fox behavior is relatively similar across the landscape because fox reproduction and predation pressure on bird nests are strongly influenced by lemming density both inside and outside the goose colony (Giroux et al., 2012; Lamarre et al., 2017; Duchesne et al., 2021).

3.7.2. Deriving mechanistic models of multi-prey functional response

General model description and model without density-dependence (model A)

The multi-prey mechanistic functional response model was derived by breaking down the predation process into steps. Our approach follows the theoretical framework proposed by Wootton et al. (2021) and we built on a mechanistic model that was developed for fox-prey dyads (Beardsell et al., 2021). Fox predation was decomposed into a maximum of 6 steps depending of the prey species: (1) search, (2) prey detection, (3) attack decision, (4) pursuit, (5) subjugation and (6) manipulation. Each step was adapted to each prey species according to their anti-predator behavior and the fox behavior observed during the bird nesting season (Beardsell et al., 2021). Figure 3.2 provides an overview of the mechanistic model (prey 1 is lemmings, prey 2 is passerine nests and prey 3 is sandpiper nests).

For the three prey species (i = 1, 2, 3), the area searched ($A_{search,i}$, km^2) by the predator is expressed by the product of the daily distance traveled when the predator is active (s, km day^{-1}), the reaction distance to a prey item (d_i, km), and the time spent searching (T_{search}, day):

$$A_{search,i} = s \cdot (2d_i) \cdot T_{search} \tag{3.1}$$

A potential encounter occurs between the predator and a prey item i when the predator is at a distance (d_i), being defined as the maximum distance at which the predator can detect a prey item i (in 2D, detection region = $2d_i$; Pawar et al. (2012)).

As not all lemmings within the searched area may be detected, attacked and subdued by the arctic fox, we introduced the detection probability ($f_{2,1}$), the attack probability ($f_{3,1}$), and the success probability of an attack ($f_{4,1}$). Capture efficiency of a lemming (α_1, km^2 day^{-1}) by the predator is expressed by:

$$\alpha_1 = s \cdot (2d_1) \cdot f_{2,1} \cdot f_{3,1} \cdot f_{4,1} \tag{3.2}$$

For passerine (prey 2) and sandpiper nests (prey 3), the capture efficiency is simply the product of s, the reaction distance (d_2 or d_3, km) and the detection probability ($f_{2,2}$ or $f_{2,3}$), because

their nests are always predated when detected (the attack and success probabilities = 1).

Handling time per lemming (h_1, day prey item $^{-1}$) sums the time spent chasing (means of successful and unsuccessful attacks) and the time spent manipulating a lemming once subdued. The average chase time for a successful and a failed attack is slightly different (110 and 70 seconds, respectively (n = 230 attacks)). Adding this source of variation in handling time to the model had negligible effects on predator acquisition rates. The manipulation time of lemmings is divided in three mutually exclusive behaviors: the lemming is either 1) consumed, 2) hoarded, or 3) delivered (Careau et al., 2007). The handling time of lemmings is hence expressed as follows:

$$h_1 = \frac{T_{pursue,1}}{f_{4,1}} + (T_{consume,1} \cdot e_1 + T_{hoard,1} \cdot o_1 + T_{deliver,1} \cdot de_1) \tag{3.3}$$

where e_1, o_1 and de_1 are respectively the probability that a lemming is consumed, hoarded or delivered to the den. The sum of e_1, o_1 and de_1 equals 1. $T_{consume,1}$, $T_{hoard,1}$ and $T_{deliver,1}$ is the average amount of time each behavior lasted. As many other carnivores (Jeschke, 2007), arctic foxes probably often meet or exceed their daily energy requirements during the summer. However, there is no evidence that short-term energy needs influence arctic fox behavior since they can harvest more prey than they consume in the short term and also cache prey for later consumption (e.g., during winter; Careau et al. 2007). Hence, prey digestion time was not included in the model. As passerines and sandpipers are unable to defend their clutches against arctic foxes (Smith and Edwards, 2018; Hussell and Montgomerie, 2020), their nests are always predated when detected (negligible chasing time) and consumed immediately upon detection (Beardsell et al., 2021). Thus, the handling time of passerine and sandpiper nests (h_2 and h_3) includes only the time spent consuming the nest ($T_{consume,2}$ and $T_{consume,3}$).

The number of prey captured ($V_{\alpha i}$) is the product of the time spent searching (T_{search}, day) and the prey density (N_i, number of i km^{-2}):

$$V_{\alpha i} = \alpha_i \cdot T_{search} \cdot N_i \tag{3.4}$$

The total time available in a day (T_{total}) is reduced by the proportion of time spent active by the predator in a day (ϕ_{active}) and by the time spent handling prey 1, 2 and 3 if subdued:

$$T_{search} = T_{total} \cdot \phi_{active} - V_{\alpha 1} \cdot h_1 - V_{\alpha_2} \cdot h_2 - V_{\alpha_3} \cdot h_3 \tag{3.5}$$

Substituting T_{search} from eq. 3.5 into eq. 3.4 and by dividing it by T_{total} to express the number of prey 1 acquired per predator per day ($FR_1(N_1, N_2, N_3)$), we obtain the following final formulation:

$$FR_1(N_1, N_2, N_3) = \frac{\phi_{active} \cdot \alpha_1 \cdot N_1}{1 + \alpha_1 \cdot h_1 \cdot N_1 + \alpha_2 \cdot h_2 \cdot N_2 + \alpha_3 \cdot h_3 \cdot N_3} \tag{3.6}$$

An equivalent equation for the predator acquisition rate on prey 2 and 3 can be obtained by substituting all 1 for 2 (or 3) in Eq. 4.14 and vice versa. Eq. 4.14 is the basic model, without density dependence in the predation components (model A). In model A, positive indirect effects between prey species can be generated only through prey handling processes. Below, we provide details on the inclusion of prey density-dependence on some components in models B and C.

Models including prey density-dependence (models B and C)

We added a dependence on lemming density in the probability that a lemming is delivered to the den (model B; see Table 3.1) by modifying Eq. 3.3 as follows:

$$h_1 = \frac{T_{pursue,1}}{f_{4,1}} + (T_{consume,1} \cdot e_1 + T_{hoard,1} \cdot o_1 + T_{deliver,1} \cdot de_1(N_1)) \tag{3.7}$$

We added a dependence on lemming density in the daily distance traveled (s), and proportion of time spent active (ϕ_{active}; model C; see Table 3.1) by modifying Eqs. 3.2 and 3.5 as follows:

$$\alpha_1 = s(N_1) \cdot (2d_1) \cdot f_{2,1} \cdot f_{3,1} \cdot f_{4,1} \tag{3.8}$$

$$T_{search} = T_{total} \cdot \phi_{active}(N_1) - V_{\alpha 1} \cdot h_1 - V_{\alpha_2} \cdot h_2 - V_{\alpha_3} \cdot h_3 \tag{3.9}$$

Although ϕ_{active} and s can be expressed as a function of all prey species densities, we have only considered lemming density as sandpipers and passerines nest at low densities (7 and 2 nests per km^2 on average, respectively). As arctic foxes cache a large proportion of they capture (Careau et al., 2007), we also assume that the proportion of time spent active is not affected by the rate of prey capture in the previous days.

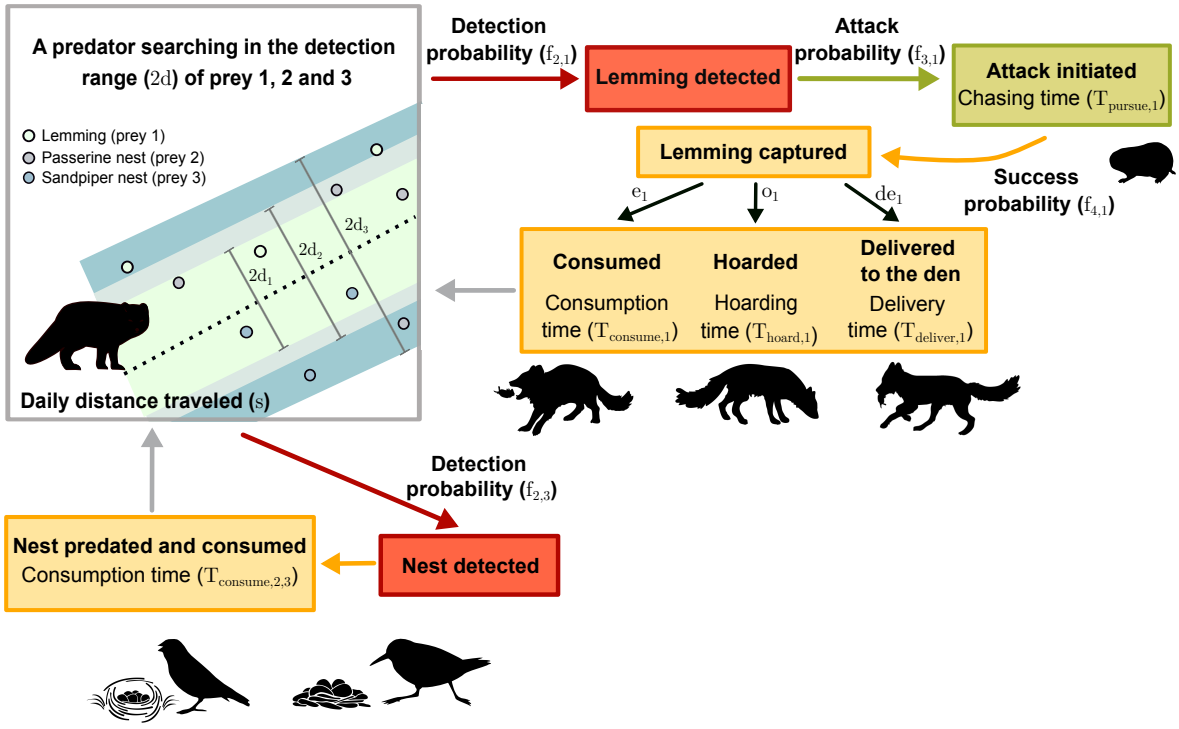

Figure 3.2. Conceptual mechanistic model of predator (arctic fox) functional response to density of a cyclic prey (prey 1; lemmings) and other prey species (prey 2 and 3; ground-nesting birds). The boxes represent the components of predation (search, prey detection, attack decision, pursuit, subjugation and manipulation). Arrows represent the probability that the predator reaches the next component. When there is no parameter near the arrow, the probability to reach the next component is assumed to be 1. The model represented has no prey density dependence in the parameters.

3.7.3. Parameter values

From June to August 2018 and 2019, 16 foxes (7 females and 9 males) were fitted with high-frequency GPS collars and tri-axial accelerometers (95 g, 2.6–3.3% of body mass; Radio Tag-

14, Milsar, Romania) to monitor their movements and behaviors. Of these, 7 were equipped in both years, for a total of 23 summer foxes (8 foxes in 2018 and 15 in 2019). Foxes were captured using cage traps (Tomahawk Live Trap Company, USA) or Softcatch #1 padded leghold traps (Oneida Victor Inc. Ltd., USA). GPS fix intervals were set to 4 minutes (360 fixes day^{-1}) and the location error was 11 m (Poulin et al., 2021); 30-second bursts of accelerometry data were collected every 4.5 minutes at 50 Hz (320 bursts day^{-1}; Clermont et al. 2021*a*). We extracted the daily activity budget of foxes from accelerometry data (Clermont et al., 2021*a*). We estimated the proportion of time spent active by subtracting the proportion of time spent resting from 1. We estimated an average proportion of time spent active using a linear mixed model with year and individual-fox as random effects. The average proportion of time spent active in a day (ϕ_{active}) was 0.50 (n = 371 fox-days; 95% CI (0.40-0.60); Table 3.2) and ranged from 0.29 to 0.64.

The distance traveled by foxes each day (km day^{-1}) was estimated by adding linear distances between successive GPS locations and was extracted from 5 June to 9 July to cover the incubation period of most birds. Days with less than 75% of observations (i.e., 270 daily fixes) were excluded from analyses to avoid underestimating daily distances. Since the distance and the proportion of time spent active were closely correlated (Fig. 3.3a), we applied a linear mixed model to estimate the average daily distance with the distance as the response, the proportion of time spent active as a fixed factor, and individual-fox and year as random effects. The predicted average daily distance traveled was 41 km (n = 371 fox-days; 95% CI (32-49 km)) and ranged from 19 to 62 km while setting the proportion of time spent active at the average (i.e., 0.50).

The probability that a lemming captured was either consumed, hoarded or delivered to the den was estimated based on behavioral observations of foraging foxes (n = 74 in 2004-2005; see Careau et al. 2007). Hoarding and consumption time were estimated with the same method and averaged 42 sec (n = 31) and 32 sec (n = 47) respectively. Average delivering time was estimated at 337 sec on the basis that i) dens are generally located close to the centroid of the home range, ii) home ranges average 10 km^2 (Grenier-Potvin et al., 2021), iii) the average speed of an active fox is 3.8 km h^{-1} (this study), and iv) foxes return an average of 5 lemmings

per trip to the den (based on 164 lemming deliveries to the den; Berteaux unpublished data).

Values for the remaining parameters of the functional response of foxes to lemmings, passerines, and sandpipers were extracted from Beardsell et al. (2021) and are summarized in Table 3.2. Parameter values were estimated using a combination of direct observations of foraging foxes (n = 124 hours, 1996-2019), camera traps (2006-2016), and information from the literature (see Beardsell et al. 2021 for more details). We conducted simulations for different values of detection probability for the three prey species since there were a high uncertainty in these parameter values Beardsell et al. (2021). We presented results of all the simulations in Figs. 3.6, 3.7, and 3.8. We used a detection and attack probability of 0.15 (the product of $f_{2,1}$ and $f_{3,1}$) since the number of lemmings captured per day predicted by the model with this value is more consistent with the highest acquisition rate of foraging foxes observed in the field at high lemming densities (i.e., 2.5 lemming h^{-1} for active foxes; Beardsell et al. 2021). We used intermediate values of 0.12 (z_2) and 0.029 (z_3) in the results.

Tableau 3.2. Values of parameters used in the multi-species functional response model of a mammalian predator (arctic fox) to density of a cyclic prey (prey 1; lemmings) and two other prey species (prey 2 and 3; passerine and sandpiper nests, respectively). Parameter values were estimated from a combination of high-frequency GPS and accelerometry (23 summer foxes, 2018-2019), behavioral observations (n = 124 hours, 1996-2019) and camera traps (2006-2016) data.

Parameter name	**Symbol**	**Value(s)**	**Unit**
Proportion of time spent active in a day	ϕ_{active}	0.5	-
Daily distance traveled (when ϕ_{active} = 0.5)	s	41	km day^{-1}
Lemmings			
Lemming density	N_1	0-700	ind. km^{-2}
Maximum reaction distance	d_1	0.0075	km
Average detection and attack probability within the reaction distance	$f_{2,1} * f_{3,1}$	0.15	-
Success probability	$f_{4,1}$	0.51	-
Chasing time	$T_{pursue,1}$	1.0 x 10^{-3}	day ind.$^{-1}$
Consumption time	$T_{consume,1}$	3.8 x 10^{-4}	day ind.$^{-1}$
Consumption probability	e_1	0.48	-
Hoarding time	$T_{hoard,1}$	4.9 x 10^{-4}	day ind.$^{-1}$
Hoarding probability	o_1	0.32	-
Delivering time	$T_{deliver,1}$	3.9 x 10^{-3}	day ind.$^{-1}$
Delivery probability	de_1	0.20	-
Passerine nests			
Passerine nest density	N_2	0-15	nests km^{-2}
Maximum reaction distance	d_2	0.02	km
Average detection probability within the reaction distance	$f_{2,2}$	0.12	-
Consumption time	$T_{consume,2}$	3.6 x 10^{-4}	day nest^{-1}
Sandpiper nests			
Sandpiper nest density	N_3	0-7	nests km^{-2}
Maximum reaction distance	d_3	0.085	km
Average detection probability within the reaction distance	$f_{2,3}$	0.029	-
Consumption time	$T_{consume,3}$	2.8 x 10^{-3}	day nest^{-1}

3.7.4. Density-dependent functions and simulations

We used data from behavioral observations of foraging foxes to define the density-dependent function of the probability that a lemming is delivered to the den. The probability that a lem-

ming captured was delivered to the den is positively related to lemming density (from 0.04 to 0.22 for a year of low and high lemming density respectively; Careau et al. 2007). As the probability that a fox pair is breeding increases markedly around a lemming density of 100 ind. km^{-2} (Juhasz et al., 2020), we used a sigmoidal function to describe the relationship between delivery probability and lemming density (Fig. 3.3c).

We used a combination of foxes accelerometry and GPS tracking data to define the parameter space of the density-dependent functions of the daily proportion of time spent active and distance traveled by the predator. These data were available for two years contrasted by very low (2 lemmings km^{-2} in 2018) and intermediate (137 lemmings km^{-2} in 2019) lemming densities. We applied a linear mixed model to estimate the distance traveled and the proportion of time spent active for both lemming densities. We included the distance traveled (km day^{-1}) as the response, the proportion of time active and lemming density as fixed effects and individual-fox as random effect. Predicted proportion of time spent active was higher at low than at intermediate lemming density (Fig. 3.3b1). Predicted daily distance traveled was also higher at low than at intermediate lemming density even when the proportion of active time was set at 0.5 (Fig. 3.3b2). Based on these results and using the range of values observed for individuals tracked with GPS, as well as the 95% confidence intervals of the average daily distance traveled and the proportion of time spent active recorded over two years, we generated 3 density-dependence functions for each parameter (Figs. 3.3d1 and d2, Fig. 3.9). The model outputs obtained with one function are presented in the results and all other simulations are presented in the supplementary figures.

3.7.5. Field evaluation of models

We evaluated the model outputs (A, B, and C) using a 15-year time series (2005-2019) of prey densities and bird nesting success. Lemming densities were estimated annually using live trapping (see Fauteux et al. 2018 for methods). Sandpiper and passerine nest densities were estimated by the maximum number of nests found in an 8 km^2 plot systematically searched during the nesting season. Each year, nests were revisited every 2-6 days to deter-

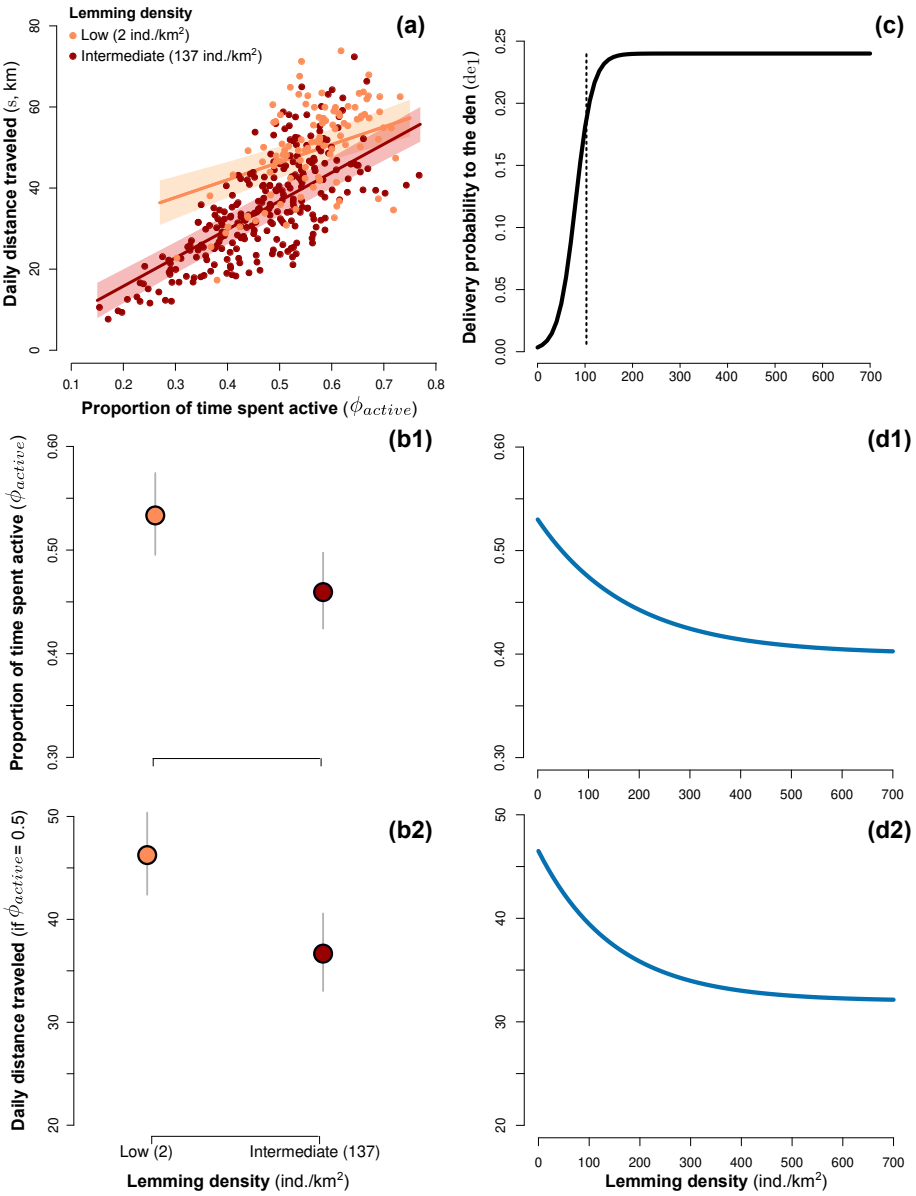

Figure 3.3. (**a**) Relationship between the daily distance traveled by the arctic fox and the proportion of time it spent active. Colored lines represent predicted relationships and 95% confidence intervals for low and intermediate lemming densities, and dots represent observed data (n = 371 fox-days). (**b1**) Predicted proportion of time spent active per day and (**b2**) predicted daily distance traveled by the fox between low and intermediate lemming densities. Error bars represent 95% confidence intervals. Density-dependent relationships of the (**c**) probability that a lemming (prey 1) is delivered to the den, (**d1**) proportion of time spent active, and (**d2**) daily distance traveled. The dashed line in (**c**) indicates a threshold at which the probability that a fox pair is breeding increases markedly (Juhasz et al., 2020). Figures **c, d1**, and **d2** are partially derived from empirical observations (see methods).

mine clutch/brood size and nest status (Gauthier et al., 2013; McKinnon et al., 2014). A nest was considered successful if at least one young left the nest (sandpipers) or fledged (passerines). Average annual daily survival rates of passerine and sandpiper nests were estimated using the logistic exposure method (Shaffer, 2004). It was then converted to nest success by increasing daily nest survival to the power of the average number of days (∼24 days) between the laying date and the fledging date (for passerines) or hatching date (for sandpipers). See Royer-Boutin (2015) for more details on these calculations.

To compare model outputs (A, B and C) to empirical data on bird nesting success, we estimated nesting success of passerines (prey 2) and sandpipers (prey 3) from predator acquisition rates using two differential equations. These equations allow us to calculate predator acquisition rates over the bird nesting period considering that nest density decreases each day. The number of nests predated after 24 days is then divided by the maximum number of nests found in the study plot (Nb_{plot}), giving us an estimate of annual nesting success. The equation given the total number of passerine nests predated (P_2) is the product of predator acquisition rate and the number of foxes foraging in the plot (Nb_{fox}):

$$\frac{dP_2}{dt} = FR_2(N_1, N_2, N_3) \cdot Nb_{fox} \tag{3.10}$$

The rate of change in passerine nest density (N_2) is expressed as follows:

$$\frac{dN_2}{dt} = \frac{(Nb_{plot} - P_2)}{plot} - N_2 \tag{3.11}$$

Where Nb_{plot} is the maximum number of nests found in the study plot, and $plot$ the plot size (8 km ^{2}). Equivalent equations for sandpiper nests can be obtained by substituting all 2's for 3's and vice versa. The model was run for 24 days which corresponds to the duration between the laying date and the fledging date (for passerines) or hatching date (for sandpipers). We assumed that 2 foxes were foraging in the study plot since foxes establish territorial pairs with little overlap between neighboring territories (Clermont et al., 2021*b*; Grenier-Potvin et al., 2021). The model was implemented in R v. 4.0.4 (R Core Team, 2022).

3.8 Results

3.8.1. Multi-prey mechanistic models of functional response

Functional response of the predator (arctic fox) to all prey species were generated for multi-prey models with or without a dependence of some model components on lemming density (Fig. 3.4). According to the model A (based on the multi-prey version of the Holling disk equation), the maximum acquisition rate within the range of lemming densities observed in our study system was 30 lemmings·fox^{-1}·day^{-1} (Fig. 3.4a). Including a dependence of lemming handling time on their density through prey delivery (model B) had almost no effect on the functional response of the predator to lemming densities (Fig. 3.4a; maximum acquisition rate remained the same). However, adding a dependence of predator activity time and distance traveled on lemming density (model C) reduced the maximum acquisition rate to 18 lemmings ·fox^{-1}·day^{-1} (Fig. 3.4a). Over the range of prey densities observed in our study system, the functional response of foxes to lemmings does not reach a plateau for all three models. The use of different density-dependence functions of the predator activity time and distance traveled (either linear or hyperbolic) led to relatively similar functional responses of arctic foxes to lemmings (Fig. 3.10). Finally, within the range of prey densities observed in our study system, variation in the density of passerine and sandpiper nests had negligible effect on the acquisition rate of lemmings by the predator and, therefore, it is not illustrated in Figure 3.4a.

Acquisition rate of passerine and sandpiper nests by the predator decreased slightly with increasing lemming density when considering only prey handling processes in the multi-prey model without density-dependence (model A). The slope of acquisition rate was 18% lower when comparing a low (0 ind. km^{-2}) and a high (700 ind. km^{-2}) lemming year (Figs. 3.4b and 3.4c). Similarly, including a dependence of lemming handling processes on their density (model B) reduced the slope of nests acquisition rate by 19% between a low and high lemming year. Finally, as illustrated in Figs. 3.4b and 3.4c, the models including a dependence of predator activity time and distance traveled on lemming density (model C) had the most

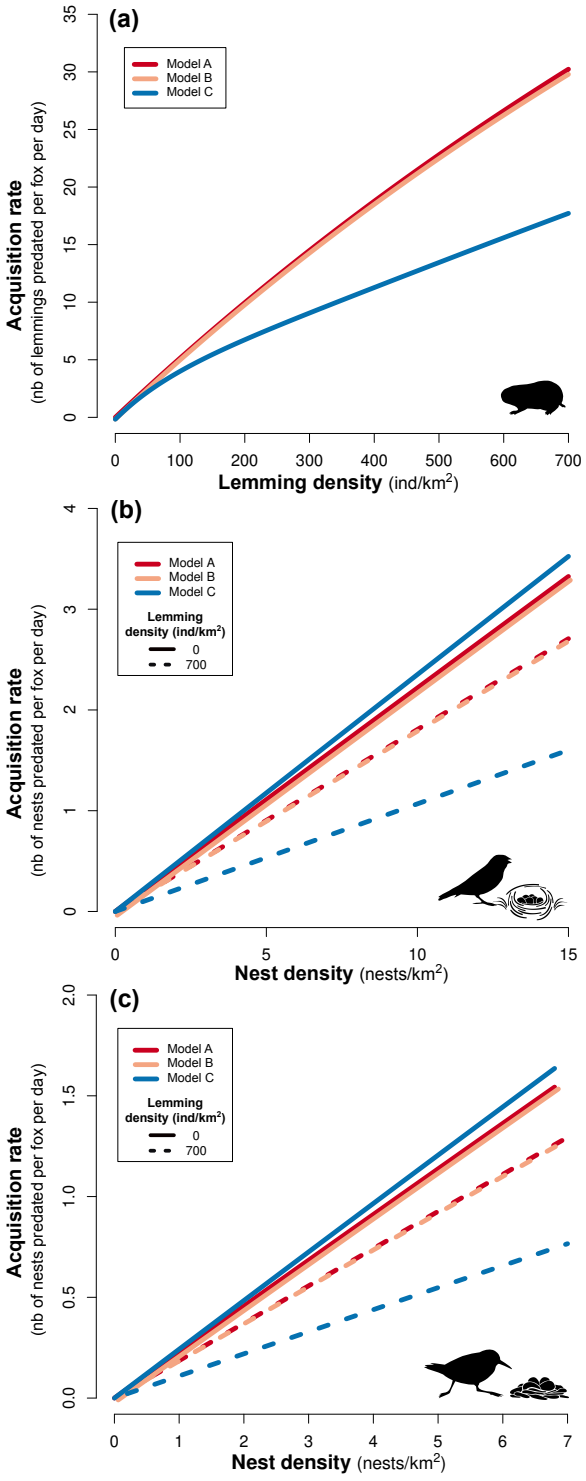

Figure 3.4. Functional response of the predator (arctic fox) to prey 1 (lemmings; **a**), prey 2 (passerine nests; **b**) and prey 3 densities (sandpiper nests; **c**) according to models A, B, and C. Model A is based on the multi-prey version of the Holling disk equation, model B modifies model A by adding density-dependence in lemmings handling processes through prey delivery, and C modifies model A by adding density-dependence in predator activity time and distance traveled. Densities of prey 2 and 3 are set at intermediate densities in **a**.

pronounced effect as it reduced the slope of passerine and sandpiper nest acquisition rate by 54% between a low and high lemming year.

3.8.2. Field evaluation of the multi-prey models

Summer lemming density varied from 2 to 648 individuals per km^2 from 2005 to 2019. A total of 625 passerine nests were monitored during this period and annual nesting success of passerines averaged 48% (range: 8 to 88%; Fig. 3.5a). From 2005 to 2019, 292 sandpiper nests were monitored and annual nesting success of sandpipers averaged 50% (range: 4 to 100%; Fig. 3.5b).

When considering only prey handling processes, model A and B generated very limited temporal variations in bird nesting success (Fig. 3.5). This indicates that lemming handling time alone cannot generate fluctuations in annual bird nesting success consistent with our time series. Model C including a dependence in predator foraging behavior with lemming density generated temporal variations in bird nesting success that were relatively consistent with those observed in our study system, including a marked release in predation pressure at high lemming densities (Fig. 3.5). However, annual variations in bird nesting success generated by model C were of smaller amplitudes than empirical observations. Our main results were robust to variation in density-dependent functions of the predator daily proportion of time spent active and distance traveled (see supplementary figures).

3.9 Discussion

In this study, we first derived a mechanistic multi-prey functional response model by breaking down key components of predation (i.e., search, attack, pursuit and handling). We also incorporated prey density-dependence in predator foraging behavior into the model. We then applied this model to an intensively studied arctic vertebrate community to evaluate the relevance of various proximate mechanisms that could explain the short-term positive indirect

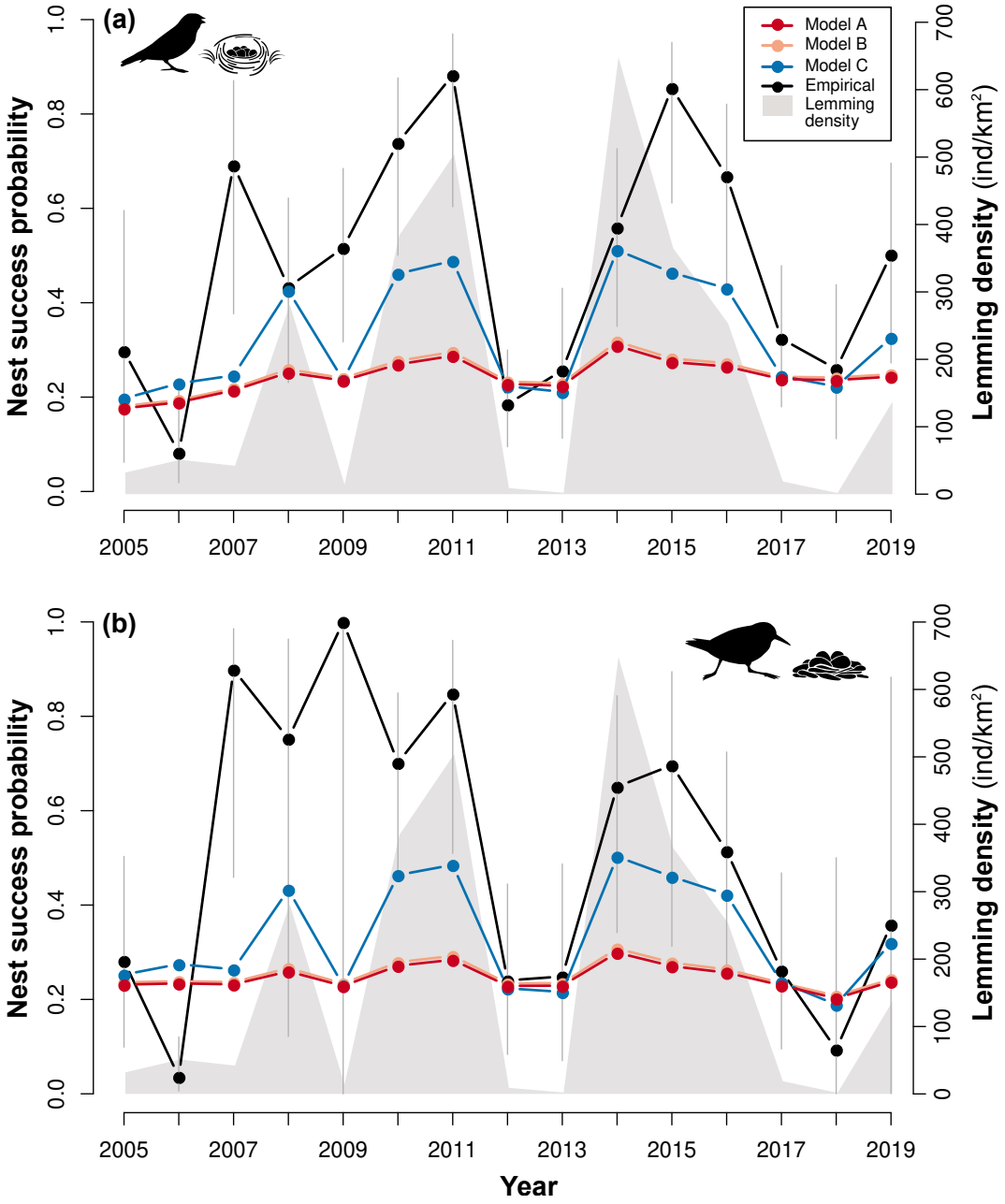

Figure 3.5. Temporal fluctuations in lemming densities (cyclic prey 1), and nesting success of passerines (**a**; prey 2) and sandpipers (**b**; prey 3). Model A is based on the multi-prey version of the Holling disk equation, model B modifies model A by adding density-dependence in lemmings handling processes through prey delivery, and C modifies model A by adding density-dependence in predator activity time and distance traveled. Model results for A and B overlap. Empirical data (lemming density and birds nest success) were acquired through long–term monitoring in the Canadian High-Arctic. Error bars are the 95% confidence intervals of nesting success estimates.

effects observed between tundra prey species. We showed that handling processes cannot explain the predation release on nesting birds observed during lemming peaks. However, we found evidence that changes in predator daily activity budget and distance traveled with respect to prey density can at least partly explain the positive indirect effects observed in a vertebrate community. These mechanisms have been little studied to date and may play a significant role in modulating species interaction strength. By disentangling the various components of predation, our approach allows for comparison of the different mechanisms modulating predator acquisition rates in order to unravel the biological underpinnings of species interactions. Although the model was inspired by an active hunting predator, modular approach could conceivably be applied to a broad range of food webs by incorporating ecological processes and constraints relevant to the study system (e.g., predator hunting strategy, predator interference; see Wootton et al. 2021).

Multi-prey quantitative models are commonly used and they traditionally assume a saturation of predator acquisition rates with increasing prey availability due to rate-limiting handling processes (Turchin and Hanski, 1997; Matthiopoulos et al., 2007; McLellan et al., 2010; Serrouya et al., 2015). However, predator saturation by prey handling processes does not appear to be frequently observed in the wild (Novak, 2010; Chan et al., 2017; Preston et al., 2018), and our results showed that fundamentally different mechanisms may limit predator acquisition rate. Handling time is often estimated by fitting a statistical functional response model to empirical data (Smout et al., 2010; Paterson et al., 2015) but as pointed out by Griffen (2021), this method does not ensure that handling time is an ecologically meaningful parameter. Thus, when traditional statistical models (Holling's type II and III) are fitted, care must be taken in interpreting predator foraging behavior.

We included density-dependence in handling processes of the main prey through prey delivery to offspring in our model. While this mechanism plays a minor role in our study system, the sensitivity of predator acquisition rate to this modification of the activity budget is likely to depend on predator home range size, prey load-size, predator movement rate and predator ability to forage while delivering food. For instance, prey delivery could represent a significant proportion of the activity budget for a predator with a large foraging range (e.g., alba-

trosses; Weimerskirch et al. (1993)) or constrained to bring one prey at a time to the breeding site. This type of prey density-dependent mechanism remains to be explored in other natural predator-prey systems.

Numerous studies highlight the relevance of improving functional response models and integrating alternative mechanisms that can modulate animal acquisition rates, such as predator activity level (Toscano and Griffen, 2014), prey digestion time (Jeschke, 2007; Papanikolaou et al., 2020) or time spent in vigilance (Sirot et al., 2021). Although many empirical studies have demonstrated links between prey availability and predator foraging behavior (Harding et al., 2007; Bertrand et al., 2014; Busdieker et al., 2019), empirically-based relationships of the dependence of predator foraging behavior on prey density are rarely included in predator-prey models (Stouffer and Novak, 2021). We recognize that the density-dependent functions used in our study were derived from limited empirical data. Further field investigations, such as long-term GPS and accelerometer tracking of predators over a wide range of prey densities, are needed to refine functions and fully integrate changes in predator foraging behavior in response to varying prey density. Overall, our results highlight the need to reinforce the links between multi-species functional response models and the dynamics of vertebrate communities.

The short-term, positive indirect effect of lemmings on tundra nesting birds due to shared predators was reported several decades ago and was studied over the circumpolar arctic since then (Underhill et al., 1993; Summers et al., 1998). Various mechanisms have been proposed to explain the observed pattern, including predator satiation, but none has been demonstrated (Underhill et al., 1993; Summers et al., 1998; Blomqvist et al., 2002; McKinnon et al., 2014; Bowler et al., 2020). Our results indicate that predation release on tundra birds at high lemming densities is primarily due to a reduction in arctic fox daily activity time and distance traveled. A change in prey preference is another potential mechanism that could contribute to predation release on birds (Bêty et al., 2002; Bowler et al., 2020). It refers to a situation where the preference for a prey i by the predator is greater when prey i is abundant relative to another prey, and inversely smaller when prey i is less abundant than other prey (Murdoch, 1969). An increase in preference for an abundant prey i may translate into an increase

in the probability of its detection, attack and/or success as prey i density increases because of changes in predator behavior or foraging strategy.

Changes in prey preference remain to be fully explored and demonstrated in our study system and more empirical data are needed to investigate the effect of lemming density on the probability of lemming and bird nest detection by foxes, as well as their attack and success probability. However, changes in prey preference are expected to play a relatively minor role. Indeed, even if foxes capture more lemmings when they are abundant, the handling time per lemming captured is still likely to be too low to have a significant effect on bird nest predation rates. Moreover, highly vulnerable prey like passerines and sandpipers are unable to protect their clutches against arctic foxes (Smith and Edwards, 2018; Hussell and Montgomerie, 2020). Consequently, once the nest is detected, the probability of nest attack by foxes is likely to remain high in all years because attacking these vulnerable prey systematically provides benefits to the predators and engenders very low costs (i.e., low handling time and no risk of injury). Inter-annual changes in the probability of nest attack by foxes may nonetheless occur in large-bodied nesting species able to fight back and defeat arctic foxes, as reported in snow geese (Bêty et al., 2002). Our multi-prey model could be adapted to explore the effects of such changes on annual nest predation rate.

Some variability in shorebird and passerine nesting success remains unexplained in our study system and this can be the result of a combination of factors. First, we assumed that lemming density and parameter values were homogeneous across the landscape. Better knowledge of potential spatial variation, especially within fox territories, would likely contribute to explaining variation in bird nesting success. Second, the empirical measurement of nesting success may be overestimated since nests predated very early in the nesting period were not necessarily found by observers. This may partly explain the relatively high nest success observed in some years of low lemming density (Fig. 3.5). Moreover, potential mechanisms that are not included in our model could also contribute to such discrepancy. For instance, we assumed that two foxes were foraging in the monitoring area of passerine and sandpiper nests in all years. Although this is most likely the predominant situation (Lai, 2017; Clermont et al., 2021*b*), slight changes in fox number could generate substantial variation in annual bird nest-

ing success.

A growing number of studies aim to predict trophic links based on species traits, especially body size (Gravel et al., 2013; Ho et al., 2019; Portalier et al., 2019), but multi-species mechanistic models quantifying interaction strength in natural communities are still lacking. With recent advances in biologging technology, high-frequency GPS, acoustic and accelerometer data are increasingly used to study free-ranging organisms (Williams et al., 2014; Pagano et al., 2018; Studd et al., 2021). As illustrated in our study system, the parametrization of mechanistic models with such data is a promising method to accurately quantify interaction strength in natural systems.

3.10 Acknowledgments

We thank Mark Novak, the subject-matter Editor, and the two anonymous reviewers for their helpful comments and suggestions on this manuscript. We also thank Éliane Duchesne for her contribution to the analyses of bird nesting success data, Madeleine-Zoé Corbeil-Robitaille for her help with illustrations, Marie-Pier Laplante for the English revision, and Guillaume Beardsell for the equations revision. The research relied on the logistic assistance of the Polar Continental Shelf Program (Natural Resources Canada) and of Sirmilik National Park of Canada. The research was funded by (alphabetical order): Arctic Goose Joint Venture, the Canada Foundation for Innovation, the Canada Research Chairs Program, the Canadian Wildlife Service (Environment Canada), the Fonds de recherche du Québec-Nature et technologies, the International Polar Year program of Indian and Northern Affairs Canada, the Natural Sciences and Engineering Research Council of Canada, the ArcticNet Network of Centers of Excellence, the Northern Scientific Training Program, Polar Knowledge Canada, Université du Québec à Rimouski, Université Laval and the W. Garfield Weston Foundation. Finally, we are especially grateful to the many people who helped us with field work over many years, the Mittimatalik Hunters and Trappers Organization and Park Canada's staff for their assistance.

3.11 Supplementary figures

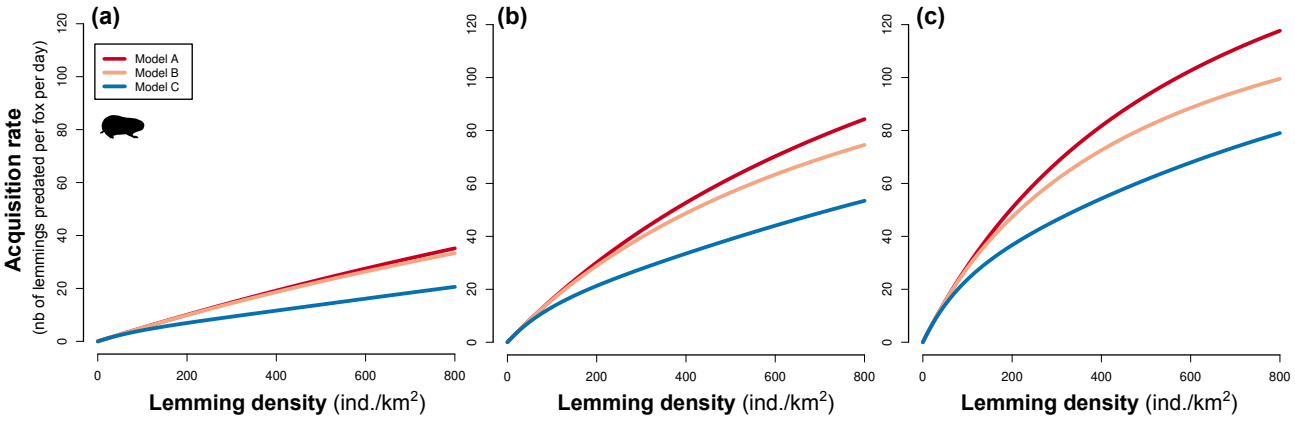

Figure 3.6. Functional response of the predator (arctic fox) to prey 1 density (lemming) for 3 values of the detection and attack probability of a lemming by the fox within the maximum reaction distance (**(a)**: $f_{2,1} * f_{3,1}$ = 0.15, **(b)**:$f_{2,1} * f_{3,1}$ = 0.50, and **(c)**: $f_{2,1} * f_{3,1}$ = 0.95). Each model is represented with a different color.

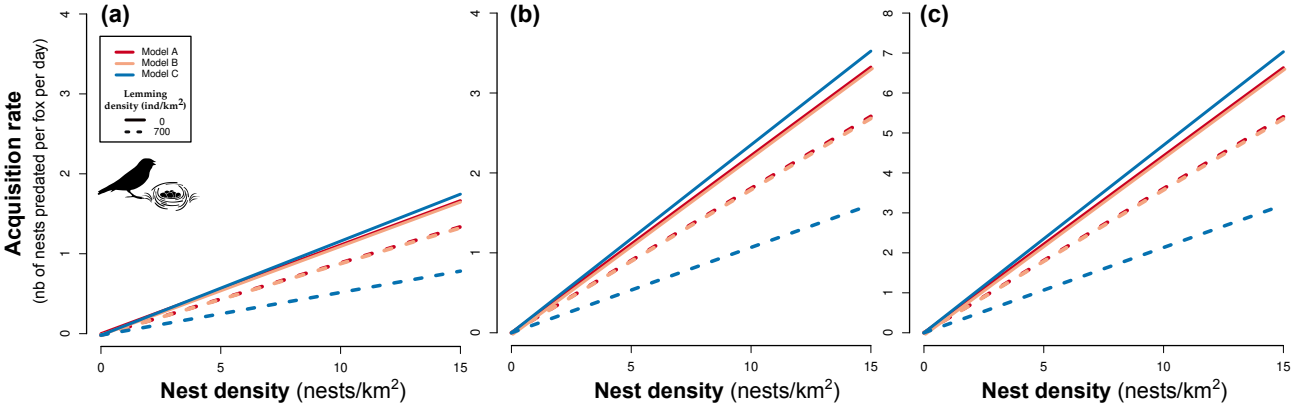

Figure 3.7. Functional response of the predator (arctic fox) to prey 2 density (passerine nests) for 3 values of the detection probability of a passerine nest by the fox within the maximum reaction distance (**(a)**: $f_{2,2}$ = 0.06, **(b)**: $f_{2,2}$ = 0.12, and **(c)**: $f_{2,2}$ = 0.24). Each model is represented by a different color at two lemming densities.

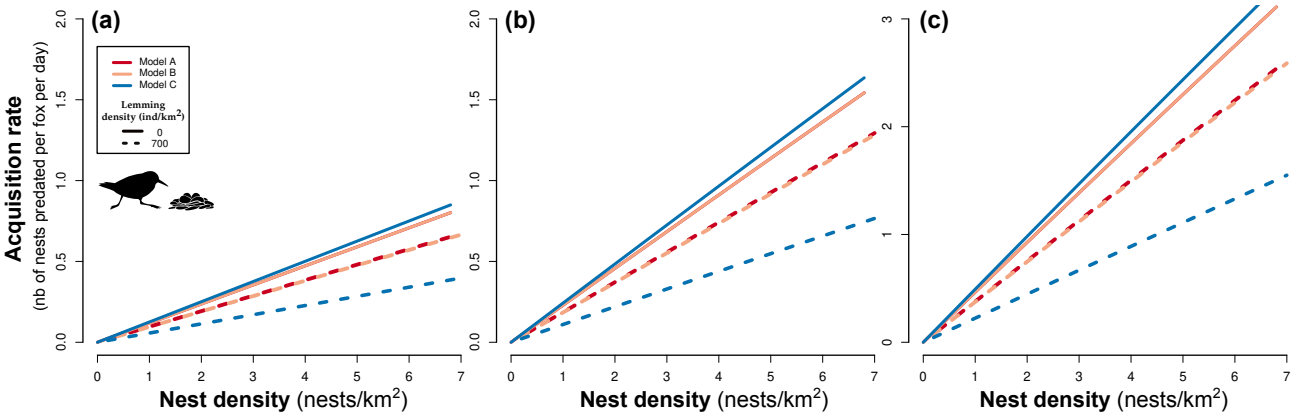

Figure 3.8. Functional response of the predator (arctic fox) to prey 3 density (sandpiper nests) for 3 values of the detection probability of a sandpiper nest by the fox within the maximum reaction distance (**(a)**: $f_{2,3}$ = 0.015, **(b)**: $f_{2,3}$ = 0.029, and **(c)**: $f_{2,3}$ = 0.059). Each model is represented by a different color at two lemming densities.

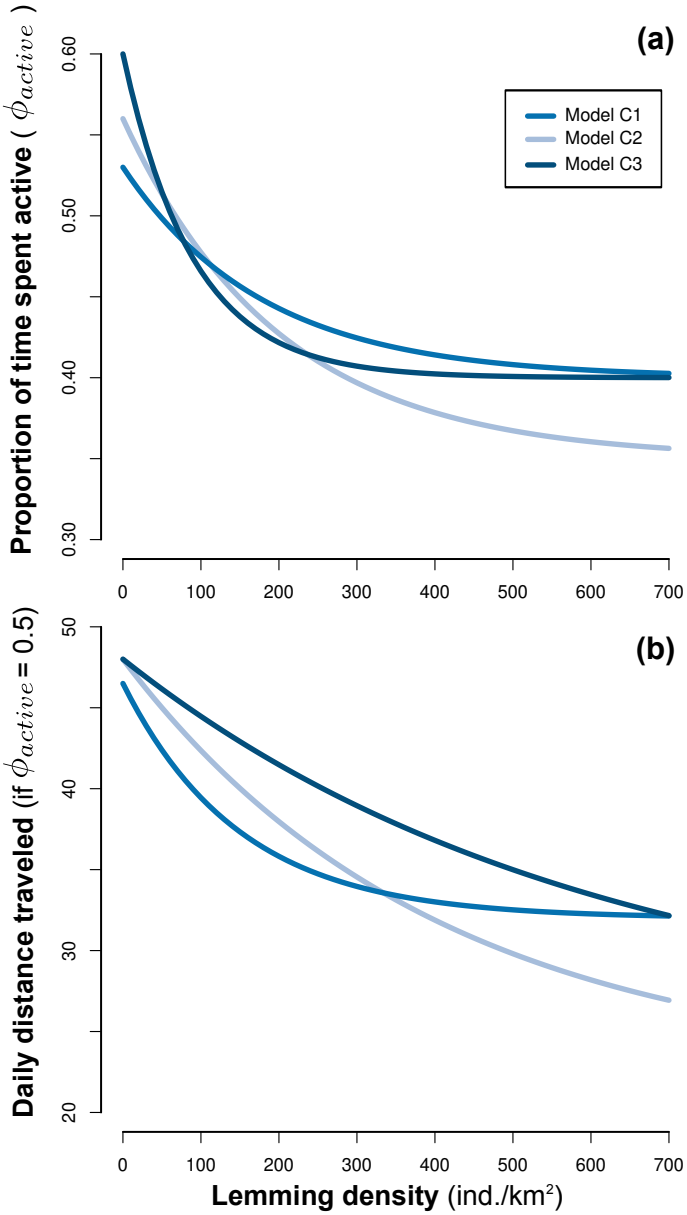

Figure 3.9. Simulations of three density-dependence functions of the predator daily proportion of time spent active (**a**) and distance traveled (**b**). Each colored line represents a simulation.

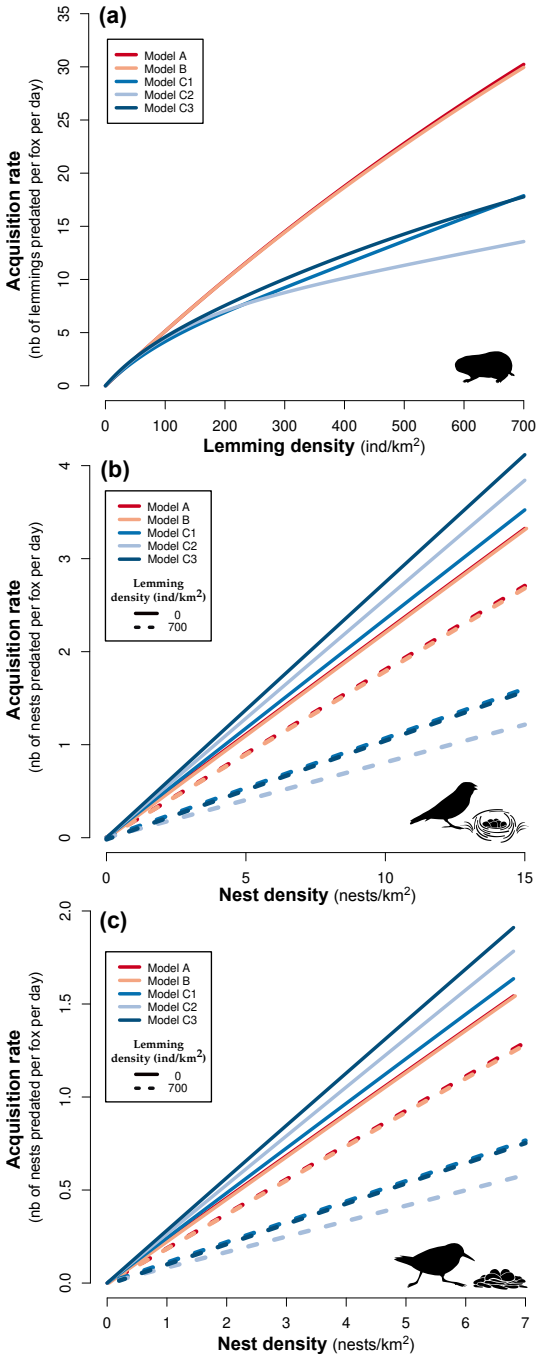

Figure 3.10. Functional response of the predator (arctic fox) to prey 1 (lemmings; **a**), prey 2 (passerine nests; **b**) and prey 3 densities (sandpiper nests; **c**) following models A, B, and C (each colored line represents a model or a simulation). Model A is based on the multi-prey version of the Holling disk equation, model B modifies model A by adding density-dependence in lemmings handling processes through prey delivery, and C modifies model A by adding density-dependence in predator activity time and distance traveled. The only difference between models C1, C2, and C3 is the density-dependence function used (see Fig.3.9). Densities of prey 2 and 3 are set at intermediate densities in **a**.

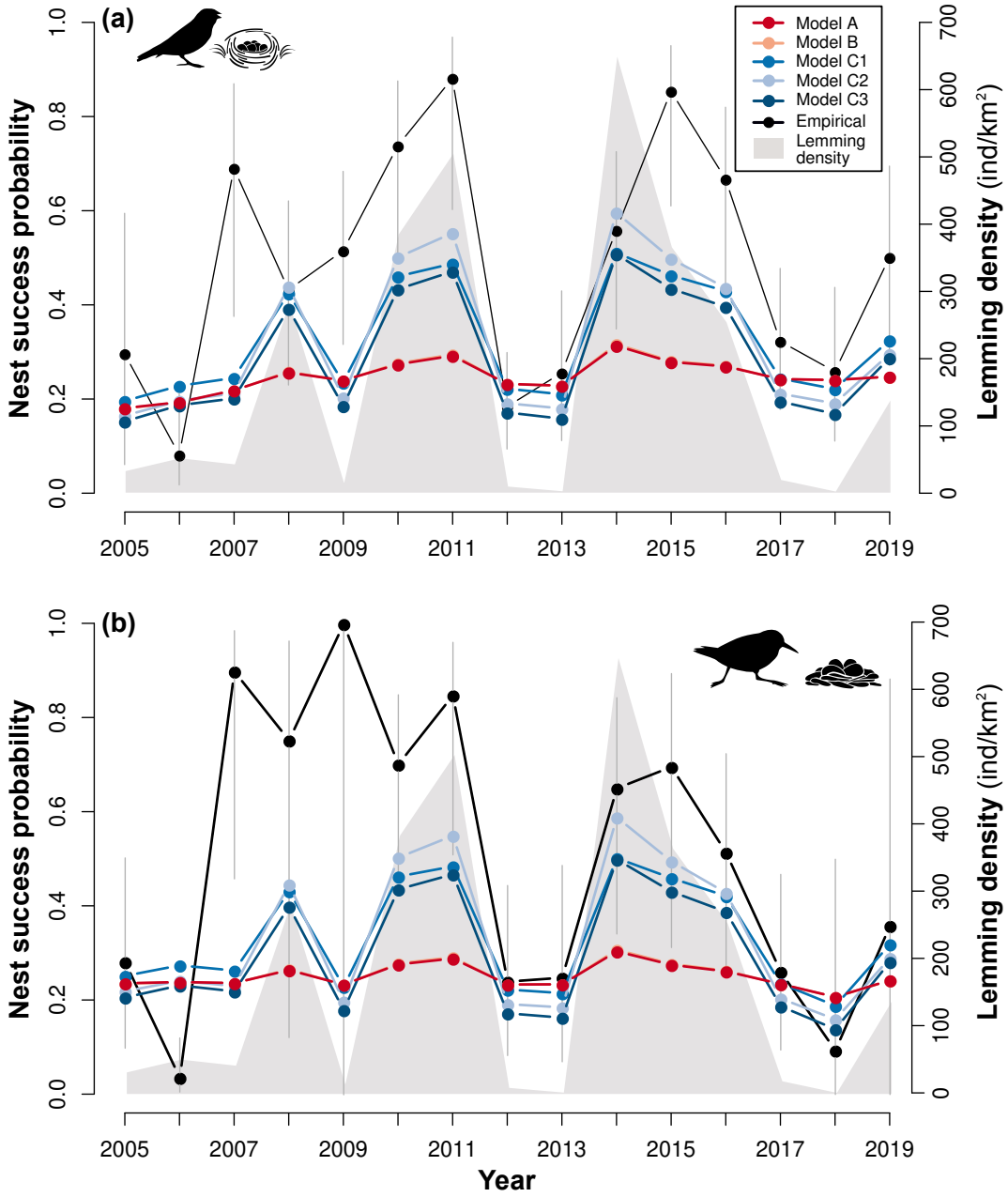

Figure 3.11. Temporal fluctuations in lemming densities (cyclic prey 1), and nesting success of passerines (**a**; prey 2) and sandpipers (**b**; prey 3). Model results and empirical time series are represented by a different color. Model A is based on the multi-prey version of the Holling disk equation, model B modifies model A by adding density-dependence in lemmings handling processes through prey delivery, and C modifies model A by adding density-dependence in predator activity time and distance traveled. The only difference between models C1, C2, and C3 is the density-dependence function used (see Fig.3.9). Model results for A and B overlap. Empirical data (lemming density and birds nest success) were acquired through long–term monitoring in the Canadian High-Arctic. Error bars are the 95% confidence intervals of nesting success estimates.

CHAPITRE 4

Des interactions indirectes à la dynamique de populations

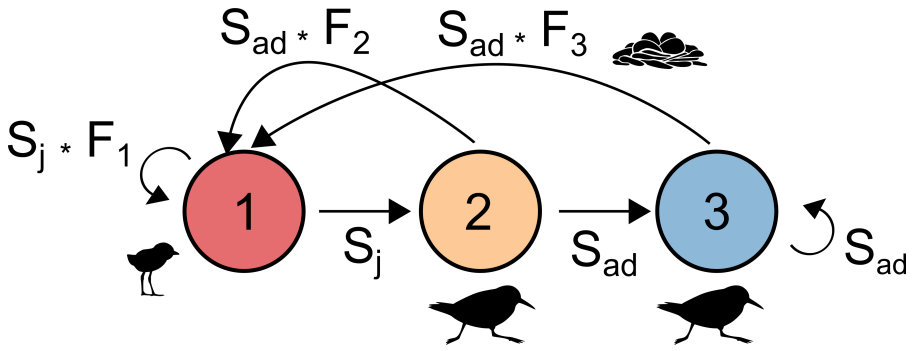

4.1 Contexte scientifique et publication associée

Cet article, intitulé *Predator-mediated interactions through changes in predator home range size can lead to local prey exclusion* a été soumis le 6 décembre 2022 à *Proceedings of the Royal Society: Biological Sciences*. En bâtissant sur les modèles mécanistiques développés dans les chapitres précédents et en les intégrant dans un modèle de dynamique de populations, cet article démontre que la présence d'une espèce de proies (l'oie des neiges) peut mener à l'exclusion locale d'une autre espèce de proie (les bécasseaux) par l'entremise d'une interaction trophique indirecte. L'originalité de cette étude est d'identifier les mécanismes proximaux af-

fectant la coexistence des proies dans une communauté naturelle de vertébrés. Cet article a été corédigé par moi-même, Dominique Berteaux, Frédéric Dulude-De-Broin, Gilles Gauthier, Jeanne Clermont, Dominique Gravel et Joël Bêty. D'une façon similaire aux chapitres précédents, cet article est le fruit de données écologiques récoltées à l'île Bylot depuis 1996 et du travail de Gilles Gauthier, Dominique Berteaux et Joël Bêty dans la coordination de ce suivi écosystémique. J'ai structuré et établi les objectifs de cet article conjointement avec Dominique Gravel et Joël Bêty. Frédéric Dulude-De-Broin a extrait la taille des domaines vitaux des renards à partir des données des colliers ARGOS. J'ai réalisé les simulations, les analyses et dirigé la rédaction de l'article. L'ensemble des co-auteurs.trices ont contribué à la rédaction et aux révisions de l'article.

Les sections suivantes sont celles de l'article soumis le 24 mai 2023.

4.2 Title

Predator-mediated interactions through changes in predator home range size can lead to local prey exclusion

4.3 Authors

Andréanne Beardsell, Dominique Berteaux, Frédéric Dulude-De-Broin, Gilles Gauthier, Jeanne Clermont, Dominique Gravel et Joël Bêty

4.4 Traduction du résumé de l'article publié

Les effets des interactions biotiques indirectes sur la coexistence des espèces sont difficiles à quantifier dans la nature. En théorie, l'exclusion d'une espèce de proie peut se produire

par le biais des réponses numériques et fonctionnelles d'un prédateur à une autre proie. Peu d'études ont évalué les effets relatifs de ces réponses sur la force d'interaction nette entre des proies partageant un prédateur, en partie parce que les modèles de réponses fonctionnelles multi-espèces basés sur des données empiriques sont très rares. Afin d'étudier si la présence d'une espèce de proie affecte les taux de prédation et le taux de croissance de la population d'une autre espèce de proie, nous avons utilisé un modèle de prédation mécanistique à proies multiples ainsi qu'un modèle matriciel de population. Les modèles ont été paramétrés en utilisant une combinaison de données comportementales, démographiques et expérimentales acquises dans une communauté de vertébrés arctiques incluant le renard arctique (*Vulpes lagopus*), un prédateur se nourrissant principalement de petits mammifères et d'œufs d'oiseaux (comme les oeufs de bécasseaux et d'oies). Nos résultats ont montré que les effets positifs de la présence d'une colonie d'oies sur le succès de nidification des bécasseaux (via le temps de manipulation des œufs par le prédateur) étaient contrebalancés par l'effet négatif d'une augmentation de la densité des renards, causée par une réduction de la taille du domaine vital des renards dans la colonie d'oies. Ainsi, l'interaction nette résultant de la présence des oies était négative. Nos résultats ont également montré que cette interaction pouvait conduire à l'exclusion locale des bécasseaux. Notre approche intègre divers mécanismes qui sous-tendent les forces d'interaction dans un système multi-proies et offre de nouvelles perspectives sur des réponses comportementales des prédateurs qui peuvent influencer la coexistence des proies dans les communautés de vertébrés.

4.5 Abstract

The strength of indirect biotic interactions are difficult to quantify in the wild and can alter community composition. To investigate whether the presence of a prey species affects population growth rate of another prey species, we quantified predator-mediated interaction strength using a multi-prey mechanistic model of predation and a population matrix model. Models were parameterized using behavioral, demographic, and experimental data from a vertebrate community that includes the arctic fox (*Vulpes lagopus*), a predator feeding on lem-

mings and eggs of various species such as sandpipers and geese. We show that the positive effects of the goose colony on sandpiper nesting success (due to reduction of search time for sandpiper nests) were outweighed by the negative effect of an increase in fox density. The fox numerical response was driven by changes in home range size. As a result, the net interaction from the presence of geese was negative and could lead to local exclusion of sandpipers. Our study provides a rare empirically based model that integrates mechanistic multi-species functional responses and behavioral processes underlying the predator numerical response. This is a major step forward in our ability to quantify the consequences of predation on community structure and dynamics.

Keywords: Functional response, numerical response, predation, indirect effects, Arctic tundra

4.6 Introduction

Understanding how and to what extent biotic interactions influence species occurrence is a major challenge because of the myriad ways species interact in natural communities (Godsoe et al., 2017). Indirect biotic interactions are especially hard to tackle because they arise through chains of direct interactions (Cazelles et al., 2016). In theory, negative indirect interactions between species that share a common predator (hereafter predator-mediated interactions) may alter community composition by excluding species that are more vulnerable to predation. Although such indirect interactions are likely widespread (Holt and Bonsall, 2017), they are difficult to quantify in complex natural communities (e.g., Schmidt and Ostfeld 2008; Iles et al. 2013; Suraci et al. 2014; Wilson et al. 2022).

Predator-mediated interactions can be quantified according to the change in the number of prey acquired per predator per unit of time (the functional response) and to the change in the number of predators (the numerical response) as a function of prey density. The net effect

of the indirect interaction on a given prey species can be either null, negative (e.g., apparent competition) or positive (e.g., apparent mutualism) depending on the relative strength of the predator functional and numerical response (Holt and Bonsall, 2017). For instance, increasing the abundance of a prey i could theoretically release predation on prey k due to reduced time spent searching for that prey (Murdoch, 1969; Murdoch and Oaten, 1975). Alternatively or additionally, increasing the density of a prey i could increase the density of predators, and consequently increase predation rate on prey k (Holt, 1977; Holt and Lawton, 1994). The balance between such opposing indirect effects has been well studied theoretically (Abrams and Matsuda, 1996) but theoretical predictions have rarely been tested in natural communities. This is in part due to difficulties in obtaining empirically-based multi-species functional response models (DeLong, 2021; Abrams, 2022) and in measuring the relative effects of the predator functional and numerical responses on the net interaction strength. Process-based mechanistic models (hereafter referred to as mechanistic models) can allow us to disentangle the relative strength of the functional and numerical responses of predators, and ultimately improve our ability to accurately quantify the strength of the net indirect interactions in ecological communities (Wootton et al., 2021; Beardsell et al., 2022).

An increase in prey densities may result in higher predator density through behavioral or demographic processes. In most predator-prey models, the numerical response of a predator is incorporated through reproduction and survival parameters (Rosenzweig and MacArthur, 1963; Courchamp et al., 2003; Serrouya et al., 2015; Abrams, 2022). Although a change in prey density is likely to influence the predator density via reproduction or survival, changes in predator behavior can also lead to marked changes in predator density. For instance, an increase in prey density modifies the costs and benefits of movements and competitive interactions, with direct effects on both home range size and local density (Loveridge et al., 2009; Payne et al., 2022). Although this idea is intuitive, the link between predator home range size and predator density is rarely explicitly incorporated in predator-multi-prey models. Yet, this is important to understand the mechanistic processes and model the net effect of predator-mediated interactions in natural communities.

Our objectives were twofold. First, we built a multi-prey mechanistic model of predation by breaking down every step of the predation process to assess whether the presence of a prey species i affects acquisition rate of a prey species k by a shared predator. We then calculated the resulting predation rates by also considering changes in predator density associated with an adjustment in predator behavior (reduction in home range size) induced by the presence of prey i. Second, we used a population matrix model to evaluate whether changes in predation rates caused by the presence of prey i can indirectly generate the local exclusion of prey k. This was illustrated in an arctic vertebrate community composed of a generalist predator, the arctic fox (*Vulpes lagopus*), feeding primarily during the summer on small cyclic mammals and eggs of various tundra bird species, including colonial nesting geese (prey i) and sandpipers (prey k).

The focal High Arctic community is characterized by high-amplitude fluctuations of lemming populations (with peaks occurring every 3–4 years), and by the presence of a large breeding colony of Snow Geese (Gauthier et al., 2013). In this community, the occurrence probability of nesting shorebirds decreases when colonial nesting geese are present, and shorebird nest predation risk (measured with artificial nests) is higher at high goose nest densities (McKinnon et al., 2013; Lamarre et al., 2017). Although the time required to handle goose eggs can reduce the time available to search for other prey like sandpiper nests, we predicted that this positive effect can be outweighed by an increase in predator density in the goose colony associated with a reduction in fox home range size (Fig. 4.1). We expected that the resulting predation rates in presence of the goose colony can be high enough to induce sandpiper local exclusion (without sandpiper immigration). The originality of this study lies in our ability to identify dominant mechanisms affecting prey coexistence (or the lack of) in a natural vertebrate community using models parameterized from a combination of behavioral, demographic, and experimental data acquired over 25 years (Gauthier et al., 2013; Weiser et al., 2020; Beardsell et al., 2021).

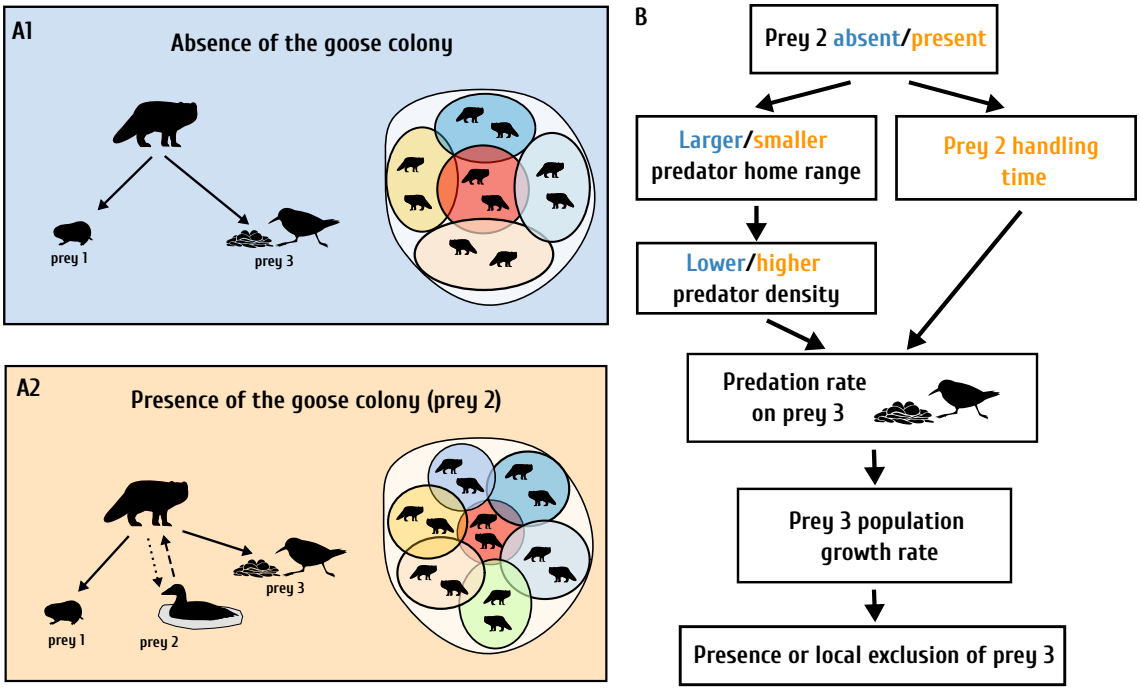

Figure 4.1. **(A)** Diagrams of simplified Arctic food webs and of fox home range size showing direct links between a predator (Arctic fox), prey 1 (lemmings), prey 2 (goose eggs), and prey 3 (sandpiper eggs) in absence (**A1**) and presence of the goose colony (**A2**). (**B**) Schematic representation of hypothesized mechanisms underlying the indirect interaction of prey 2 (goose eggs) on prey 3 (sandpiper eggs) through a shared predator (arctic fox). Although the time required to handle goose eggs can reduce the time available to search for sandpiper nests (dotted arrow), we predicted that this positive effect can be outweighed by an increase in predator density in the goose colony associated with a reduction in fox home range size (dashed arrow).

4.7 Methods

4.7.1. Study area and species

The mechanistic model of predation was built using detailed empirical data from a long-term ecological study on Bylot Island, Nunavut, Canada (73° N; 80° W). The study area ($\sim$ 500 km^2) encompasses a greater snow geese colony (*Anser caerulescens atlanticus*) of $\sim$ 20 000 pairs, which is concentrated in an area of 50-70 km^2 (McKinnon et al., 2014). The location of the goose colony centroid is relatively stable across years (Duchesne et al., 2021). Two cyclic species of small mammals are present: the brown (*Lemmus trimucronatus*) and collared

(*Dicrostonyx groenlandicus*) lemmings (Gauthier et al., 2013). The most common ground-nesting sandpipers found in the study area are the Baird's (*Calidris bairdii*) and White-rumped (*Calidris fuscicollis*) sandpipers. Both species nest on the ground at relatively low densities (<6 nests/km^2; Beardsell et al. 2021).The arctic fox is an active-searching predator (Poulin et al., 2021) and the main predator of goose and sandpiper eggs (Bêty et al., 2002; McKinnon and Bêty, 2009). In the study area, the same home range is used throughout the summer, and the degree of overlap is generally low in the population studied (Clermont et al., 2021*b*). Arctic foxes are also generally faithful to their home range year after year (Lai et al., 2017; Rioux et al., 2017). In the study area, the majority of juveniles disperse at the end of the summer (Gravel et al., 2023), and hence the density of adult foxes does not appear to be influenced by the local reproduction of the previous year. Adult survival of arctic foxes is not driven by resource variation (goose eggs and lemmings) in the study area (Chevallier et al., 2020).

4.7.2. Multi-prey model of predation

We built on a mechanistic model of arctic fox functional response to lemming and sandpiper nests developed at the same study area (Beardsell et al., 2022). We incorporated goose nests into this model based on a mechanistic model previously developed for the fox-goose dyad (Beardsell et al., 2021). This model used the Holling disk equation as a starting point and follows the theoretical framework of Wootton et al. (2021). The model was derived by breaking down fox predation into a maximum of 6 steps: (1) search, (2) prey detection, (3) attack decision, (4) pursuit, (5) capture and (6) manipulation. Each step was adapted to each prey species according to their anti-predator behavior and the fox hunting behavior (Beardsell et al., 2021, 2022). Figure 4.2 provides an overview of the multi-prey mechanistic model (prey 1 is lemmings, prey 2 is goose nests and prey 3 is sandpiper nests).

For the three prey species (i = 1, 2, 3), the area searched ($A_{search,i}$, km^2) by the predator is expressed by the product of the daily distance traveled by the predator (s; km/day), the reaction distance to a prey item (d_i, km), and the time spent searching (T_{search}, day):

$$A_{search,i} = s \cdot (2d_i) \cdot T_{search} \tag{4.1}$$

A potential encounter occurs between the predator and a prey item i when the predator is at a distance (d_i), being defined as the maximum distance at which the predator can detect a prey item i (in 2D, detection region = $2d_i$; Pawar et al. 2012). As not all prey within the searched area may be detected, attacked and subdued by the predator, we introduced the detection probability ($f_{2,i}$), the attack probability ($f_{3,i}$), and the success probability of an attack ($f_{4,i}$).

The number of sandpiper nests predated per fox per day (the predator acquisition rate) is expressed as:

$$FR_3(N_1, N_2, N_3) = \frac{\phi_{active}(N_1) \cdot \alpha_3(N_1) \cdot N_3}{1 + \alpha_1(N_1) \cdot h_1 \cdot N_1 + \alpha_2(N_1) \cdot h_2 \cdot N_2 + \alpha_3(N_1) \cdot h_3 \cdot N_3} \tag{4.2}$$

Where ϕ_{active} is the proportion of time the predator spent active in a day, N the density of each prey (ind/km^2), α the capture efficiency (km^2/day), and h the handling time per prey item (day/per prey item). Capture efficiency of a lemming (α_1) is expressed by the product of the daily distance traveled by the predator (s; km/day), the reaction distance (d_1; km), the detection probability ($f_{2,1}$), the attack probability ($f_{3,1}$) and the success probability of an attack ($f_{4,1}$):

$$\alpha_1(N_1) = s(N_1) \cdot (2 \cdot d_1) \cdot f_{2,1} \cdot f_{3,1} \cdot f_{4,1} \tag{4.3}$$

Because sandpipers cannot protect their nests once they are detected by a fox, we assumed that once a nest is detected, it is consumed. Thus, the capture efficiency of sandpiper nests is simply the product of s, the reaction distance (d_3, km) and the detection probability ($f_{2,3}$). Since we have evidence that the values of ϕ_{active} and s depend on lemming density (Model C in Beardsell et al. 2022), the value of ϕ_{active} and α are expressed as a function of lemming density (Fig. 4.4). The handling time equations for all prey and capture efficiency equations for geese can be found in the supplementary methods and associated parameter values in Table 4.1.

The predator acquisition rate of sandpiper nests in absence of a goose colony is obtained by setting the density of geese (N_2) to 0 in equation 4.2. Detailed equations of the functional response model for each prey species can be found in supplementary methods and associated parameter values in Table 4.1. For more details on the construction of the model see Beardsell et al. (2021, 2022).

We estimated predator density (NR_j; number of predators per km^2) as follows:

$$NR_j = \frac{Np}{H_{0,j}} \tag{4.4}$$

Where Np is the number of predators sharing the same home range and H_{0j} is the size of the home range exclusively shared by Np (km^2). As fox pair members share a home range (Clermont et al., 2021*b*), we assumed that two foxes were foraging per home range (Np = 2). We calculated H_{0j} as follows:

$$H_{0,j} = H_j \cdot (1 - V) \tag{4.5}$$

Where H_j is the home range size (km^2), and V is the proportion of overlap between adjacent home ranges. The value of H_j simply depends on whether a goose colony is absent (j=0) or present (j=1). We calculated fox density for the whole range of home range sizes observed in the presence or the absence of a goose colony (Fig. 4.3A). We assumed that a part of the home range is always used exclusively by Np (V cannot be equal to 1). We did not consider the presence of floaters (non-resident foxes) in the number of predators.

The number of sandpiper nests predated per day per km^2 ($P_{3,j}(N_1, N_2, N_3)$, hereafter the predation rate) is given by the product of the predator acquisition rate ($FR_3(N_1, N_2, N_3)$; nests

predated per fox per day; Eq. 4.2) and predator density (NR_j; fox per km^2; Eq. 4.4):

$$P_{3,j}(N_1, N_2, N_3) = FR_3(N_1, N_2, N_3) \cdot NR_j \tag{4.6}$$

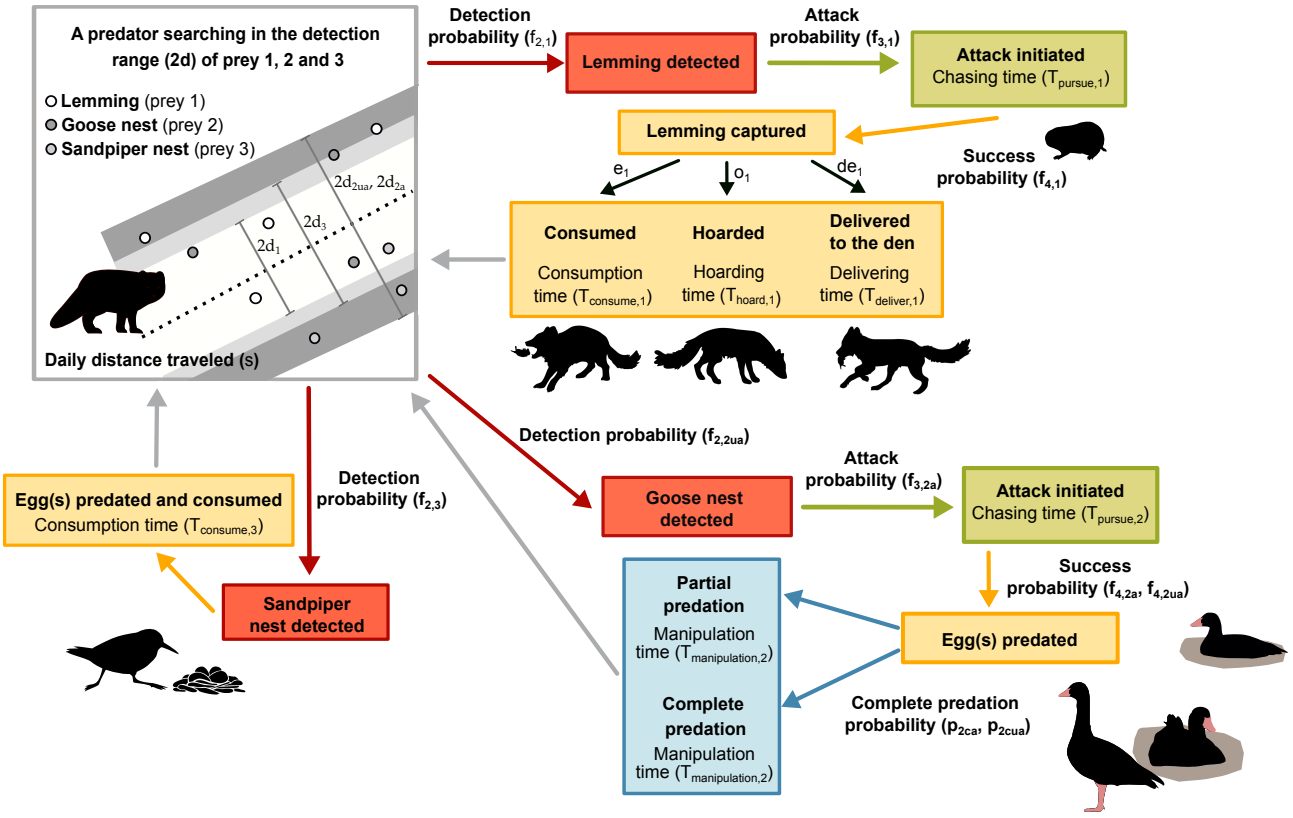

Figure 4.2. Conceptual multi-prey mechanistic model of arctic fox functional response to density of lemmings (prey 1), goose eggs (prey 2) and sandpiper eggs (prey 3). Each box represents one or more components of predation (search, prey detection, attack decision, pursuit, capture and manipulation). Arrows represent the probability that the predator reaches the next component. When there is no parameter near an arrow, the probability of reaching the next component is 1. As incubating geese can actively protect their nests from arctic foxes, their presence at the nest strongly influences fox foraging behavior. Thus, most parameter values were estimated separately for goose nests that were attended and unattended (indicated by two symbols near the arrows). Unlike geese, sandpipers cannot protect their nests once they are detected by a fox. We therefore assumed that once a nest is detected, it is consumed.

4.7.3. Parameter values

We estimated summer home range size of arctic foxes using telemetry data (Argos) of 113 foxes from 2008 to 2016 on Bylot Island. Foxes were captured and equipped with Argos radio collars as described in Tarroux et al. (2010), providing a location every 1-2 days. We estimated the area of the 95% home range contour for each individual-year between May-October using the autocorrelation-informed home range estimation workflow described in Fleming et al. (2015), and implemented in $ctmm$ R package (Calabrese et al. 2016, Dulude et al. in prep.). Home range size averages 10.8 km^2 (n = 56 home ranges) and 18.2 km^2 (n = 57) in presence and absence of the goose colony respectively (Fig. 4.3A). Based on high-frequency gps-data (13 foxes in summer 2019), the average overlap between adjacent home ranges is 0.18 on Bylot Island (Clermont et al., 2021*b*).

We set the average density of goose nests within fox home ranges at 255 nests per km^2. We derived this estimate from an exhaustive count of all goose nests present within the colony (an area of 56 km^2 in 2019; methods in Grenier-Potvin et al. 2021). The year 2019 falls within the long-term average of goose nest density measured in an intensive monitoring area (0.5 km^2) in the core of the colony from 1989-2019 (Gauthier et al., 2019).

Values for the remaining parameters of the functional response of foxes to lemmings, sandpipers and geese were extracted from Beardsell et al. (2021) and Beardsell et al. (2022), and are summarized in Table 4.1. In short, parameter values were estimated from a combination of high-frequency GPS and accelerometry data (23 summer foxes, 2018-2019), behavioral observations in the field (n = 124 hours, 1996-2019), field experiments, and camera traps deployed at nests (2006-2016).

4.7.4. Estimating nesting success

We estimated annual nesting success of sandpipers (prey 3) for the whole range of home range sizes observed in presence (N_2 = 255 nests per km^2) and absence (N_2 = 0 nests per km^2) of the goose colony using a set of differential equations. These equations allowed us to calculate the total number of nests predated per km^2 over the sandpiper nesting period (i.e., the average duration between the laying date and hatching date) while considering that the density of nests decreases each day. We assumed that the bird nesting period is synchronized, that fox predation is the only cause of nest failure, and that predated nests are not replaced. The rates of change in the total number of goose (prey 2) and sandpiper (prey 3) nests predated per day per km^2 are given by:

$$\frac{dPR_2}{dt} = P_{2,j}(N_1, N_2, N_3) \tag{4.7}$$

$$\frac{dPR_3}{dt} = P_{3,j}(N_1, N_2, N_3) \tag{4.8}$$

The rates of change in goose and sandpiper nest density (respectively N_2 and N_3) are expressed as follows:

$$\frac{dN_2}{dt} = -PR_2 \tag{4.9}$$

$$\frac{dN_3}{dt} = -PR_3 \tag{4.10}$$

The total number of sandpiper nests predated (nests per km^2) over the nesting period (24 days) was divided by the number of nests present at day 1 of nest initiation (the density of N_3 at day 1), giving us an estimate of the proportion of nests predated annually (1 minus this proportion gives the annual nesting success). The annual nesting success in absence of the goose colony was obtained by setting the density of geese (N_2) to 0 and by using only equations 4.8 and 4.10.

We also estimated annual nesting success of geese with equations 4.7 and 4.9. The total number of goose nests predated (nests per km^2) over the nesting period (28 days) was divided by the number of nests present at day 1 of nest initiation (the density of N_2 at day 1), giving us an estimate of the proportion of nests predated annually (1 minus this proportion gives the annual nesting success).

Since lemming densities fluctuate with high amplitude between years, we computed the average sandpiper nesting success over the 13-year time series of lemming densities on Bylot Island (Fig. 4.5). Inclusion of interannual variability in lemming density (from 2 to 648 ind./km^2) results in a 7% decrease in average nesting success of sandpipers relative to a constant average lemming density (i.e., 204 ind/km^2). This is consistent with the results of a different system (Barraquand et al., 2015). We conducted all models and simulations in R v. 4.2.2 (R Core Team, 2022).

4.7.5. Sensitivity analysis

We quantified the relative influence of model parameter values on the estimation of sandpiper annual nesting success by using the Latin hypercube sampling technique (an efficient implementation of the Monte Carlo methods; Marino et al. 2008). This analysis allowed us to investigate the uncertainty in the model output generated by the uncertainty and variability in parameter values. Each parameter was represented by a probability distribution (uniform or normal truncated) based on the distribution of empirical data. For some parameters, the biological information was limited, so we assigned a uniform distribution allowing for a large range bounded by minimum and maximum values. Latin hypercube sampling was then applied to each distribution (N = 1,000 iterations). For simplicity, the sensitivity analysis was conducted on the predation model (Eq. 4.6) including the presence of the goose colony (j = 1), without density-dependence in parameters s and ϕ_{active}, and with fixed prey densities (N_1 = 204 individuals/km^2 , N_2 = 255 nests/km^2, N_3 = 3.1 nests/km ^{2}).

4.7.6. Sandpiper population model

We evaluated if changes in nest predation rates caused by the presence of the goose colony can indirectly generate local exclusion of sandpipers. We used a population matrix model to link estimated nesting success to sandpiper population growth rate. Since most demographic parameters for white-rumped sandpiper and/or Baird's sandpiper are poorly documented on Bylot Island, we built upon a projection matrix model developed by Weiser et al. (2020) for the semipalmated sandpiper (*Calidris pusilla*; hereafter sandpiper), a tundra nesting species for which the demographic parameters are relatively well documented across the North American Arctic (Fig. 4.11). We calculated growth rate (λ) using the mean values of each vital rate while varying average nesting success values (NS_{ini} and NS_{renest}; see Table 4.2). Given the strong influence of annual adult survival on λ (Weiser et al., 2020), we calculated λ values for different values of adult survival. We used the $popbio$ package v. 2.7 (Stubben and Milligan, 2007) in R (R Core Team, 2022) to calculate λ. Details regarding the matrix model are available in supplementary methods.

Tableau 4.1. Symbol definition and parameter values used in the multi-prey mechanistic model of fox predation as a function of the density of lemmings (prey 1), goose nests (prey 2) and sandpiper nests (prey 3). Parameter values were estimated from a combination of high-frequency GPS and accelerometry data (23 summer foxes, 2018-2019), ARGOS telemetry data (113 summer-foxes), behavioral observations in the field (n = 124 hours, 1996-2019), the litterature, and camera traps (2006-2016). Most details regarding the estimation of parameter values can be found in Beardsell et al. (2021). Parameters related to lemming manipulation times and the fox activity budget can be found in Beardsell et al. (2022).

Parameter name	Symbol	Value(s)	Unit
Arctic Fox			
Home range size	H	3.7-48.4	km^2
Average proportion of overlap between adjacent home ranges	V	0.18	-
Daily proportion of time the predator spent active (function of N_1)	ϕ_{active}	Fig. 4.4	-
Daily distance traveled (function of N_1)	s	Fig. 4.4	km day^{-1}
Lemmings			
Lemming density	N_1	0-700	ind. km^{-2}
Maximum reaction distance	d_1	0.0075	km
Average detection and attack probability within the reaction distance	$f_{2,1} * f_{3,1}$	0.15	-
Success probability	$f_{4,1}$	0.51	-
Chasing time	$T_{pursue,1}$	1.0 x 10^{-3}	day ind.$^{-1}$
Consumption time	$T_{consume,1}$	3.8 x 10^{-4}	day ind.$^{-1}$
Consumption probability	e_1	0.48	-
Hoarding time	$T_{hoard,1}$	4.9 x 10^{-4}	day ind.$^{-1}$
Hoarding probability	o_1	0.32	-
Delivering time	$T_{deliver,1}$	3.9 x 10^{-3}	day ind.$^{-1}$
Delivering probability	de_1	0.20	-
Goose nests			
Goose nest density	N_2	255	nests km^{-2}
Nest unattendance probability	w	0.021	-
Chasing time	$T_{pursue,2}$	8.3 x 10^{-4}	day nest^{-1}
Manipulation time (includes consumption and hoarding time)	$T_{manipulation,2}$	5.8 x 10^{-3}	day nest^{-1}
Goose attended nests			
Maximum reaction distance	d_{2a}	0.033	km
Average attack probability within the reaction distance	$f_{3,2a}$	0.05	-
Success probability	$f_{4,2a}$	0.098	-
Complete predation probability	p_{2ca}	0.47	-
Goose unattended nests			
Maximum reaction distance	d_{2ua}	0.11	km
Average detection probability within the reaction distance	$f_{2,2ua}$	0.37	-
Success probability	$f_{4,2ua}$	0.93	-
Complete predation probability	p_{2cua}	0.69	-
Sandpiper nests			
Sandpiper nest density	N_3	3.1	nests km^{-2}
Maximum reaction distance	d_3	0.085	km
Average detection probability within the reaction distance	$f_{2,3}$	0.029	-
Consumption time	$T_{consume,3}$	2.8 x 10^{-3}	day nest^{-1}

4.8 Results

Summer home range size of arctic foxes varied from 3.7 to 48.4 km^2 in the study area (Fig. 4.3A). The average home range size was smaller within the colony (18.2 km^2) than outside (10.8 km^2), hence the estimated fox density was on average 1.7 times higher in the goose colony (Fig. 4.3A). The estimated goose nesting success was 77%, which is consistent with the average success estimated from intensive annual goose nest monitoring in the colony (68% between 1991 and 2015; Reséndiz-Infante et al. 2020). In absence of nesting geese, the estimated nesting success of sandpiper was 56% (Fig. 4.3B). This is also consistent with the average nesting success observed in a monitoring area located $\sim$30 km away from the goose colony on Bylot Island (50% $\pm$ 0.08 (SE) between 2005 and 2019; Beardsell et al. 2022). There is no estimate of annual sandpiper nesting success in the goose colony because sandpiper nest density is too low (Lamarre et al., 2017). Functional and total responses of the predator (arctic fox) to sandpiper nests as a function of each prey density are shown in Fig. 4.6.

Sensitivity analysis indicated that four parameters had a significant effect on annual sandpiper nesting success (Fig. 4.7). A change in the value of these four parameters by 50% generated changes in sandpiper annual nesting success by 24%, 15%, 12%, and 11% respectively for predator home range size, daily distance traveled by the predator, proportion of time spent active by the predator, and detection probability of sandpiper nests (Fig. 4.8). Neither daily distance traveled nor activity level was correlated to fox home range sizes based on high-frequency GPS and accelerometry data (Fig. 4.9). Although some parameters directly related to goose nest predation had a statistically significant influence on sandpiper nesting success (Fig. 4.7), their biological effects were limited as indicated by the low correlation coefficient (<0.21) of the relationship (Fig. 4.8). Predator home range size was thus the most influential parameter in the model.

We evaluated the net effect of colonial geese on the average sandpiper nesting success. We

first computed nesting success of sandpipers from the multi-prey mechanistic models over the range of fox densities (home range sizes) observed in the study area (Fig. 4.3B). For a given arctic fox density, the presence of nesting geese increased the estimated sandpiper nesting success by 7% (functional response effect only: Fig. 4.3B). This release of predation pressure was the result of time constraints related to goose egg handling (including chasing, hoarding, consumption), which reduced the time available to search for other prey like sandpiper nests. On the other hand, when considering only the increase in fox density caused by the presence of colonial geese (from 0.13 ind./km^2 to 0.22 ind./km^2; Fig. 4.3A), the estimated sandpiper nesting success decreased by 18% (numerical response effect only: Fig. 4.3B). The negative effect mediated by arctic fox home range size adjustment thus outweighed the predation release due to goose egg handling time, resulting in an 11% decrease in average sandpiper success in the goose colony overall (see combined effects in Fig. 4.3B).

We investigated the net effect of the goose colony on sandpipers demography. Population growth rate (λ) derived from the sandpiper matrix population model indicated that changes in sandpiper nesting success caused by the presence of colonial geese can affect local sandpiper population dynamics (Fig. 4.3C). While the predation release on sandpiper nests generated by the goose egg handling time could increase λ by 3% (functional response effect only), the reduction in sandpiper nesting success caused by higher density of foxes in the goose colony resulted in a 7% decrease of λ (numerical response effect only: Fig. 4.3C). The negative effect mediated by the increased predator density thus outweighed the positive effect generated by the functional response. When fox home range size is smaller than 13.5 km^2, which includes 80% of empirically estimated home range sizes in presence of the goose colony (n=56), the local growth rate of sandpipers is <1, in absence of immigration (Fig. 4.3C). In absence of the goose colony, the local growth rate of sandpipers is >1 when fox home range is larger than 16 km^2 (which includes 54% of empirically estimated home range sizes in absence of the goose colony (n=57: Fig. 4.3C). For the average fox home range size observed in the goose colony on Bylot Island, model outputs indicated that sandpiper adult survival has to reach a minimum of 0.78 for a λ>1 without immigration (Fig. 4.10).

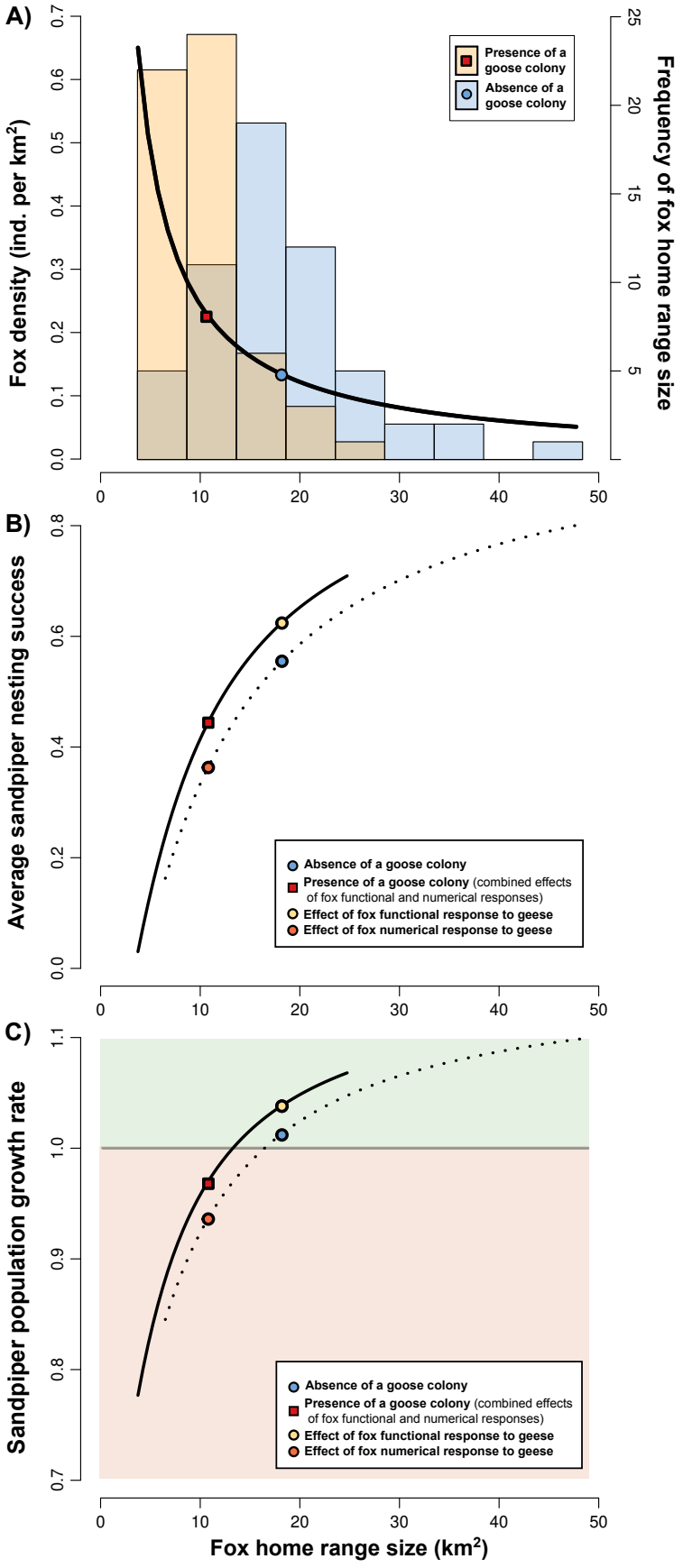

Figure 4.3. Legend on next page

Legend figure 3: (**A**) Relationship between fox density and summer home range size of arctic foxes derived from equation 4.4, and histograms of home range size (estimated from telemetry data; n = 113) in presence and absence of the goose colony. Points indicate average home range size in presence and absence of the goose colony. (**B**) Relationship between average nesting success of sandpipers and summer home range size of arctic foxes in presence (plain line) and absence (dashed line) of the goose colony. (**C**) Relationship between local growth rate (λ) of sandpipers and summer home range size of foxes in presence (plain line) and absence (dashed line) of the goose colony. Points show the average nesting success (**B**) or the local growth rate (**C**) of sandpipers for an average fox home range size in absence of geese and in presence of geese when considering the functional response of foxes to geese, the numerical response of foxes to geese, or the combined effects (functional and numerical response of foxes to geese). Areas where λ is >1 are in green and <1 in red.

4.9 Discussion

In this study, we used a mechanistic multi-prey predation model to quantify predator-mediated interaction strength in a natural system. We analyzed the model to quantify the indirect interaction between two prey species (colonial nesting geese and sandpipers) sharing a common predator (the arctic fox). We incorporated predation rates into a population matrix model to evaluate the consequences of predator-mediated interactions on local prey growth rates. Our results showed that the positive effects of the presence of the goose colony on sandpiper nesting success (due to a reduction of search time for sandpiper nests by the predator) were outweighed by the negative effect of an increase in fox density, associated with a reduction in fox home range size in the goose colony. Thus, the net interaction resulting from the presence of the goose colony on sandpiper nesting success was negative. The strength of the negative net interaction obtained could be sufficient to cause local exclusion of sandpipers for various values of adult sandpiper survival rate observed in the wild. Overall, our results indicate that predator-mediated effects could explain the low occurrence of Arctic-nesting shorebirds in areas of high goose nesting density (Flemming et al., 2016; Lamarre et al., 2017; Duchesne

et al., 2021).

The strength of the negative indirect interaction of geese on sandpipers was potentially underestimated due to a combination of factors. First, in addition to reducing home range size, the presence of abundant resources could also increase overlap between fox home ranges (Eide et al., 2004; Lai, 2017). This was not taken into account in our models because adjacent fox home ranges were not systematically monitored. Second, in addition to causing lower egg survival, higher fox density is likely to reduce chick survival. However, empirical data on chick survival is limited because sandpiper chicks leave the nest shortly after hatching. Finally, a higher density of avian predators within the goose colony (Lamarre et al., 2017) may also decrease survival rate of sandpiper chicks. These three factors would have amplified the strength of the negative effect of the presence of geese on sandpipers.

Along with changes in the predator home range size, additional components of predator behavior are likely to change in the presence of geese and more data is needed to fully explore the possible links between those parameters. Our sensitivity analysis indicated that three parameters have a notable influence on sandpiper nesting success, namely 1) daily distance traveled by the predator, 2) proportion of time spent active by the predator, and 3) sandpiper nest detection probability by the predator. We recognize that further field investigations, such as long-term GPS and accelerometer tracking of predators over a wide range of prey densities, are needed to investigate the effect of prey densities on the value of predator movement parameters. This would be especially important in our study system since changes in these movement parameters are known to be related to lemming density (Beardsell et al., 2022). Regarding the detection probability of sandpiper nests, there is no evidence that this parameter is affected by the presence of geese. This absence of effect probably reflects that attacking sandpiper nests provides systematic benefits to foxes and entails very low costs (e.g., risk of injury, handling time; Beardsell et al. 2022).

Predator-mediated interactions in natural systems have been investigated using various approaches, including statistical analyses linking prey occurrence probability with density of other prey (Flemming et al., 2019; Duchesne et al., 2021), and field experiments involving the addition or removal of prey or predator species (Menge, 1995; Spiller and Schoener, 2001). Although these approaches can help identifying the presence of indirect effects, they provide a limited ability to tease apart and infer proximate mechanisms underlying biotic indirect interactions. Moreover, field experiments in natural food webs can be impossible to implement when predator home range size is large (but see Wilson et al. 2022). Although extensive empirical data and detailed knowledge of the study system are needed to use a mechanistic approach, the growing number of technologies allowing remote monitoring of wildlife behavior (e.g., high-frequency GPS, acoustic and heart rate monitoring devices) should facilitate the application of this approach to more complex systems (Williams et al., 2014; Pagano et al., 2018; Studd et al., 2021).

Variations in the shape of the functional response can have important ecological consequences for the structure and dynamics of communities by altering the coexistence among prey, and the strength and signs of the interactions among them (Abrams et al., 1998; Abrams and Matsuda, 2004; Brose et al., 2006; Abrams and Cortez, 2015; Coblentz, 2020). However, very few empirically-based, multi-species functional responses have been developed (Abrams, 2022; DeLong, 2021). The evaluation of functional response using phenomenological models often fails to discriminate between different response shapes (e.g., between a type 2 and 3) (Novak and Stouffer, 2020), which limits our ability to quantify the strength of predator-mediated interactions in the wild. Although strong empirical foundation of multi-species functional response in natural communities is lacking, they are widely used in predator-prey models (Roemer et al., 2002; Courchamp et al., 2000, 2003; McLellan et al., 2010; Serrouya et al., 2015). To our knowledge, our study provides a rare empirically-based model that integrates mechanistic multi-species functional responses while also taking into account behavioural processes underlying the numerical response of a generalist predator. Our study is a step towards mechanistic approaches and should increase our ability to accurately quantify the consequences of

predation on wild animal community structure and dynamics.

Our results show that finer-scale behavioral processes may actually be the main drivers of predator density and prey persistence in the wild. Along with the link between predator home range size and prey availability (Loveridge et al., 2009; Bino et al., 2010; Payne et al., 2022), other processes could be explored such as the presence of predator social or aggressive interactions and predator group hunting. For instance, we might expect overlap between predator home ranges to vary with the abundance of food resources (e.g., higher overlap when prey density is very high or very low; Sells and Mitchell 2020). In arctic foxes, this could occur during years of low lemming density, in absence of a goose colony or when foxes mainly feed on unpredictable prey (e.g., carcasses). Such effects remain to be explored. As pointed out by Abrams (2022), our understanding of numerical responses is much more limited than functional responses. To date, the numerical response is typically modeled through demographic processes in classical models (see MacArthur-Rosenzweig equations; Rosenzweig and MacArthur 1963). Our approach takes into account diverse proximate mechanisms underpinning interaction strengths in a multi-prey system and generates novel insights on some of the predator behavioral responses that may influence prey coexistence (or the lack of) in vertebrate communities. Overall, this study underlines the need to explicitly investigate the consequences of various behavioral processes underlying predator numerical response.

4.10 Acknowledgments

We are grateful to the many people who helped us with field work over the years, to the Mittimatalik Hunters and Trappers Organization, and to Park Canada staff for their assistance. We also thank Marie-Pier Laplante for the English revision. The research relied on the logistic assistance of the Polar Continental Shelf Program (Natural Resources Canada) and of Sirmilik National Park of Canada. The research was funded by (alphabetical order): Arctic Goose Joint Venture, the ArcticNet Network of Centers of Excellence, the Canada Foundation for In-

novation, the Canada Research Chairs Program, the Canadian Wildlife Service (Environment Canada), the Fonds de recherche du Québec-Nature et technologies, the International Polar Year program of Indian and Northern Affairs Canada, the Kenneth M Molson Foundation, the Natural Sciences and Engineering Research Council of Canada, the Northern Scientific Training Program, Polar Knowledge Canada, Université du Québec à Rimouski, Université Laval and the W. Garfield Weston Foundation.

4.11 Supplementary figures

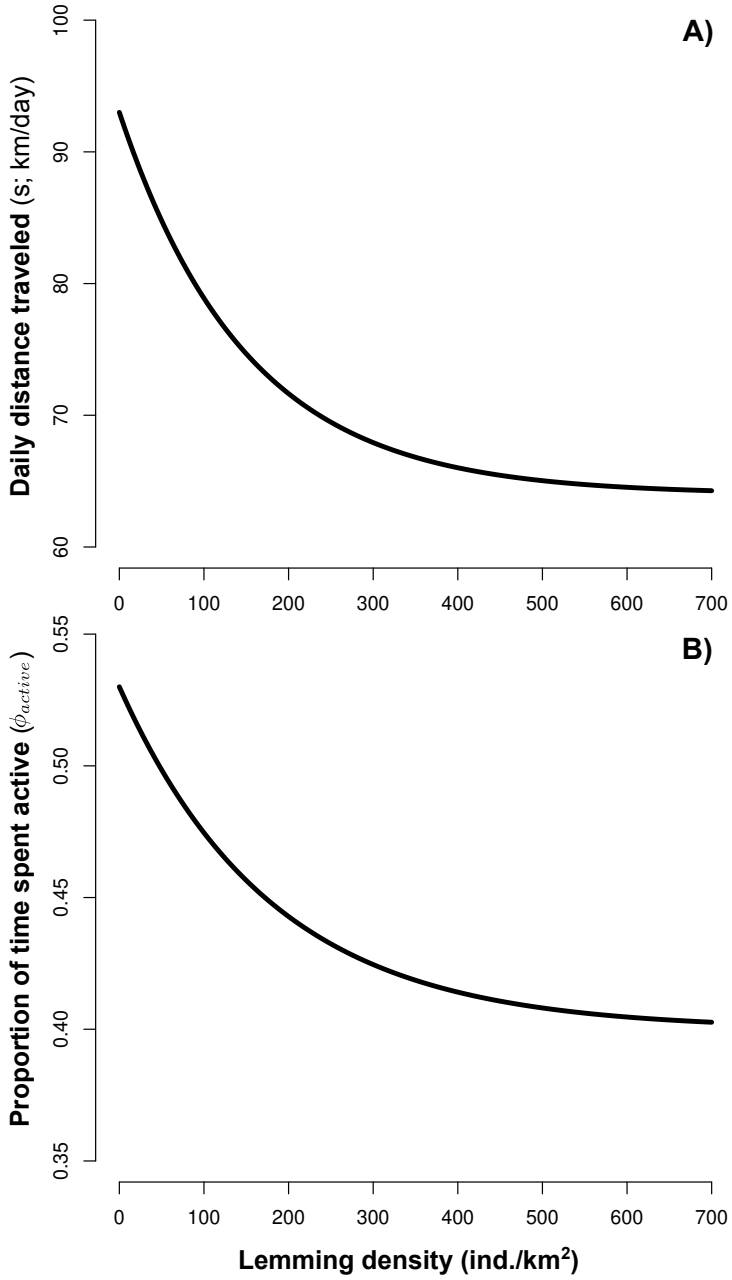

Figure 4.4. Relationships between lemming density and (**A**) the proportion of time the arctic fox spent active in a day, and (**B**) the daily distance traveled by the arctic fox. Relationships are partially derived from empirical observations (see Beardsell et al. 2022).

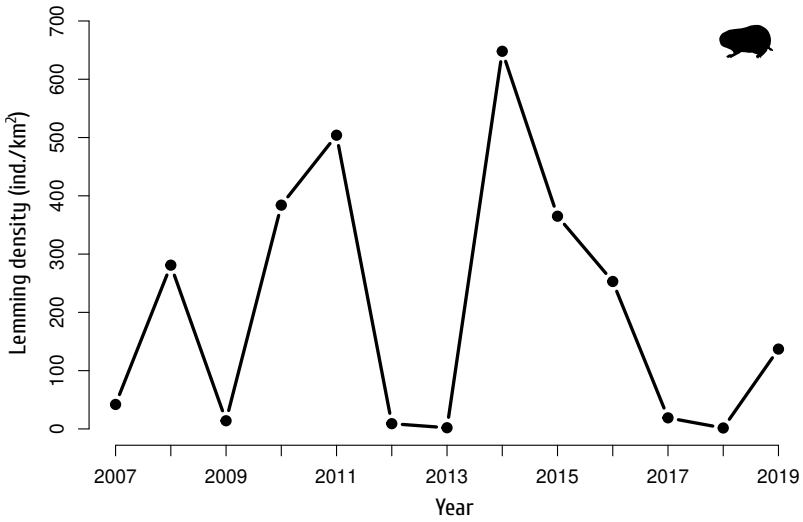

Figure 4.5. Empirical time series of lemming density on Bylot Island from 2007 to 2019 measured by live-trapping (see methods in Fauteux et al. 2018). The density of brown and collared lemmings was summed.

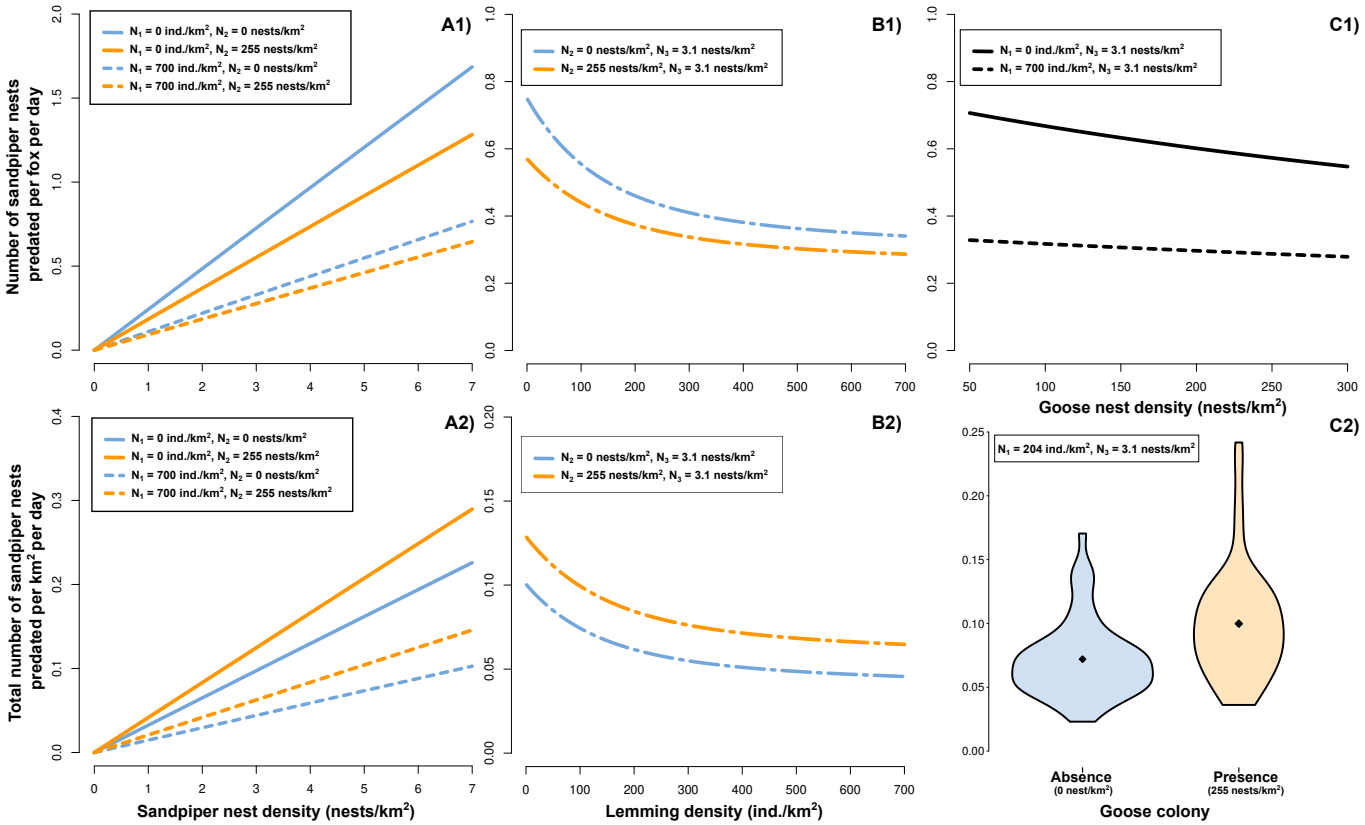

Figure 4.6. Functional response of arctic fox to the density of sandpiper nests (N_3; **A1**), lemmings (N_1; **B1**) and goose nests (N_2; **C1**). Predation rate (the product of the predator functional and numerical response) of arctic fox to the density of sandpiper nests (**A2**), lemmings (**B2**) and goose nests (**C2**). The average home range size of arctic foxes in presence (N_2=255 nests/km^2) or absence (N_2=0 nest/km^2) of the goose colony is used in **A2** and **B2** to compute predation rate. The violon plot in **C2** illustrates the distribution, and the whole range of predation rates calculated for each fox home range observed in presence (n=56 home ranges) and absence (n=57) of the goose colony. Lozenges indicate the predation rate for an average home range size.

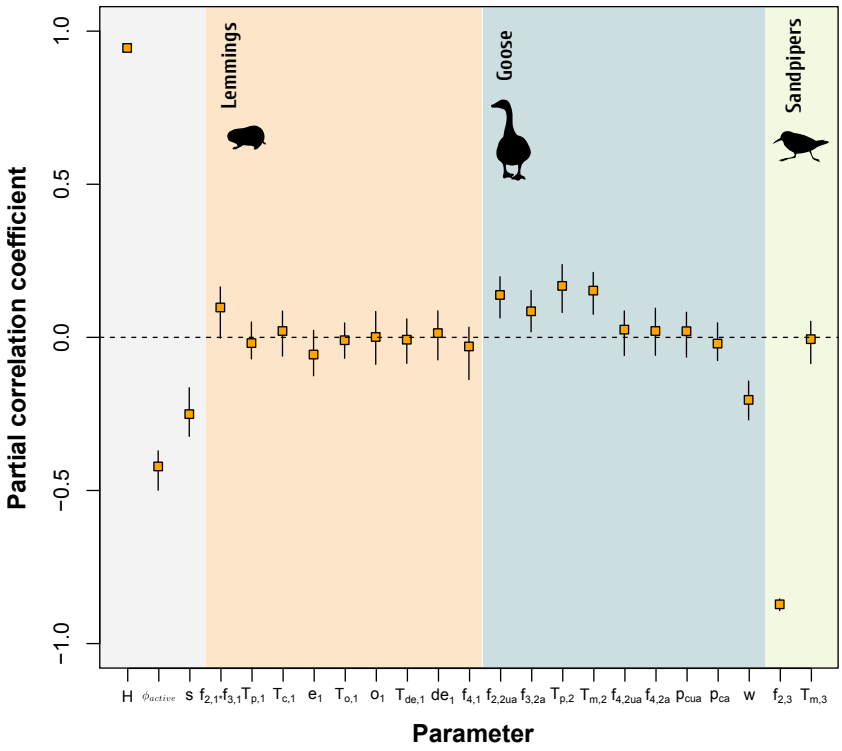

Figure 4.7. Partial correlation coefficient between the values of each parameter and annual nesting success of sandpipers. The predation model used in the simulation includes the presence of the goose colony (Eq. 4.6). The bars are 95% confidence intervals, generated by bootstrapping 40 times (n = 1000 simulations). See Table 4.1 for a description of each parameter.

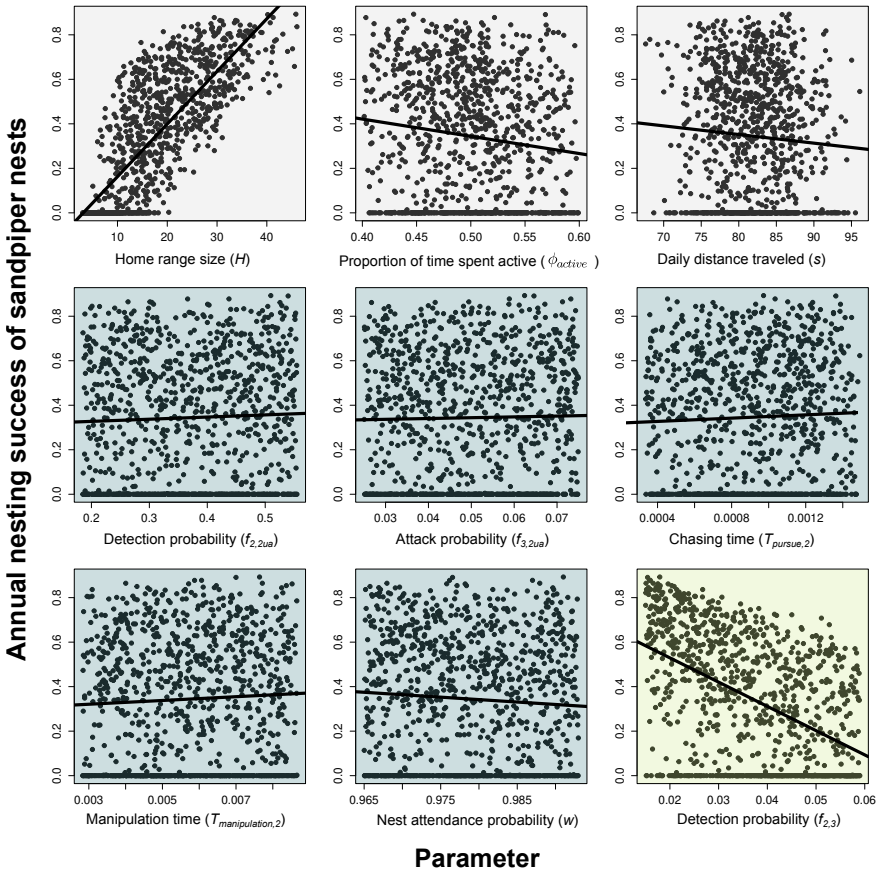

Figure 4.8. Scatterplots linking the value of input parameters on the annual nesting success of sandpipers. Parameters with a correlation coefficient in Fig. 4.7 significantly different from 0 are represented. See Table 4.1 for a description of each parameter.

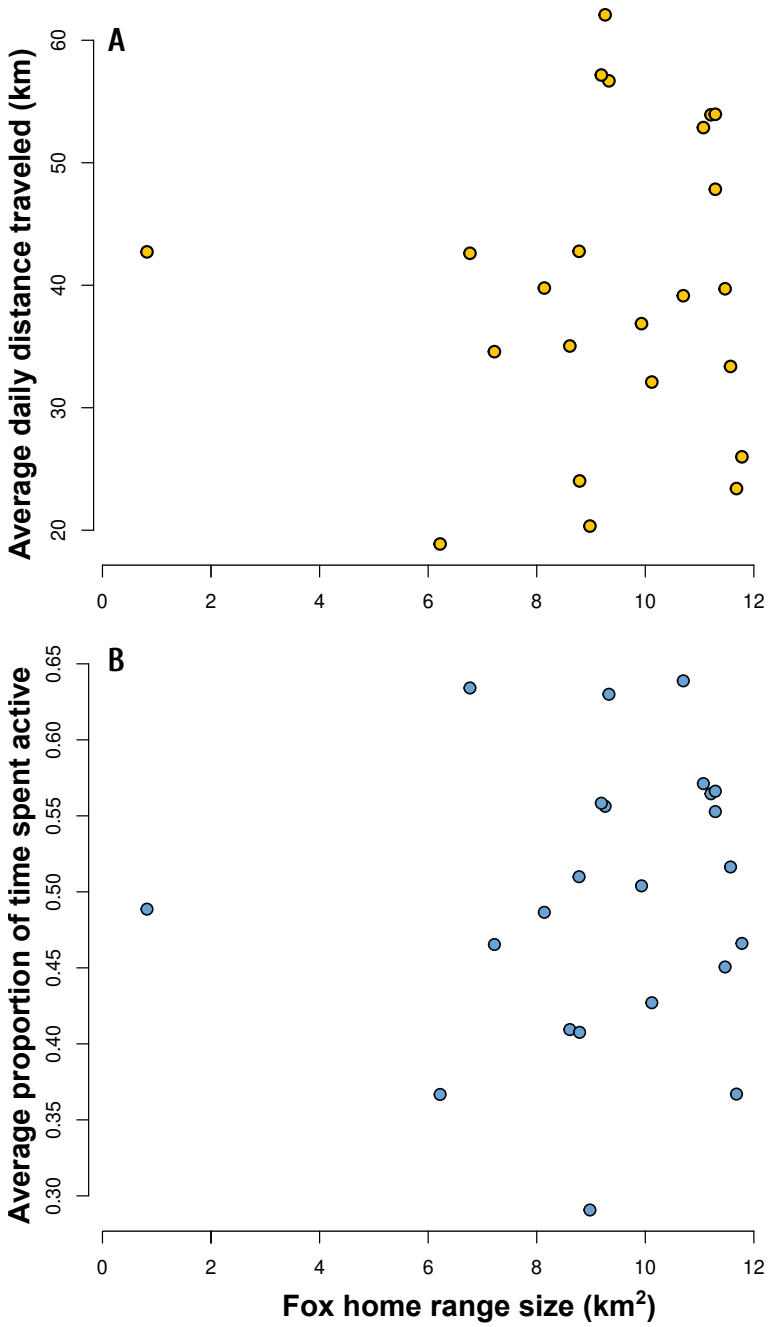

Figure 4.9. **A)** Relationship between the average daily distance traveled by arctic foxes during the bird incubation period (from June 10 to July 14) and the summer home range size of arctic foxes. **B)** Relationship between the average proportion of time spent active by arctic foxes during the bird incubation period and the summer home range size of arctic foxes. Dots in **A)** and **B)** represent empirical home range size, average daily distance traveled and average proportion of time spent active by arctic foxes calculated from high-frequency GPS-data and accelerometry data from 23 foxes monitored during the summer (8 foxes in 2018 and 15 in 2019).

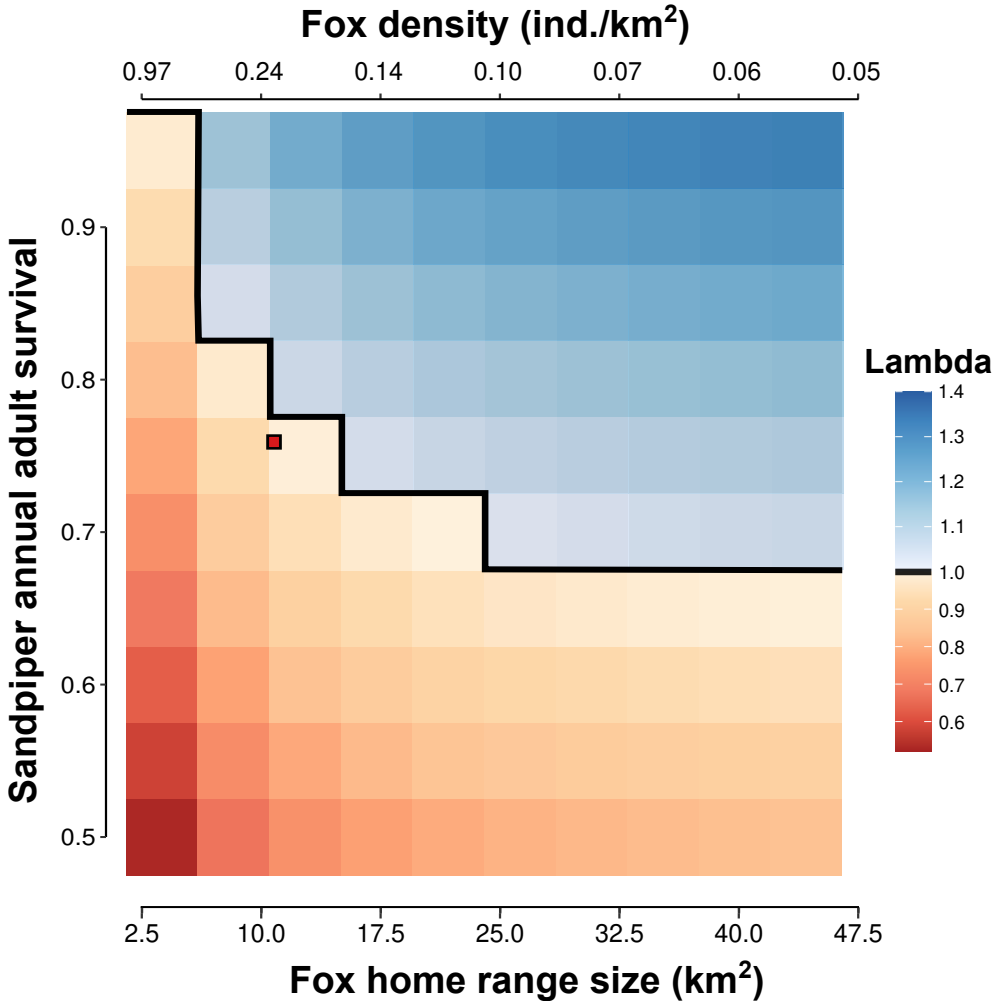

Figure 4.10. Predicted local growth rate of sandpipers derived from the population model of semipalmated sandpiper for various combinations of adult survival and fox home range size. Average sandpiper nesting success, used to calculate local growth rate, was calculated over a 13-year period covering different lemming densities, for a goose nest density of 255 nests/km^2 and a sandpiper nest density of 3.1 nests/km^2. The red square is the average home range size observed in the goose colony on Bylot Island along with the average adult survival estimated in semipalmated sandpipers in North America (Weiser et al., 2018).

4.12 Supplementary methods: Equations of the multi-prey mechanistic model of functional response

This appendix presents mainly the equations. See Beardsell et al. (2021) and Beardsell et al. (2022) for the full details.

4.12.1. Functional response model of arctic fox to lemmings (prey 1)

The number of lemmings captured per fox per day is expressed as:

$$FR_1(N_1, N_2, N_3) = \frac{\phi_{active}(N_1) \cdot \alpha_1(N_1) \cdot N_1}{1 + \alpha_1(N_1) \cdot h_1 \cdot N_1 + \alpha_{2a}(N_1) \cdot h_{2a} \cdot N_{2ua} + \alpha_{2ua}(N_1) \cdot h_{2ua} \cdot N_{2ua} + \alpha_3(N_1) \cdot h_3 \cdot N_3} \tag{4.11}$$

Where capture efficiency (km^2/day) is defined as:

$$\alpha_1(N_1) = s(N_1) \cdot (2 \cdot d_1) \cdot f_{2,1} \cdot f_{3,1} \cdot f_{4,1} \tag{4.12}$$

Handling time per lemming (h_1, day/prey item) sums the time spent chasing (means of successful and unsuccessful attacks) and the time spent manipulating a lemming once subdued. The manipulation time of lemmings is divided in three mutually exclusive behaviors: the lemming is either 1) consumed, 2) hoarded, or 3) delivered (Careau et al., 2007). The handling time per lemming is hence expressed as follows:

$$h_1 = \frac{T_{pursue,1}}{f_{4,1}} + (T_{consume,1} \cdot e_1 + T_{hoard,1} \cdot o_1 + T_{deliver,1} \cdot de_1) \tag{4.13}$$

4.12.2. Functional response model of arctic fox to goose nests (prey 2)

Since a successful fox attack does not necessarily result in predation of the whole clutch (Bêty et al., 2002), we included the probability that an attack would result in partial or total clutch predation (p_{2ca} and p_{2cua}) in the goose model. Also, since geese can actively protect their nests from arctic foxes, their presence at the nest strongly influences fox foraging behavior (Bêty et al., 2002). Thus, the model was divided into two components. A first component models the rate of acquisition of goose nests when the female is incubating or when a protective adult is <10 m from the nest (attended nest). A second component models the rate of goose nest acquisition during incubation recesses when both adults are >10 m from the nest (unattended nest). See Beardsell et al. 2021 for more details on the goose model. The number of goose nests acquired per fox per day (the predator acquisition rate) is expressed as:

$$FR_2(N_1, N_2, N_3) = FR_{2ua}(N_1, N_{2ua}, N_3) + FR_{2a}(N_1, N_{2a}, N_3) \tag{4.14}$$

Functional response model of arctic fox to unattended goose nests (prey 2)

The number of unattended nests acquired per fox per day is expressed as:

$$FR_{2ua}(N_1, N_{2ua}, N_3) = \frac{\phi_{active}(N_1) \cdot \alpha_{2ua}(N_1) \cdot N_{2ua}}{1 + \alpha_1(N_1) \cdot h_1 \cdot N_1 + \alpha_{2a}(N_1) \cdot h_{2a} \cdot N_{2a} + \alpha_{2ua}(N_1) \cdot h_{2ua} \cdot N_{2ua} + \alpha_3(N_1) \cdot h_3 \cdot N_3} \tag{4.15}$$

where the density of unattended nests is the product of goose nest density and nest attendance probability (w):

$$N_{2ua} = N_2 \cdot w \tag{4.16}$$

capture efficiency (km^2/day) of unattended nests is defined by two components to include complete and partial nest predation:

$$\alpha_{2ua}(N_1) = s(N_1) \cdot (2 \cdot d_{2ua}) \cdot f_{2,2ua} \cdot f_{4,2ua} \cdot P_{2cua} + \frac{s(N_1) \cdot (2 \cdot d_{2ua}) \cdot f_{2,2ua} \cdot f_{4,2ua} \cdot (1 - P_{2cua})}{3.7*} \tag{4.17}$$

and handling time (day/per nest) of unattended nests is defined as:

$$h_{2ua} = \frac{T_{pursue,2}}{f_{4,2ua} \cdot P_{2cua}} + T_{manipulation,2} \tag{4.18}$$

*This value refers to the average clutch size of the greater snow goose (Gauthier et al., 2013).

Functional response model of arctic fox to attended goose nests (prey 2)

The number of attended nests acquired per fox per day is expressed as:

$$FR_{2a}(N_1, N_{2a}, N_3) = \frac{\phi_{active}(N_1) \cdot \alpha_{2a}(N_1) \cdot N_{2a}}{1 + \alpha_1(N_1) \cdot h_1 \cdot N_1 + \alpha_{2a}(N_1) \cdot h_{2a} \cdot N_{2ua} + \alpha_{2ua}(N_1) \cdot h_{2ua} \cdot N_{2ua} + \alpha_3(N_1) \cdot h_3 \cdot N_3} \tag{4.19}$$

where density of attended goose nest is expressed as:

$$N_{2a} = N_2 \cdot (1 - w) \tag{4.20}$$

capture efficiency (km^2/day) of attended nests is defined as:

$$\alpha_{2a}(N_1) = s(N_1) \cdot (2 \cdot d_{2a}) \cdot f_{3,2a} \cdot f_{4,2a} \cdot P_{2ca} + \frac{s(N_1) \cdot (2 \cdot d_{2a}) \cdot f_{3,2a} \cdot f_{4,2a} \cdot (1 - P_{c2a})}{3.7*} \tag{4.21}$$

and handling time (day/per nest) of attended nests is defined as:

$$h_{2a} = \frac{T_{pursue,2}}{f_{4,2a} \cdot P_{2ca}} + T_{manipulation,2} \tag{4.22}$$

.

*This value refers to the average clutch size of the greater snow goose (Gauthier et al., 2013).

4.12.3. Functional response model of arctic fox to sandpiper nests (prey 3)

The number of sandpiper nests acquired per fox per day is expressed as:

$$FR_3(N_1, N_2, N_3) = \frac{\phi_{active}(N_1) \cdot \alpha_3(N_1) \cdot N_3}{1 + \alpha_1(N_1) \cdot h_1 \cdot N_1 + \alpha_{2a}(N_1) \cdot h_{2a} \cdot N_{2ua} + \alpha_{2ua}(N_1) \cdot h_{2ua} \cdot N_{2ua} + \alpha_3(N_1) \cdot h_3 \cdot N_3} \tag{4.23}$$

Where capture efficiency (km^2/day) is defined as:

$$\alpha_3(N_1) = s(N_1) \cdot (2 \cdot d_3) \cdot f_{2,3} \tag{4.24}$$

and handling time (day/per nest) is defined as:

$$h_3 = T_{consume,3} \tag{4.25}$$

4.13 Supplementary methods - Details of the sandpiper population model

We used a projection matrix model developed by Weiser et al. (2020) for the semipalmated sandpiper but with a modification. As it is a post-breeding model, we added either adult or juvenile survival to the fecundity terms of the model. Using the the original model of Weiser et al. (2020) leads to similar results and the same conclusions. No information on density dependence of survival and/or fecundity is available for the semipalmated sandpiper, so we did not include density dependence in the model (Weiser et al., 2020).

The post-breeding projection matrix model is male-based and includes three age classes composed of juveniles, yearlings and 2+ years old (Fig. 4.11). Variations in the size (Z) of the age structured population between times t and t + 1 can be computed from:

$$Z_{t+1} = M \cdot Z_t \tag{4.26}$$

where M is a population projection matrix and Z is a vector describing the age-structured population. The projection matrix is:

$$Z_{t+1} = \begin{bmatrix} Z_1 \\ Z_2 \\ Z_3 \end{bmatrix}_{t+1} = \begin{bmatrix} S_j \cdot F_1 & S_{ad} \cdot F_2 & S_{ad} \cdot F_3 \\ S_j & 0 & 0 \\ 0 & S_{ad} & S_{ad} \end{bmatrix} \cdot \begin{bmatrix} Z_1 \\ Z_2 \\ Z_3 \end{bmatrix}_t$$

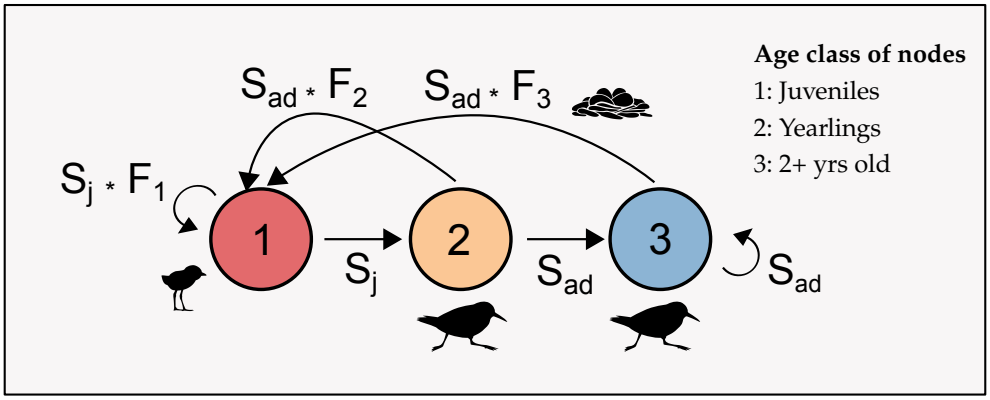

Figure 4.11. Diagram for the age-structured population model of semipalmated sandpiper.

Transitions among age classes are described by annual juvenile survival (S_j) and adult survival (S_{ad}). Age-specific probabilities of returning to the breeding area resulted in age-specific fecundity values (F_1, F_2, and F_3), but survival values (S_j and S_{ad}) did not vary among classes after the first year because insufficient data were available to develop age-specific estimates. The fecundity value (F) associated with each age class is defined by the sum of F_{ini} and F_{renest} and the probability of returning to breeding area (e.g, $P1_{return}$ for yearlings), which is essentially an age-specific recruitment probability, as follows:

$$F_1 = P1_{return} \cdot (F_{ini} + F_{renest}) \tag{4.27}$$

$$F_2 = P2_{return} \cdot (F_{ini} + F_{renest}) \tag{4.28}$$

$$F_3 = P3_{return} \cdot (F_{ini} + F_{renest}) \tag{4.29}$$

The mean number of male fledglings produced per breeding adult male for initial nests (F_{ini}) and renesting attempt (F_{renest}) is calculated as follows:

$$F_{ini} = P_{nest} \cdot NS_{ini} \cdot (CS_{ini} \cdot P_{hatch}) \cdot Sc_{ini} \cdot sexr \tag{4.30}$$

$$F_{renest} = P_{nest} \cdot (1 - NS_{ini}) \cdot P_{renest} \cdot NS_{renest} \cdot (CS_{renest} \cdot P_{hatch}) \cdot Sc_{renest} \cdot sexr \tag{4.31}$$

where fecundity of initial nests is defined by the probability of nesting in a given year (P_{nest}),

the average nesting success (NS_{ini}), the number of eggs expected to hatch (the average clutch size, CS_{ini}, multiplied by the hatching probability, P_{hatch}), the survival rate of chicks to fledging (SC_{ini}), and the sex ratio (the proportion of eggs that were expected to be male, $sexr$). The fecundity of renesting birds was conditional on the failure of the initial nest ($1 - NS_{ini}$). See Table 4.2 for a complete description of the model parameters.

Tableau 4.2. Parameters used in the population matrix model of semipalmated sandpiper. Details regarding the estimation of parameter values can be found in Weiser et al. (2020).

Parameter name	Symbol	Value (sd)
Probability of returning to breeding area (yearlings)	$P1_{return}$	0.67 (0.10)
Probability of returning to breeding area (age 2)	$P2_{return}$	0.925 (0.10)
Probability of returning to breeding area (age 3+)	$P3_{return}$	1
Probability of nesting in a given year	P_{nest}	0.8 (0.10)
Mean clutch size (initial nests)	CS_{ini}	3.89
Mean clutch size (renests)	CS_{renest}	3.76
Sex ratio of eggs	$sexr$	0.5
Average nesting success probability (initial nests)	NS_{ini}	Values from the predation model
Average nesting success probability (renests)	NS_{renest}	Values from the predation model
Proportion of eggs that hatch	P_{hatch}	0.94 (0.01)
Probability of renesting in a given year	P_{renest}	0.73 (0.20)
Chick survival probability (initial nests)	Sc_{ini}	0.71 (0.07)
Chick survival probability (renests)	Sc_{renest}	0.23 (0.19)
Juvenile survival probability	S_j	0.44 (0.10)
Adult (1+ yr old) survival probability	S_{ad}	0.76 (0.09)

We calculated growth rate (λ) using the mean values of each vital rates (Table 4.2) and average nesting success value obtained from different predation models. Given the strong influence of annual adult survival on λ (Weiser et al., 2020), we calculated λ values for different values of adult survival.

CHAPITRE 5

Conclusion

La combinaison de modélisation et de données empiriques détaillées peut permet de construire des modèles mécanistiques multi-espèces de la réponse fonctionnelle. Cette approche consiste à décomposer la séquence de la prédation (p.ex., la rencontre avec la proie, la capture et la manipulation de la proie) et de paramétrer ces composantes avec des données empiriques. Cette approche repousse la frontière des connaissances en écologie et permet de répondre à des questions inédites, tel que souligné récemment dans les perspectives du livre de DeLong (2021) : « *if we had empirically parameterized multi-species functional responses for food webs, we might have the ability to predict the consequences of climate change, invasive species, or extinctions on the structure and function of ecological communities*». C'est dans ce contexte que cette thèse fait progresser notre compréhension du fonctionnement des systèmes écologiques.

Le premier chapitre présente l'un des premiers modèle mécanistique de la réponse fonctionnelle paramétré dans une communauté naturelle de verterbrés. Ensuite, en utilisant les modèles développés dans ce chapitre comme point de départ, nous présentons l'un des premiers modèles mécanistiques de la prédation impliquant plusieurs espèces de proies (ce qui a été souligné récemment dans une revue de littérature écrite par une sommité en écologie; Abrams 2022). Le deuxième chapitre démontre que l'intégration de changements dépendants de la

densité dans des composantes de la réponse fonctionnelle peuvent générer des interactions indirectes positives. Contrairement à des hypothèses classiques qui mettent l'emphase sur la manipulation et la préférence des proies, les résultats montrent que des changements dans le comportement du renard (soit dans le budget d'activité quotidien et la distance parcourue) peuvent générer une interaction indirecte positive entre les lemmings et les oiseaux. Enfin, le dernier chapitre démontre que la présence d'une proie (l'oie des neiges) peut mener à l'exclusion locale d'une autre proie (les bécasseaux) via des interactions trophiques indirectes. L'originalité de cette étude est d'identifier les mécanismes proximaux affectant la coexistence des proies dans une communauté naturelle de vertébrés en faisant le pont entre la taille du domaine vital du prédateur, le risque de prédation, jusqu'à la dynamique de populations. Cette thèse apporte des contributions théoriques pour l'écologie par le développement et l'utilisation d'approches novatrices (modèles mécanistiques de la prédation) pour quantifier les interactions prédateurs-proies.

Historiquement, une approche catégorique a été adoptée par les écologistes pour définir les réponses fonctionnelles. Cette catégorisation est solidement ancrée en écologie et une réponse fonctionnelle linéaire a été traditionnellement attribuée aux organismes filtreurs (Jeschke et al., 2004), une forme hyperbolique (type II) aux invertébrés et une forme sigmoïdale (type III) aux prédateurs vertébrés (Holling 1965, mais voir Hassell et al. 1977). Il importe de souligner qu'Holling (1959*b*) avait conclut que son modèle reproduisait bien la dynamique du système simple qu'il étudiait (expérience avec des disques de papier) et qu'il servira de base à partir duquel des réponses fonctionnelles plus complexes pourraient être dérivées. Bien que cette catégorisation ait une certaine valeur heuristique et puisse être utile dans certains aspects de la recherche où la catégorisation est nécessaire, les types I, II et III devraient être considérés simplement comme des cas particuliers sur le long d'un continuum. Cette thèse illustre comment les modèles mécanistiques peuvent générer des fonctions reliant la densité des proies et les taux d'acquisition des prédateurs qui sont propres au système prédateur-proie étudié et à la gamme de densités de proies observée sur le terrain. Considérant l'impact de la réponse fonctionnelle sur le résultat des modèles prédateur-proie (Abrams et al.,

1998; Sinclair et al., 1998), de telles fonctions spécifiques devraient améliorer notre capacité à simuler et à quantifier fidèlement la force des interactions entre les espèces dans les communautés naturelles.

Nos résultats corroborent d'autres recherches indiquant que le taux d'acquisition des prédateurs n'est pas systématiquement limitée aux plus fortes densités de proies observées dans la nature (Novak, 2010; Chan et al., 2017; Preston et al., 2018; Coblentz et al., 2022). Les modèles de réponses fonctionnelles de type II (hyperbolique) et III (sigmoïdale) sont couramment utilisés dans les modèles de dynamique des populations (Turchin and Hanski, 1997; Gervasi et al., 2012; Serrouya et al., 2015) et prédisent que les taux d'acquisition des prédateurs devraient saturer à haute densité de proies via le temps de manipulation. Sur la base de modèles mécanistiques, il n'y avait pas d'évidences que le taux d'acquisition du renard arctique est limité par le temps de manipulation aux plus fortes densités de proies observées dans un système naturel, et ce, même en présence d'une colonie d'oies où la densité de nids peut être assez élevée ($\sim$255 nids/km^2 en moyenne dans un domaine vital de renard).

Les densités de proies requises pour atteindre un point de saturation du taux d'acquisition pourraient être rarement observées dans les systèmes naturels (Coblentz et al., 2022). C'est en utilisant des densités bien supérieures à celles observées en milieu naturel que le renard devient éventuellement limité par le temps de manipulation (Fig. 5.1). De plus, les évidences empiriques d'une réponse fonctionnelle hyperbolique dans la nature sont relativement rares (voir le cas de lynx et des lièvres dans Chan et al. 2017) et proviennent principalement d'expériences contrôlées en laboratoire, dans lesquelles la gamme de densités de proies peut dépasser celle observée dans la nature ou les conditions ne sont pas nécessairement représentatives de celles rencontrées par le prédateur en milieu naturel (99 % de toutes les réponses fonctionnelles de type II proviennent d'expériences contrôlées en laboratoire (n = 61 études) ; revue par Rall et al. 2012). Ceci étant dit, le temps de manipulation est probablement un mécanisme limitant le taux d'acquisition chez plusieurs prédateurs en milieu naturel, particulièrement quand la digestion d'une proie empêche ou limite l'acquisition d'une autre. C'est

le cas notamment chez des serpents arboricoles, où la digestion d'une proie réduit considérablement leur niveau d'activité pendant 5 à 7 jours (Siers et al., 2018). Depuis les travaux de Holling (1959*b*), le temps de manipulation est solidement ancré dans les modèles de réponses fonctionnelles alors qu'il est connu qu'une panoplie de mécanismes différents modulent le taux d'acquisition des prédateurs (Fryxell et al., 2007; Fletcher et al., 2010; Toscano and Griffen, 2013; Sirot et al., 2021). Les interactions prédateurs-proies sont encore rarement modélisés en intégrant explicitement ces mécanismes et à mon avis, cela ferait progresser énormément notre capacité de modéliser les interactions prédateurs-proies.

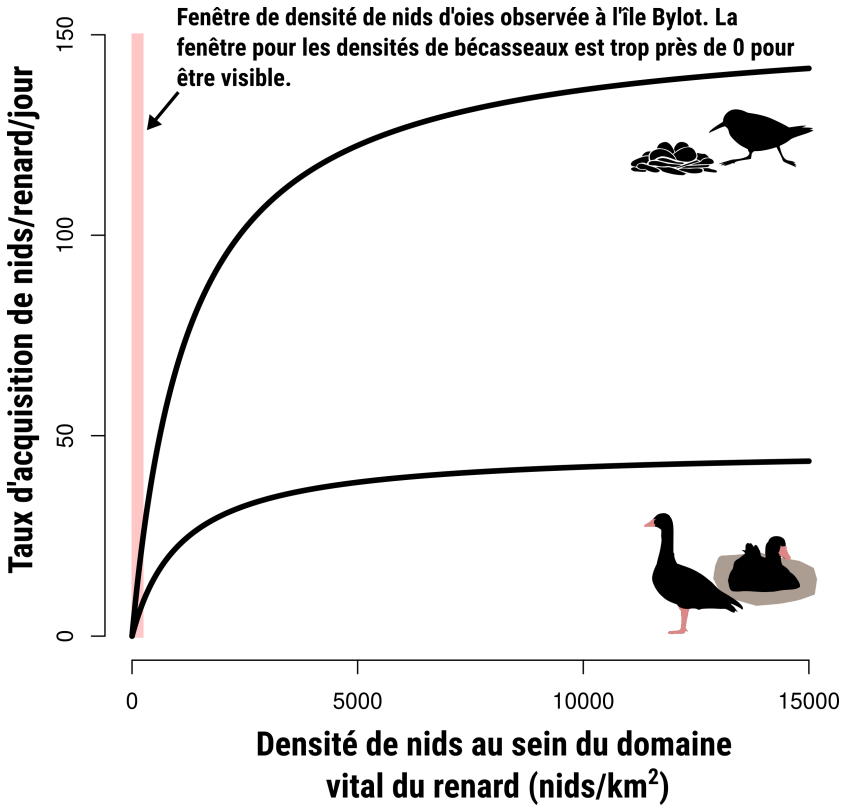

Figure 5.1. Réponse fonctionnelle du renard arctique à la densité de nids d'oies des neiges et de bécasseaux obtenue avec le modèle mécanistique présenté au chapitre 3. La densité des lemmings est fixée à une densité intermédiaire (204 ind./km^2). Le renard est limité par le temps de manipulation (qui inclut le temps de chasse) à environ 44 nids par jour pour l'oie des neiges et 142 nids par jour pour les bécasseaux. Le rectangle rosé indique la fenêtre de densité d'oies observée à l'île Bylot. La fenêtre pour les densités de bécasseaux est trop près de 0 pour être visible.

Une compréhension détaillée des composantes de la réponse fonctionnelle (la rencontre, la détection, l'attaque et la capture) est nécessaire pour estimer le taux de prédation et identifier les mécanismes qui le module. Cette thèse est un premier pas dans cette direction. Nous avons démontré que des changements dans la distance parcourue par le prédateur et le temps que le prédateur passe en activité en fonction de la densité d'une proie peuvent générer des interactions indirectes positives entre des proies partageant ce prédateur. Ces changements sont rarement intégrés dans les modèles prédateurs-proies (Stouffer and Novak, 2021) et ont été peu étudiés en milieu naturel. Les mécanismes expliquant les patrons observés entre l'abondance des lemmings et le succès des oiseaux n'étaient pas connu (Summers et al., 1998; Blomqvist et al., 2002; McKinnon et al., 2014) et nos résultats mettent en avant des mécanismes pouvant expliquer une partie de la variation observée dans le succès des oiseaux. La combinaison de technologies émergentes (p.ex., GPS à haute fréquence, enregistreurs acoustiques et photosensibles) devrait faciliter l'intégration de ces mécanismes (ou de ceux pertinents au système étudié) dans des modèles mécanistiques multi-espèces de la réponse fonctionnelle (Williams et al., 2014; Pagano et al., 2018; Studd et al., 2021).

Une hypothèse classique en écologie est que les prédateurs stabilisent les populations de proies en ajustant leurs préférences alimentaires selon l'abondance relative des proies (concept de *prey switching*; Murdoch 1969). Le terme "préférence" du prédateur fait référence à une vaste gamme de mécanismes allant de la probabilité de détection, d'attaque et de capture d'une proie (Chesson, 1984). Un changement de comportement du prédateur positif (*positive prey switching*) survient lorsque son taux d'acquisition pour une proie augmente lorsque son abondance relative est élevée, et génère de la non-linéarité dans la réponse fonctionnelle. À l'opposé si le taux d'acquisition du prédateur pour une proie diminue lorsque son abondance relative est élevée, cela fait référence à un changement de comportement inverse ou négatif (*negative prey switching*; Murdoch 1969; Baudrot et al. 2016). Toutefois, les évidences empiriques qui soutiennent ce concept sont quasi-inexistantes en milieu naturel (Tallian et al., 2017). Cela s'explique notamment car la plupart des réponses fonctionnelles sont évaluées à l'aide de modèles statistiques qui peinent à identifier les mécanismes proximaux modulant les

taux d'acquisition des prédateurs (Novak and Stouffer, 2020; Pawar et al., 2012). De plus, bien que les changements de comportement du prédateur permettent de stabiliser les populations de proies dans les modèles de réseaux trophiques, ils sont rarement inclus explicitement dans les modèles (ils sont plutôt intégrés à travers la réponse fonctionnelle de type III qui n'a pas une origine mécanistique), ce qui ne permet pas de mettre le doigt sur les mécanismes qui sous-tendent ce concept.

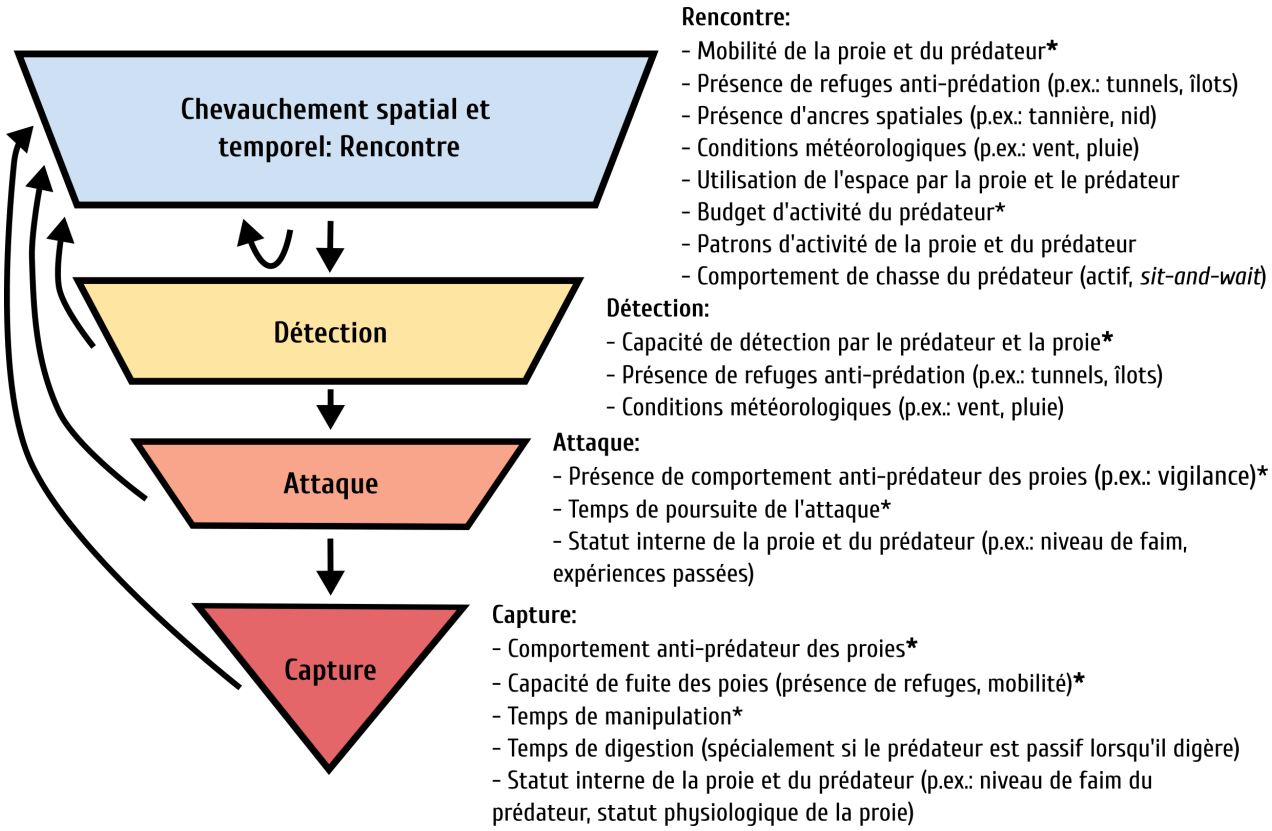

Figure 5.2. Séquence de prédation et processus potentiels pouvant intervenir à différents endroits dans la séquence. Notez que les processus énumérés ne sont pas nécessairement indépendant les uns des autres. Les processus marqués d'un astérisque ont été considéré dans le modèle mécanistique présenté dans cette thèse. Figure inspirée de Suraci et al. 2022.

Le concept de *prey switching* mérite d'être revisité en tirant profit de modèles mécanistiques multi-espèces pour évaluer comment différentes composantes de la réponse fonctionnelle (qui dépendent de la densité d'une ou de plusieurs proies) peuvent influencer les interactions multi-espèces en milieu naturel. Par exemple, dans notre système d'étude, lorsque la densité

totale de proies est faible (principalement les nids d'oies et les lemmings), le renard pourrait être plus enclin à prendre des risques (ayant un impact potentiel sur sa survie) pour récolter des proies situées dans des refuges anti-prédateurs partiels (comme des îlots, des falaises escarpés). Dans le modèle, cela pourrait se réfléter par des changements dans la probabilité d'attaquer certains nids, comme des nids de bernaches ou de buses en fonction de la densité totale de proies disponibles (Fig. 5.2). Dans cette thèse, j'ai intégré des paramètres dépendant de la densité de seulement une proie (chapitre 1 et 2) alors qu'il est probable que la densité totale des proies influencent le comportement du prédateur.

Les caractéristiques de l'habitat (p.ex., type de végétation, le relief, étendue d'eau) sont susceptibles d'influencer plusieurs composantes de la réponse fonctionnelle des prédateurs (Lipcius and Hines, 1986; Barrios-O'Neill et al., 2015). Par exemple, la distance de détection d'un nid par les renards arctiques pourrait être plus faible dans une végétation dense (Flemming et al., 2016), la probabilité d'attaque pourrait être plus faible pour les nids situés dans des zones humides ou sur des îlots accessibles uniquement par le renard à la nage (Lecomte et al., 2008; Gauthier et al., 2015), et la probabilité de succès d'une attaque pourrait être modulée par la présence de réseaux de tunnels offrant des refuges aux lemmings. Enfin, la probabilité de rencontre entre une proie et le prédateur variera selon l'utilisation de l'espace par le prédateur (Clermont et al., 2021*b*). Dans une première étape, des expériences et ou observations directes du prédateur pourraient être réalisées pour identifier les composantes principales (p.ex., probabilité d'attaque) et quantifier leurs variations selon certaines caractéristiques de l'habitat offrant par exemple un refuge partiel à la proie (p.ex., présence de tunnels, d'îlot) ou modifiant les déplacements du prédateur (p.ex., falaises, lac; Fig. 5.3). Ensuite, le modèle mécanistique pourrait être couplé à des cartes d'habitats, de distribution des proies et des données de mouvement du prédateur. Une partie de cette intégration fait l'objet actuellement d'un projet de doctorat (F. Dulude-de-Broin) où le modèle mécanistique développé dans cette thèse sera jumelé à un modèle de mouvement du renard à fine échelle spatiale.

Dans le contexte où il y a présence de refuges pour les lemmings (tunnels) dans le paysage et en supposant que ces refuges sont limitants, on pourrait s'attendre à ce que la probabilité

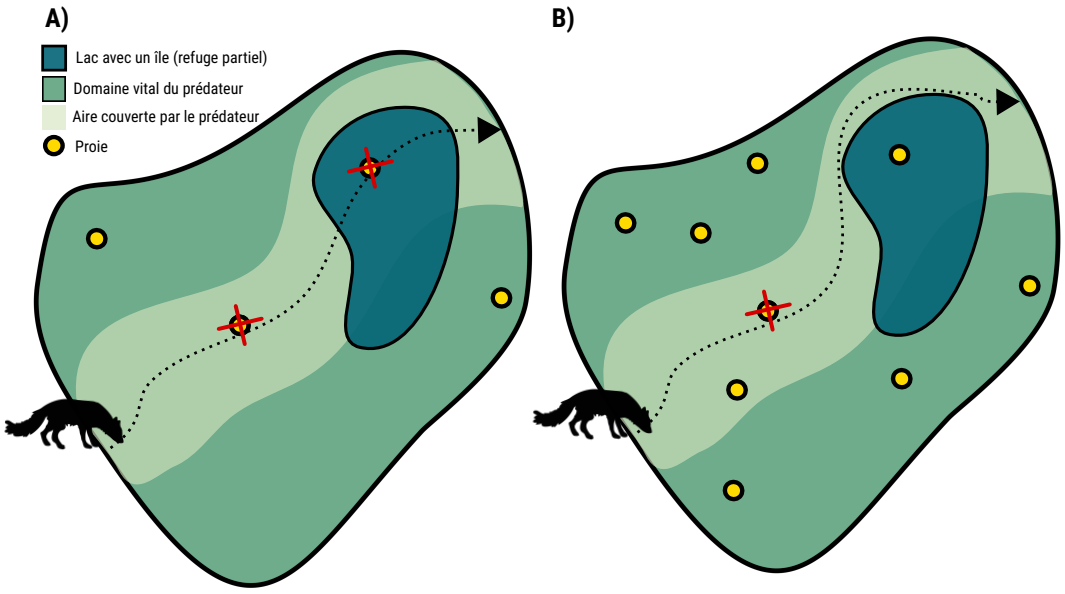

Figure 5.3. Représentation schématique d'un prédateur se déplaçant dans son domaine vital et où la probabilité qu'il attaque la proie (p.ex., un nid) située sur un îlot est modulée par deux facteurs: la densité totale de proies et les caractéristiques de l'habitat (présence/absence d'eau entourant le nid). La densité totale de proies est plus faible en **A** et plus élevée en **B**.

de détection par le renard (détection réduite si un refuge est disponible) et de succès d'une attaque qu'il initie (la fuite est possible) soient réduites à faible densité de lemmings (Fig. 5.2). On pourrait prédire que ces deux probabilités augmentent avec la densité de lemmings, à partir d'un certain seuil où les refuges deviennent limitants. Ainsi, ces deux paramètres dépendraient de la densité de lemmings et la forme de ces effets s'apparenterait à une forme sigmoïdale. Donc, la réponse fonctionnelle du renard aux lemmings pourrait avoir une allure de type III, sans plateau lié au temps de manipulation mais un léger aplatissement lié à la distance parcourue par jour et à la proportion de temps passée en activité. Cet exemple était purement spéculatif, mais illustre comment des liens entre des caractéristiques du paysage peuvent être intégrés dans le modèle mécanistique et utimement avoir des impacts sur la dynamique des populations.

Dans le premier chapitre, j'ai illustré les variations dans le taux d'acquisition de proies par le prédateur générés par l'incertitude et la variabilité dans la valeur des paramètres du modèle (Fig. 2.2). Cette variabilité peut provenir de variations dans les composantes abiotiques (p.ex., météo, présence de refuges) et biotiques (densité des proies, variabilité intra et inter individuelle des proies et des prédateurs). Il serait intéressant, d'une part, de dissocier la variabilité générée par l'incertitude de celle générée par des processus biologiques. D'autre part, une meilleure quantification de plusieurs paramètres (p.ex., la probabilité que le nid soit sous surveillance d'un adulte chez les oies, la probabilité d'attaque d'un nid d'oies) seraient utiles pour raffiner le modèle et réduire les variations causées par l'incertitude dans la valeur des paramètres. Enfin, il faut aussi garder en tête que la valeur de certains paramètres est possiblement légèrement biaisée. Certains paramètres ont été mesurés dans un contexte qui n'était pas nécessairement représentatif de la gamme de densité de proies observées ou encore via des expériences impliquant des humains comme prédateur (p.ex., la probabilité de détection d'un nid de passereaux), ce qui a pu biaiser leurs valeurs.

Les modèles mécanistiques présentés dans cette thèse font abstraction de l'impact potentiel de l'interférence entre les prédateurs sur le taux d'acquisition. En théorie, cet effet serait plus marqué à haute densité de la proie où la compétition par exploitation et les conflits entre les prédateurs peuvent être plus importants (Abrams and Ginzburg, 2000). Certains modèles mathématiques intègrent l'interférence entre les prédateurs soit comme composante de la réponse fonctionnelle elle-même (Hassel and Varley, 1969; DeAngelis et al., 1975), ou via l'abondance relative de proies par prédateur (Arditi and Ginzburg, 2012). Dans notre système, nous n'avions pas d'indication que ce mécanisme est important puisque les renards arctiques ont des domaines vitaux pendant l'été avec un faible chevauchement (Clermont et al., 2021*b*), ce qui limite l'interférence potentielle au sein des domaines vitaux. De plus, les renards se rencontrent et interagissent rarement avec d'autres individus dans leurs domaines vitaux pendant l'été (49 interactions, ce qui représente 0.9 % du temps sur 118 h d'observations directes de renards). Ainsi, ces rencontres ne devraient pas représenter une part importante du budget d'activité des renards. Toutefois, le modèle mécanistique pourrait être adapté à des systèmes

prédateurs-proies où l'interférence entre les prédateurs représente une composante importante. Cela pourrait se réfléter notamment dans le budget d'activité ou l'utilisation de l'espace par le prédateur (Novak et al. 2017; Fig. 5.2).

La saisonnalité peut aussi complexifier la réponse fonctionnelle des prédateurs, particulièrement dans des écosystèmes qui connaissent de fortes variations saisonnières où des composantes centrales de la réponse fonctionnelle (comme la probabilité de rencontre, de détection ou d'attaque d'une proie; Fig. 5.2) peuvent changer fondamentalement en fonction des saisons. Dans les écosystèmes boréaux et arctiques, la phénologie de chute et de fonte de la neige est une composante abiotique qui détermine grandement les saisons. La présence de neige et ses caractéristiques (l'épaisseur et la dureté) sont susceptibles de moduler notamment la probabilité de détection (camouflage) ou de capture (réduction de la capacité de fuite dans la neige) d'une proie par le prédateur (Stenseth et al., 2004). Des études théoriques récentes soulignent la nécessité d'intégrer la saisonnalité dans les modèles prédateurs-proies pour comprendre la dynamique des communautés et la persistance des espèces (Tyson and Lutscher, 2016). Toutefois, mesurer empiriquement le taux d'attaque d'un prédateur selon différentes densités de proies et sous différentes conditions abiotiques (comme des caractéristiques de neige) est extrêmement difficile à réaliser dans des systèmes naturels. La construction de modèles mécanistiques de la réponse fonctionnelle, solidement appuyés par des données empiriques, permettrait d'intégrer la saisonnalité et d'évaluer comment différents scénarios d'enneigement influencent les dynamiques prédateurs-proies. Une telle intégration fournira des informations essentielles sur la manière dont la composition des communautés sera affectée par le changement climatique, notamment pour les espèces aux latitudes nordiques (là où le réchauffement est le plus prononcé sur la planète) qui sont particulièrement vulnérables aux changements des conditions d'enneigement (Peers et al., 2020).

RÉFÉRENCES

Abrams, P. A. 1982. Functional responses of optimal foragers. American Naturalist, 120:382–390.

Abrams, P. A. 1987. Indirect interactions between species that share a predator: varieties of indirect effects. In W. C. K. Sih and A., editors, Predation: direct and indirect impacts on aquatic communities, pages 38–54. University edition.

Abrams, P. A. 2022. Food web functional responses. Frontiers in Ecology and Evolution, 10:984384.

Abrams, P. A. and M. H. Cortez. 2015. The many potential indirect interactions between predators that share competing prey. Ecological Monographs, 85:625–641.

Abrams, P. A. and L. R. Ginzburg. 2000. The nature of predation : prey dependent, ratio dependent or neither? Trends in Ecology & Evolution, 15:337–341.

Abrams, P. A., R. D. Holt, and J. D. Roth. 1998. Apparent competition or apparent mutualism? Shared predation when population cycle. Ecology, 79:201–212.

Abrams, P. A. and H. Matsuda. 1993. Effects of adaptive predatory and anti-predator behaviour in a two-prey-one-predator system. Evolutionary Ecology, 7:312–326.

Abrams, P. A. and H. Matsuda. 1996. Positive indirect effects between prey species that share predators. Ecology, 77:610–616.

Abrams, P. A. and H. Matsuda. 2004. Consequences of behavioral dynamics for the population dynamics of predator-prey systems with switching. Population Ecology, 46:13–25.

Alisauskas, R. T., R. F. Rockwell, K. W. Dufour, E. G. Cooch, G. Zimmerman, K. L. Drake, J. O. Leafloor, T. J. Moser, and E. T. Reed. 2011. Harvest, survival, and abundance of midcontinent lesser snow geese relative to population reduction efforts. Wildlife Monographs, 179:1–42.

Angerbjörn, A., M. Tannerfeldt, and S. Erlinge. 1999. Predator-prey relationships: Arctic foxes and lemmings. Journal of Animal Ecology, 68:34–49.

Arditi, R. and L. Ginzburg. 2012. How Species Interact: Altering the Standard View on Trophic Ecology. Oxford University Press, New York.

Audet, A. M., C. B. Robbins, and S. Larivière. 2002. Alopex lagopus. Mammalian Species, 713:1–10.

Baker, A., P. Gonzales, T. Piersma, L. Niles, I. d. L. Serrano do Nascimento, P. Atkinson, N. Clark, C. Minton, M. Peck, and G. Aarts. 2004. Rapid population decline in red knots: fitness consequences of decreased refuelling rates and late arrival in Delaware Bay. Proceedings of the Royal Society of London. Series B: Biological Sciences, 271:875 LP – 882.

Barraquand, F., L. F. New, S. Redpath, and J. Matthiopoulos. 2015. Indirect effects of primary prey population dynamics on alternative prey. Theoretical Population Biology, 103:44–59.

Barrios-O'Neill, D., J. T. Dick, M. C. Emmerson, A. Ricciardi, and H. J. MacIsaac. 2015. Predator-free space, functional responses and biological invasions. Functional Ecology, 29:377–384.

Barrios O'Neill, D., R. Kelly, and M. C. Emmerson. 2019. Biomass encounter rates limit the size scaling of feeding interactions. Ecology Letters, 22:1870–1878.

Baudrot, V., A. Perasso, C. Fritsch, P. Giraudoux, and F. Raoul. 2016. The adaptation of generalist predators' diet in a multi-prey context: Insights from new functional responses. Ecology, 97:1832–1841.

Beardsell, A., D. Gravel, D. Berteaux, G. Gauthier, J. Clermont, V. Careau, N. Lecomte, C.-C. Juhasz, P. Royer-Boutin, and J. Bêty. 2020. Derivation of predator functional responses using a mechanistic approach in a natural system. bioRxiv.

Beardsell, A., D. Gravel, D. Berteaux, G. Gauthier, J. Clermont, V. Careau, N. Lecomte, C. C. Juhasz, P. Royer-Boutin, and J. Bêty. 2021. Derivation of predator functional responses using a mechanistic approach in a natural system. Frontiers in Ecology and Evolution, 9:630944.

Beardsell, A., D. Gravel, J. Clermont, D. Berteaux, G. Gauthier, and J. Bêty. 2022. A mechanistic model of functional response provides new insights into indirect interactions among arctic tundra prey. Ecology, e3734.

Bertrand, A., D. Grados, F. Colas, S. Bertrand, X. Capet, A. Chaigneau, G. Vargas, A. Mousseigne, and R. Fablet. 2014. Broad impacts of fine-scale dynamics on seascape structure from zooplankton to seabirds. Nature Communications, 5:1–9.

Bêty, J., G. Gauthier, J.-F. Giroux, and E. Korpimäki. 2001. Are goose nesting success and lemming cycles linked? Interplay between nest density and predators. Oikos, 93:388–400.

Bêty, J., G. Gauthier, E. Korpimäki, and J.-F. Giroux. 2002. Shared predators and indirect trophic interactions: lemming cycles and arctic-nesting geese. Journal of Animal Ecology, 71:88–98.

Bino, G., A. Dolev, D. Yosha, A. Guter, R. King, D. Saltz, and S. Kark. 2010. Abrupt spatial and numerical responses of overabundant foxes to a reduction in anthropogenic resources. Journal of Applied Ecology, 47:1262–1271.

Blomqvist, S., N. Holmgren, S. Akesson, A. Hedenström, and J. Pettersson. 2002. Indirect effects of lemming cycles on sandpiper dynamics : 50 years of counts from southern Sweden. Oecologia, 133:146–158.

Bonsall, M. B. and M. P. Hassell. 1997. Apparent competition structures ecological assemblages. Nature, 388:371–373.

Bowler, D. E., M. A. J. Kvasnes, H. C. Pedersen, B. K. Sandercock, and E. B. Nilsen. 2020. Impacts of predator-mediated interactions along a climatic gradient on the population dynamics of an alpine bird: Climate-dependent species interactions. Proceedings of the Royal Society B: Biological Sciences, 287.

Brose, U., E. L. Berlow, and N. D. Martinez. 2005. Scaling up keystone effects from simple to complex ecological networks. Ecology Letters, 8:1317–1325.

Brose, U., R. J. Williams, and N. D. Martinez. 2006. Allometric scaling enhances stability in complex food webs. Ecology Letters, 9:1228–1236.

Busdieker, K. M., S. C. Patrick, S. Descamps, and A. M. Trevail. 2019. Prey density affects predator foraging strategy in an Antarctic ecosystem. Ecology and Evolution, 10:350–359.

Calabrese, J. M., C. H. Fleming, and E. Gurarie. 2016. ctmm: an R Package for analyzing animal relocation data as a continuous-time stochastic process. Methods in Ecology and Evolution, 7:1124–1132.

Careau, V., J.-F. Giroux, and D. Berteaux. 2007. Cache and carry : hoarding behavior of arctic fox. Behavioral Ecology and Sociobiology, 62:87–96.

Careau, V., N. Lecomte, J. Bêty, J.-F. Giroux, G. Gauthier, and D. Berteaux. 2008. Hoarding of pulsed resources: Temporal variations in egg-caching by arctic fox. Ecoscience, 15:268–276.

Cazelles, K., M. B. Araújo, N. Mouquet, and D. Gravel. 2016. A theory for species co-occurrence in interaction networks. Theoretical Ecology, 9:39–48.

Chan, K., S. Boutin, T. J. Hossie, C. J. Krebs, M. O'Donoghue, and D. L. Murray. 2017. Improving the assessment of predator functional responses by considering alternate prey and predator interactions. Ecology, 98:1787–1796.

Chaneton, E. J. and M. B. Bonsall. 2000. Enemy-mediated apparent competition: Empirical patterns and the evidence. Oikos, 88:380–394.

Chesson, P. L. 1984. Variable Predators and Switching Behavior. Theoretical Population Biology, 26.

Chevallier, C., G. Gauthier, S. Lai, and D. Berteaux. 2020. Pulsed food resources affect reproduction but not adult apparent survival in arctic foxes. Oecologia, 193:557–569. URL https://doi.org/10.1007/s00442-020-04696-8.

Chivers, W. J., W. Gladstone, R. D. Herbert, and M. M. Fuller. 2014. Predator–prey systems depend on a prey refuge. Journal of Theoretical Biology, 360:271–278.

Clark, K. L. and R. J. Robertson. 1979. Spatial and temporal multi-species nesting aggregations in birds as anti-parasite and anti-predator defenses. Behavioral Ecology and Sociobiology, 5:359–371.

Clermont, J., S. W. Gagné, and D. Berteaux. 2021*a*. Digging into the behaviour of an active hunting predator : arctic fox prey caching events revealed by accelerometry. Movement Ecology, 9:1–12.

Clermont, J., A. Grenier-Potvin, É. Duchesne, C. Couchoux, F. Dulude-de Broin, A. Beardsell, J. Bêty, and D. Berteaux. 2021*b*. The predator activity landscape predicts the anti-predator behavior and distribution of prey in a tundra community. Ecosphere, 12:1–17.

Coblentz, K. E. 2020. Relative prey abundance and predator preference predict individual diet variation in prey-switching experiments. Ecology, 101:1–10.

Coblentz, K. E. and J. P. DeLong. 2020. Predator-dependent functional responses alter the coexistence and indirect effects among prey that share a predator. Oikos, 129:1404–1414.

Coblentz, K. E., M. Novak, J. P. Delong, and C. Author. 2022. Predator feeding rates may often be unsaturated under typical prey densities. Ecology Letters, pages 1–22.

Connolly, S. R., S. A. Keith, R. K. Colwell, and C. Rahbek. 2017. Process, mechanism, and modeling in macroecology. Trends in Ecology & Evolution, 32:835–844.

Courchamp, F., M. Langlais, and G. Sugihara. 2000. Rabbits killing birds: Modelling the hyperpredation process. Journal of Animal Ecology, 69:154–164.

Courchamp, F., R. Woodroffe, and G. W. Roemer. 2003. Removing Protected Populations to Save Endangered Species. Science, 302:1532.

DeAngelis, D., R. Goldstean, and R. O'Neill. 1975. A Model for Tropic Interaction. Ecology, 56:881–892.

DeCesare, N. J., M. Hebblewhite, H. S. Robinson, and M. Musiani. 2010. Endangered, apparently: The role of apparent competition in endangered species conservation. Animal Conservation, 13:353–362.

Deinet, S., C. Zöckler, D. Jacoby, E. Tresize, V. Marconi, L. McRae, M. Svobods, and T. Barry. 2015. Arctic Species Trend Index : Migratory Birds Index. Conservation of Arctic Flora and Fauna, Akureyri, Iceland.

DeLong, J. P. 2021. Predator Ecology : Evolutionary Ecology of the Functional Response. Oxford University Press, Oxford, United Kingdom.

Duchesne, É., J.-f. Lamarre, G. Gauthier, D. Berteaux, D. Gravel, and J. Bêty. 2021. Variable strength of predator-mediated effects on species occurrence in an arctic terrestrial vertebrate community. Ecography, 44:1–13.

Eide, N. E., P. M. Eid, P. Prestrud, and J. E. Swenson. 2005. Dietary responses of arctic foxes *Alopex lagopus* to changing prey availability across an Arctic landscape. Wildlife Biology, 11:109–121.

Eide, N. E., J. U. Jepsen, and P. Å. L. Prestrud. 2004. Spatial organization of reproductive Arctic foxes Alopex lagopus : responses to changes in spatial and temporal. Journal of Animal Ecology, 73:1056–1068.

Ellis, K., R. T. Larsen, and D. N. Koons. 2019. The importance of functional responses among competing predators for avian nesting success. Functional Ecology, 34:252–264.

Fauteux, D., G. Gauthier, and D. Berteaux. 2015. Seasonal demography of a cyclic lemming population in the Canadian Arctic. Journal of Animal Ecology, 84:1412–1422.

Fauteux, D., G. Gauthier, M. J. Mazerolle, N. Coallier, J. Bêty, and D. Berteaux. 2018. Evaluation of invasive and non-invasive methods to monitor rodent abundance in the Arctic. Ecosphere, 9:1–18.

Fleming, C. H., W. F. Fagan, T. Mueller, K. A. Olson, P. Leimgruber, and J. M. Calabrese. 2015. Rigorous home range estimation with movement data: a new autocorrelated kernel density estimator. Ecology, 96:1182–1188.

Flemming, S. A., A. Calvert, E. Nol, and P. A. Smith. 2016. Do hyperabundant Arctic-nesting geese pose a problem for sympatric species ? Environmental Reviews, 10:1–10.

Flemming, S. A., E. Nol, L. V. Kennedy, A. Bédard, M. A. Giroux, and P. A. Smith. 2019. Spatio-temporal responses of predators to hyperabundant geese affect risk of predation for sympatric-nesting species. PLoS ONE, 14.

Fletcher, Q. E., S. Boutin, J. E. Lane, J. M. Lamontagne, A. G. Mcadam, C. J. Krebs, and M. M. Humphries. 2010. The functional response of a hoarding seed predator to mast seeding. Ecology, 91:2673–2683.

Fox, A. D., J. Madsen, H. Boyd, E. Kuijken, D. W. Norriss, I. M. Tombre, and D. A. Stroud. 2005. Effects of agricultural change on abundance, fitness components and distribution of two arctic-nesting goose populations. Global Change Biology, 11:881–893.

Fryxell, J. M., A. Mosser, A. R. E. Sinclair, and C. Packer. 2007. Group formation stabilizes predator–prey dynamics. Nature, 449:1041–1043.

Gauthier, G., J. Bêty, M.-C. Cadieux, P. Legagneux, M. Doiron, C. Chevallier, S. Lai, A. Tarroux, and D. Berteaux. 2013. Long-term monitoring at multiple trophic levels suggests heterogeneity in responses to climate change in the Canadian Arctic tundra. Philosophical Transactions of the Royal Society of London B: Biological Sciences, 368.

Gauthier, G., J. Bêty, J.-F. Giroux, and L. Rochefort. 2004. Trophic interactions in a high arctic snow goose colony. Integrative and Comparative Biology, 44:119–129.

Gauthier, G., M.-C. Cadieux, P. Legagneux, J. Lefebvre, J. Bêty, and D. Berteaux. 2019. Population study of greater snow geese and its nesting habitat on Bylot Island, Nunavut in 2019: A progress report. Technical report.

Gauthier, G., P. Legagneux, M.-A. Valiquette, M.-C. Cadieux, and J.-F. Therrien. 2015. Diet and reproductive success of an Arctic generalist predator: Interplay between variations in prey abundance, nest site location, and intraguild predation. The Auk, 132:735–747.

Gervasi, V., E. B. Nilsen, H. Sand, M. Panzacchi, G. R. Rauset, H. C. Pedersen, J. Kindberg, P. Wabakken, B. Zimmermann, J. Odden, O. Liberg, J. E. Swenson, and J. D. C. Linnell. 2012. Predicting the potential demographic impact of predators on their prey: a comparative

analysis of two carnivore–ungulate systems in Scandinavia. Journal of Animal Ecology, 81:443–454.

Gilg, O., I. Hanski, and B. Sittler. 2003. Cyclic dynamics in a simple vertebrate predator-prey community. Science, 302:866–868.

Gilg, O., B. Sittler, and I. Hanski. 2009. Climate change and cyclic predator-prey population dynamics in the high Arctic. Global Change Biology, 15:2634–2652.

Gilg, O., B. Sittler, B. Sabard, A. Hurstel, R. Sané, P. Delattre, and I. Hanski. 2006. Functional and numerical responses of four lemming predators in high arctic Greenland. Oikos, 113:193–216.

Giroux, M.-A., D. Berteaux, N. Lecomte, G. Gauthier, G. Szor, and J. Bêty. 2012. Benefiting from a migratory prey: spatio-temporal patterns in allochthonous subsidization of an arctic predator. Journal of Animal Ecology, 81:533–542.

Godsoe, W., J. Jankowski, R. D. Holt, and D. Gravel. 2017. Integrating Biogeography with Contemporary Niche Theory. Trends in Ecology & Evolution, 32:488–499.

Gravel, D., T. Poisot, C. Albouy, L. Velez, and D. Mouillot. 2013. Inferring food web structure from predator-prey body size relationships. Methods in Ecology and Evolution, 4:1083–1090.

Gravel, R., S. Lai, and D. Berteaux. 2023. Long-term satellite tracking reveals patterns of long-distance dispersal in juvenile and adult Arctic foxes (Vulpes lagopus). Royal Society Open Science, 10:220729. URL https://royalsocietypublishing.org/doi/abs/10.1098/rsos.220729.

Grenier-Potvin, A., J. Clermont, G. Gauthier, and D. Berteaux. 2021. Prey and habitat distribution are not enough to explain predator habitat selection: addressing intraspecific interaction constraints, behavioural state and time. Movement Ecology, 9:1–13.

Griffen, B. D. 2021. Considerations When Applying the Consumer Functional Response Measured Under Artificial Conditions. Frontiers in Ecology and Evolution, 9:1–8.

Griffen, B. D., D. van den Akker, E. R. DiNuzzo, L. Anderson, and A. Vernier. 2021. Comparing methods for predicting the impacts of invasive species. Biological Invasions, 23:491–505.

Gruyer, N., G. Gauthier, and D. Berteaux. 2008. Cyclic dynamics of sympatric lemming populations on Bylot Island, Nunavut, Canada. Canadian Journal of Zoology, 86:910–917.

Harding, A. M., J. F. Piatt, J. A. Schmutz, M. T. Shultz, T. I. Van Pelt, A. B. Kettle, and S. G. Speckman. 2007. Prey density and the behavioral flexibility of a marine predator: The common murre (Uria aalge). Ecology, 88:2024–2033.

Hassel, M. P. and G. C. Varley. 1969. New Inductive Population Model for Insect Parasites and its Bearing on Biological Control. Nature, 223:1133.

Hassell, M. P., J. H. Lawton, and J. R. Beddington. 1977. Sigmoid functional responses by invertebrate predators and parasitoids. The Journal of Animal Ecology, 46:249–262.

Ho, H.-C., J. M. Tylianakis, J. X. Zheng, and S. Pawar. 2019. Predation risk influences food web structure by constraining species diet choice. Ecology Letters, 22:1734–1745.

Holling, C. S. 1959*a*. Some characteristics of simple types of predation and parasitism. The Canadian Entomologist, pages 385–398.

Holling, C. S. 1959*b*. The components of predation as revealed by a study of small-mammal predation of the European pine sawfly. The Canadian Entomologist, 91:293–320.

Holling, C. S. 1965. The functional response of predators to prey density and its role in mimicry and population regulation. Memoirs of the Entomological Society of Canada, 97:5–60.

Holt, R. D. 1977. Predation, apparent competition, and the structure of prey communities. Theoretical Population Biology, 12:197–229.

Holt, R. D. and M. Bonsall. 2017. Apparent Competition. Annual Review of Ecology, Evolution, and Systematics, 48:447–471.

Holt, R. D. and J. H. Lawton. 1994. The Ecological Consequences of Shared Natural Enemies. Annual Review of Ecology and Systematics, 25:495–520.

Hone, J., C. J. Krebs, and M. O'Donoghue. 2011. Is the relationship between predator and prey abundances related to climate for lynx and snowshoe hares? Wildlife Research, 38:419–425.

Hussell, D. J. T. and R. Montgomerie. 2020. Lapland Longspur (Calcarius lapponicus), version 1.0. In Birds of the World (S. M. Billerman, B. K. Keeney, P. G. Rodewald, and T. S. Schulenberg, Editors).

Iles, D. T., R. F. Rockwell, P. Matulonis, G. J. Robertson, K. F. Abraham, J. C. Davies, and D. N. Koons. 2013. Predators, alternative prey and climate influence annual breeding success of a long-lived sea duck. Journal of Animal Ecology, 82:683–693.

Ims, R. A., J. A. Henden, and S. T. Killengreen. 2008. Collapsing population cycles. Trends in Ecology and Evolution, 23:79–86.

Ishii, Y. and M. Shimada. 2010. The effect of learning and search images on predator-prey interactions. Population Ecology, 52:27–35.

Jefferies, R. L., R. F. Rockwell, and K. F. Abraham. 2004. The embarrassment of riches: agricultural food subsidies, high goose numbers, and loss of Arctic wetlands -a continuing saga. Environmental Reviews, 11:193–232.

Jehl, J. R. 2007. Disappearance of breeding semipalmated sandpipers from Churchill, Manitoba: More than a local phenomenon. Condor, 109:351–360.

Jeschke, J. M. 2007. When carnivores are "full and lazy". Oecologia, 152:357–364.

Jeschke, J. M., M. Kopp, and R. Tollrian. 2002. Predator functional responses: Discriminating between handling and digesting prey. Ecological Monographs, 72:95–112.

Jeschke, J. M., M. Kopp, and R. Tollrian. 2004. Consumer-food systems: Why type I functional responses are exclusive to filter feeders. Biological Reviews of the Cambridge Philosophical Society, 79:337–349.

Juhasz, C., B. Shipley, G. Gauthier, D. Berteaux, and N. Lecomte. 2020. Direct and indirect effects of regional and local climatic factors on trophic interactions in the Arctic tundra. Journal of Animal Ecology, 89:704–715.

Lai, S. 2017. Organisation socio-spatiale et stratégie de mouvement d'une population de renards arctiques dans un contexte de fluctuations spatio-temporelles des ressources. Phd, Université du Québec à Rimouski.

Lai, S., J. Bêty, and D. Berteaux. 2017. Movement tactics of a mobile predator in a meta-ecosystem with fluctuating resources: the arctic fox in the High Arctic. Oikos, 126:937–947. URL http://doi.wiley.com/10.1111/oik.03948.

Lamarre, J. F., P. Legagneux, G. Gauthier, E. T. Reed, and J. Bêty. 2017. Predator-mediated negative effects of overabundant snow geese on arctic-nesting shorebirds. Ecosphere, 8:1–13.

Lecomte, N., V. Careau, G. Gauthier, and J. F. Giroux. 2008. Predator behaviour and predation risk in the heterogeneous Arctic environment. Journal of Animal Ecology, 77:439–447.

Lefebvre, J., G. Gauthier, J. F. Giroux, A. Reed, E. T. Reed, and L. Bélanger. 2017. The greater snow goose Anser caerulescens atlanticus: Managing an overabundant population. Ambio, 46:262–274.

Legagneux, P., G. Gauthier, D. Berteaux, J. Bêty, M.-C. Cadieux, F. Bilodeau, E. Bolduc, L. McKinnon, A. Tarroux, J.-F. Therrien, L. Morissette, and C. J. Krebs. 2012. Disentangling trophic relationships in a High Arctic tundra ecosystem through food web modeling. Ecology, 93:1707–1716.

Legagneux, P., G. Gauthier, N. Lecomte, N. M. Schmidt, D. Reid, M.-C. Cadieux, D. Berteaux, J. Bêty, C. J. Krebs, R. A. Ims, N. G. Yoccoz, R. I. G. Morrison, S. J. Leroux, M. Loreau, and D. Gravel. 2014. Arctic ecosystem structure and functioning shaped by climate and herbivore body size. Nature Climate Change, 4:379–383.

Lipcius, R. N. and A. H. Hines. 1986. Variable functional responses of a marine predator in dissimilar homogeneous microhabitats. Ecology, 67:1361–1371.

Loveridge, A. J., M. Valeix, Z. Davidson, F. Murindagomo, H. Fritz, and D. W. MacDonald. 2009. Changes in home range size of African lions in relation to pride size and prey biomass in a semi-arid savanna. Ecography, 32:953–962.

Marino, S., I. B. Hogue, C. J. Ray, and D. E. Kirschner. 2008. A methodology for performing global uncertainty and sensitivity analysis in systems biology. Journal of Theoretical Biology, 254:178–196.

Matthiopoulos, J., K. Graham, S. Smout, C. Asseburg, S. Redpath, S. Thirgood, P. Hudson, and J. Harwood. 2007. Sensitivity to Assumptions in Models of Generalist Predation on a Cyclic Prey. Ecology, 88:2576–2586.

McKinnon, L., D. Berteaux, and J. Bêty. 2014. Predator-mediated interactions between lemmings and shorebirds: A test of the alternative prey hypothesis. The Auk, 131:619–628.

McKinnon, L., D. Berteaux, G. Gauthier, and J. Bêty. 2013. Predator-mediated interactions between preferred, alternative and incidental prey in the arctic tundra. Oikos, 122:1042–1048.

McKinnon, L. and J. Bêty. 2009. Effect of camera monitoring on survival rates of High-Arctic shorebird nests. Journal of Field Ornithology, 80:280–288.

McLellan, B., R. Serrouya, H. U. Wittmer, and S. Boutin. 2010. Predator-mediated Allee effects in multi-prey systems. Ecology, 91:286–292.

Menge, B. A. 1995. Indirect Effects in Marine Rocky Intertidal Interaction Webs : Patterns and Importance. Ecological Monographs, 65:21–74.

Morin, C. 2015. Effets des ressources alimentaires sur la date d'émergence et de la taille de portée du renard arctique à l'île Bylot, Nunavut. M.sc., Université du Québec à Rimouski.

Murdoch, W. W. 1969. Switching in General Predators : Experiments on Predator Specificity and Stability of Prey Populations. Ecological Monographs, 39:335–354.

Murdoch, W. W. 1973. The functional response of predators. Journal of Applied Ecology, 10:335–342.

Murdoch, W. W. and A. Oaten. 1975. Predation and Population Stability. Advances in Ecological Research, 9:1–131.

Nams, V. O. 1997. Density-dependent predation by skunks using olfactory search images. Oecologia, 110:440–448.

Nolet, B. A., S. Bauer, N. Feige, Y. I. Kokorev, I. Y. Popov, and B. S. Ebbinge. 2013. Faltering lemming cycles reduce productivity and population size of a migratory Arctic goose species. Journal of Animal Ecology, 82:804–813.

Novak, M. 2010. Estimating interaction strengths in nature: experimental support for an observational approach. Ecology, 91:2394–2405.

Novak, M. and D. B. Stouffer. 2020. Systematic bias in studies of consumer functional responses. Ecology Letters, 24:580–593.

Novak, M., C. Wolf, K. E. Coblentz, and I. D. Shepard. 2017. Quantifying predator dependence in the functional response of generalist predators. Ecology Letters, 20:761–769.

Oaten, A. and W. W. Murdoch. 1975. Switching, Functional Response, and Stability in Predator-Prey Systems. The American Naturalist, 109:299–318.

O'Donoghue, M., S. Boutin, C. J. Krebs, G. Zuleta, D. L. Murray, and E. J. Hofer. 1998. Functional responses of coyotes and lynx to the snowshoe hare cycle. Ecology, 79:1193–1208.

Oksanen, T., L. Oksanen, and P. T. Fretwell. 1985. Surplus killing in the hunting strategy of small predators. The American Naturalist, 126:328–346.

Okuyama, T. 2010. Prey density-dependent handling time in a predator-prey model. Community Ecology, 11:91–96.

Okuyama, T. 2012. Flexible components of functional response. Journal of Animal Ecology, 81:185–189.

Pagano, A. M., G. M. Durner, K. D. Rode, T. C. Atwood, S. N. Atkinson, E. Peacock, D. P. Costa, M. A. Owen, and T. M. Williams. 2018. High-energy, high-fat lifestyle challenges an Arctic apex predator, the polar bear. Science, 359:568–572.

Papanikolaou, N. E., G. D. Broufas, D. P. Papachristos, M. L. Pappas, C. Kyriakaki, K. Samaras, and T. Kypraios. 2020. On the mechanistic understanding of predator feeding behavior using the functional response concept. Ecosphere, 11:1–9.

Paterson, R. A., J. T. A. Dick, D. W. Pritchard, M. Ennis, M. J. Hatcher, and A. M. Dunn. 2015. Predicting invasive species impacts: A community module functional response approach reveals context dependencies. Journal of Animal Ecology, 84:453–463.

Pawar, S., A. I. Dell, and Van M. Savage. 2012. Dimensionality of consumer search space drives trophic interaction strengths. Nature, 486:485–489.

Payne, E., O. Spiegel, D. L. Sinn, S. T. Leu, M. G. Gardner, S. S. Godfrey, C. Wohlfeil, and A. Sih. 2022. Intrinsic traits, social context, and local environment shape home range size and fidelity of sleepy lizards. Ecological Monographs, pages 1–18.

Peers, M. J. L., Y. N. Majchrzak, A. K. Menzies, E. K. Studd, G. Bastille-Rousseau, R. Boonstra, M. Humphries, T. S. Jung, A. J. Kenney, C. J. Krebs, D. L. Murray, and S. Boutin. 2020. Climate change increases predation risk for a keystone species of the boreal forest. Nature Climate Change.

Pivovaroff, A., Santia, and L. S. Santiago. 2017. Isohydric and anisohydric stomatal strategies under exceptional drought conditions. Plant Cell and Environment, 8:0–22.

Portalier, S. M. J., G. F. Fussmann, M. Loreau, and M. Cherif. 2019. The mechanics of predator–prey interactions: First principles of physics predict predator–prey size ratios. Functional Ecology, 33:323–334.

Poulin, M.-P., J. Clermont, and D. Berteaux. 2021. Extensive daily movement rates measured in territorial arctic foxes. Ecology and Evolution, 11:2503–2514.

Poussart, C., J. Larochelle, and G. Gauthier. 2000. The thermal regime of eggs during laying and incubation in greater snow geese. The Condor, 102:292–300.

Preston, D. L., J. S. Henderson, L. P. Falke, L. M. Segui, T. J. Layden, and M. Novak. 2018. What drives interaction strengths in complex food webs? A test with feeding rates of a generalist stream predator. Ecology, 99:1591–1601.

R Core Team. 2022. R: A language and environment for statistical computing. URL https://www.r-project.org/.

Rall, B. C., U. Brose, M. Hartvig, G. Kalinkat, F. Schwarzmüller, O. Vucic-Pestic, and O. L. Petchey. 2012. Universal temperature and body-mass scaling of feeding rates. Philosophical Transactions of the Royal Society B: Biological Sciences, 367:2923–2934.

Reed, A., R. J. Hughes, and G. Gauthier. 1995. Incubation behavior and body mass of female greater snow geese. The Condor, 97:993–1001.

Reséndiz-Infante, C., G. Gauthier, and G. Souchay. 2020. Consequences of a changing environment on the breeding phenology and reproductive success components in a long-distance migratory bird. Population Ecology, 62:284–296.

Rioux, M. J., S. Lai, N. Casajus, J. Bêty, and D. Berteaux. 2017. Winter home range fidelity and extraterritorial movements of Arctic fox pairs in the Canadian High Arctic. Polar Research, 36.

Roemer, G. W., C. J. Donlan, and F. Courchamp. 2002. Golden eagles, feral pigs, and insular carnivores: How exotic species turn native predators into prey. Proceedings of the National Academy of Sciences, 99:791–796.

Rosenzweig, M. L. and R. H. MacArthur. 1963. Graphical representation and stability conditions of predator-prey interactions. The American Naturalist, 97:209–223.

Roth, J. D. 2003. Variability in marine resources affects arctic fox. Journal of Animal Ecology, 72:668–676.

Royer-Boutin, P. 2015. Effets des cycles de lemmings sur le succès de nidification d'oiseaux différant par leur taille corporelle et leur comportement. M.sc., Université du Québec à Rimouski.

Samelius, G. and R. T. Alisauskas. 2000. Foraging patterns of arctic foxes at a large arctic goose colony. Arctic, 53:279–288.

Samelius, G. and R. T. Alisauskas. 2001. Deterring arctic fox predation: the role of parental nest attendance by lesser snow geese. Canadian Journal of Zoology, 79:861–866.

Samelius, G., R. T. Alisauskas, and S. Larivière. 2011. Seasonal pulses of migratory prey and annual variation in small mammal abundance affect abundance and reproduction by arctic foxes. Polar Biology, 34:1475–1484.

Schmidt, K. A. and R. S. Ostfeld. 2008. Numerical and Behavioral Effects within a Pulse-Driven System : Consequences for Shared Prey. Ecology, 89:635–646.

Schneider, F. D., U. Brose, B. C. Rall, and C. Guill. 2016. Animal diversity and ecosystem functioning in dynamic food webs. Nature Communications, 7:1–8.

Sells, S. N. and M. S. Mitchell. 2020. The economics of territory selection. Ecological Modelling, page 109329.

Serrouya, R., M. J. Wittmann, B. N. McLellan, H. U. Wittmer, and S. Boutin. 2015. Using predator-prey theory to predict outcomes of broadscale experiments to reduce apparent competition. The American Naturalist, 185:665–679.

Shaffer, T. L. 2004. A unified Approach to Analyzing Nest Success. The Auk, 121:526–540.

Siers, S. R., A. A. Y. Adams, and R. N. Reed. 2018. Behavioral differences following ingestion of large meals and consequences for management of a harmful invasive snake : A field experiment. Ecology and Evolution, pages 10075–10093.

Sinclair, A. R. E., R. P. Pech, C. R. Dickman, D. Hik, P. Mahon, and A. E. Newsome. 1998. Predicting effects of predation on conservation of endangered prey. Conservation Biology, 12:564–575.

Sirot, E., P. Blanchard, A. Loison, and O. Pays. 2021. How vigilance shapes the functional response of herbivores. Functional Ecology, 35:1491–1500.

Sittler, B., O. Gilg, and T. B. Berg. 2000. Low abundance of king eider nests during low lemming years in Northeast Greenland. Arctic, 53:53–60.

Smith, P. A. and D. B. Edwards. 2018. Deceptive nest defence in ground-nesting birds and the risk of intermediate strategies. PLoS ONE, 13:1–12.

Smout, S., C. Asseburg, J. Matthiopoulos, C. Fernnadez, S. Redpath, S. Thirgood, and J. Harwood. 2010. The functional response of a generalist predator. PLoS ONE, 5.

Solomon, M. E. 1949. The natural control of animal populations. Journal of Animal Ecology, 18:1–35.

Spalinger, D. E. and N. T. Hobbs. 1992. Mechanisms of foraging in mammalian herbivores: new models of functional response. American Naturalist, 140:325–348.

Spiller, D. A. and T. W. Schoener. 2001. An experimental test for predator-mediated interactions among spider species. Ecology, 82:1560–1570.

Stenseth, N. C., A. Shabbar, K. S. Chan, S. Boutin, E. K. Rueness, D. Ehrich, J. W. Hurrell, O. C. Lingjærde, and K. S. Jakobsen. 2004. Snow conditions may create an invisible barrier for lynx. Proceedings of the National Academy of Sciences of the United States of America, 101:10632–10634.

Stickney, A. 1991. Seasonal patterns of prey availability and the foraging behavior of arctic foxes (*Alopex lagopus*) in a waterfowl nesting area. Canadian Journal of Zoology, 69:2853–2859.

Stouffer, D. B. and M. Novak. 2021. Hidden layers of density dependence in consumer feeding rates. Ecology Letters, 24:520–532.

Stubben, C. J. and B. G. Milligan. 2007. Estimating and analyzing demographic models using the popbio package in R. Journal of Statistical Software, 22.

Studd, E. K., R. Derbyshire, A. K. Menzies, J. Simms, M. M. Humphries, D. L. Murray, and S. Boutin. 2021. The Purr-fect Catch: using accelerometers and audio recorders to document kill rates and hunting behaviour of a small prey specialist, the Canada lynx. Methods in Ecology and Evolution, 12:1277–1287.

Studds, C. E., B. E. Kendall, N. J. Murray, H. B. Wilson, D. I. Rogers, R. S. Clemens, K. Gosbell, C. J. Hassell, R. Jessop, D. S. Melville, D. A. Milton, C. D. T. Minton, H. P. Possingham, A. C. Riegen, P. Straw, E. J. Woehler, and R. A. Fuller. 2017. Rapid population decline in migratory

shorebirds relying on Yellow Sea tidal mudflats as stopover sites. Nature Communications, 8:14895.

Summers, R. W., L. G. Underhill, and E. E. Syroechkovski JR. 1998. The breeding productivity of dark-bellied brent geese and curlew sandpipers in relation to changes in the numbers of arctic foxes and lemmings on the Taimyr Peninsula, Siberia. Ecography, 21:573–580.

Suraci, J. P., M. Clinchy, L. Y. Zanette, C. M. Currie, and L. M. Dill. 2014. Mammalian mesopredators on islands directly impact both terrestrial and marine communities. Oecologia, 176:1087–1100.

Suraci, J. P., J. A. Smith, S. Chamaillé-Jammes, K. M. Gaynor, M. Jones, B. Luttbeg, E. G. Ritchie, M. J. Sheriff, and A. Sih. 2022. Beyond spatial overlap: harnessing new technologies to resolve the complexities of predator–prey interactions. Oikos, 2022:1–15.

Suryawanshi, K. R., S. M. Redpath, Y. V. Bhatnagar, U. Ramakrishnan, V. Chaturvedi, S. C. Smout, and C. Mishra. 2017. Impact of wild prey availability on livestock predation by snow leopards. Royal Society Open Science, 4.

Tallian, A., D. W. Smith, D. R. Stahler, M. C. Metz, R. L. Wallen, C. Geremia, J. Ruprecht, C. T. Wyman, and D. R. Macnulty. 2017. Predator foraging response to a resurgent dangerous prey. Functional Ecology, 31:1418–1429.

Tarroux, A., D. Berteaux, and J. Bêty. 2010. Northern nomads: Ability for extensive movements in adult arctic foxes. Polar Biology, 33:1021–1026.

Terraube, J., A. Villers, L. Ruffino, L. Iso-Iivari, H. Henttonen, T. Oksanen, and E. Korpimäki. 2015. Coping with fast climate change in northern ecosystems: mechanisms underlying the population-level response of a specialist avian predator. Ecography, 38:690–699.

Therrien, J.-F., G. Gauthier, E. Korpimäki, and J. Bêty. 2014. Predation pressure by avian predators suggests summer limitation of small-mammal populations in the Canadian Arctic. Ecology, 95:56–67.

Toscano, B. J. and B. Griffen. 2013. Predator size interacts with habitat structure to determine the allometric scaling of the functional response. Oikos, 122:454–462.

Toscano, B. J. and B. D. Griffen. 2014. Trait-mediated functional responses: Predator behavioural type mediates prey consumption. Journal of Animal Ecology, 83:1469–1477.

Turchin, P. and I. Hanski. 1997. An empirically based model for latitudinal gradient in vole population dynamics. The American Naturalist, 149:842–874.

Tyson, R. and F. Lutscher. 2016. Seasonally Varying Predation Behavior and Climate Shifts Are Predicted to Affect Predator-Prey Cycles. The American Naturalist, 188:539–553.

Underhill, L. G., R. P. Prŷs-Jones, E. E. Syroechkovski JR., N. M. Groen, V. Karpov, H. G. Lappo, M. W. J. V. Roomen, A. Rybkin, H. Schekkerman, H. Spiekman, and R. W. Summers. 1993. Breeding of waders (Charadrii) and Brent Geese Branta bernicla bernicla at Pronchishcheva Lake, northeastern Taimyr, Russia, in a peak and a decreasing lemming year. Ibis, 135:277–292.

Vander Wall, S. 1990. Food Hoarding in Animals. University of Chicago Press.

Vucetich, J. A., R. O. Peterson, and C. L. Schaefer. 2002. The effect of prey and predator densities on wolf predation. Ecology, 83:3003–3013.

Weimerskirch, H., M. Salamolard, F. Sarrazin, and P. Jouventin. 1993. Foraging Strategy of Wandering Albatrosses Through The Breeding Season: A Study Using Satellite Telemetry. The Auk, 110:325–342.

Weiser, E. L., R. B. Lanctot, S. C. Brown, H. R. Gates, R. L. Bentzen, J. Bêty, M. L. Boldenow, W. B. English, S. E. Franks, L. Koloski, E. Kwon, J.-F. Lamarre, D. B. Lank, J. R. Liebezeit, L. McKinnon, E. Nol, J. Rausch, S. T. Saalfeld, N. R. Senner, D. H. Ward, P. F. Woodard, and B. K. Sandercock. 2018. Environmental and ecological conditions at Arctic breeding sites have limited effects on true survival rates of adult shorebirds. The Auk, 135:29–43.

Weiser, E. L., R. B. Lanctot, S. C. Brown, H. R. Gates, J. Bêty, M. L. Boldenow, R. W. Brook, G. S. Brown, W. B. English, and S. A. Flemming. 2020. Annual adult survival drives trends in Arctic-breeding shorebirds but knowledge gaps in other vital rates remain. The Condor, 122:1–14.

Williams, T. M., L. Wolfe, T. Davis, T. Kendall, B. Richter, Y. Wang, C. Bryce, G. H. Elkaim, and C. C. Wilmers. 2014. Instantaneous energetics of puma kills reveal advantage of felid sneak attacks. Science, 346:81–85.

Wilson, E. C., B. Zuckerberg, M. Z. Peery, and J. N. Pauli. 2022. Experimental repatriation of snowshoe hares along a southern range boundary reveals historical community interactions. Ecological Monographs, pages 1–18.

Wootton, K. L., A. Curtsdotter, T. Roslin, R. Bommarco, and T. Jonsson. 2021. Toward a modular theory of trophic interactions. Functional Ecology, 00:1–18.